INTEGRATIVE ANALYSIS of BRANCH POINTS in the EVOLUTION of CHEMOSENSORY RECEPTOR REPERTORIES: UNEXPECTED PROPERTIES of AMPHIBIAN OLFACTORY and COELACANTH TASTE RECEPTORS

Inaugural-Dissertation

zur

Erlangung des Doktorgrades

der Mathematisch-Naturwissenschaftlichen Fakultät

der Universität zu Köln

vorgelegt von

Adnan Shahzad Syed

aus Rawalpindi, Pakistan

Köln 2014/15

INTEGRATIVE ANALYSIS of BRANCH POINTS in the EVOLUTION of CHEMOSENSORY RECEPTOR REPERTORIES: UNEXPECTED PROPERTIES of AMPHIBIAN OLFACTORY and COELACANTH TASTE RECEPTORS

Inaugural-Dissertation

zur

Erlangung des Doktorgrades

der Mathematisch-Naturwissenschaftlichen Fakultät

der Universität zu Köln

vorgelegt von

Adnan Shahzad Syed

aus Rawalpindi, Pakistan

Köln 2014/15

Berichterstatter: Prof. Dr. Sigrun I. Korsching
Prof. Dr. Kay Hofmann

Tag der mündlichen Prüfung: 23 January, 2015

To Shah Baba Family

1 INTRODUCTION 7
1.1 OLFACTION 7
1.1.1 OLFACTORY SYSTEM 8
1.1.1.1 MAMMALIAN OLFACTORY SYSTEM 8
1.1.1.2 TELEOST OLFACTORY SYSTEM 9
1.1.1.3 AMPHIBIAN OLFACTORY SYSTEM 9
1.2 EVOLUTIONARY DYNAMICS of OLFACTORY RECEPTOR GENE REPERTOIRES 11
1.2.1.1 ODORANT RECEPTORS (ORs) 11
1.2.1.2 VOMERONASAL RECEPTORS (VRs) 11
1.2.1.3 TRACE AMINE-ASSOCIATED RECEPTORS (TAARs) 15
1.2.1.4 MEMBRANE GUANYLYL CYCLASE (GC-D) 15
1.3 GUSTATORY (TASTE) SYSTEM 16
1.3.1 TASTE RECEPTOR GENE FAMILY REPERTOIRES 16
1.3.1.1 FREQUENT EXPANSION of the BITTER TASTE RECEPTOR GENE REPERTOIRE DURING EVOLUTION of TETRAPODS 16
1.3.1.2 UMAMI and SWEET TASTE RECEPTORS 17
1.3.1.3 SALT and SOUR TASTE RECEPTORS 17
1.4 EXPERIMENTAL MODEL 18
1.4.1 AFRICAN CLAWED FROG 18
1.4.2 COELACANTH 19
1.5 AIMS of this DISSERTATION 21
2 PUBLICATIONS of the DISSERTATION 22
2.1 *XENOPUS laevis* (AFRICAN CLAWED FROG) 22
2.1.1 EXPRESSION of V2R GENE FAMILY 22
2.1.2 TRPC2 is EXPRESSED in TWO OLFACTORY SUBSYSTEMS 29
2.1.3 ODOR MAPPING to the OLFACTORY RECEPTORS EXPRESSION in MOE 34
2.2 *LATIMERIA chalumnae* (COELACANTH) 55

2.2.1 CHARACTERIZATION of TWO CHEMOSENSORY RECEPTOR FAMILIES 55
3 EXTENDED DISCUSSION 71
3.1 *XENOPUS laevis* (AFRICAN CLAWED FROG) 71
3.1.1 EARLY DIVERGING V2R GENES are EXPRESSED in MOE 71
3.1.2 TRPC2 EXPRESSION in BOTH OLFACTORY SUBSYSTEMS of *XENOPUS* PARALLELS THE COMBINED V2R EXPRESSION 72
3.1.3 SPATIAL EXPRESSION ARCHITECTURE of *XENOPUS* OLFACTORY RECEPTOR FAMILIES in MOE 73
3.1.4 MAPPING the ODOR RESPONSES to the OLFACTORY RECEPTORS SPATIAL DISTRIBUTION in MOE 75
3.2 COELACANTH CHEMOSENSORY RECEPTOR REPERTOIRE MORE SIMILAR to TETRAPODS than RAY-FINNED FISHES 77
3.2.1 AN UNPRECEDENTEDLY LARGE T2R FAMILY of LIVING FOSSIL 77
3.2.2 V1R GENE REPERTOIRE SIMILAR to TETRAPOD V1R REPERTOIRES 79
4 REFERENCES 81
5 SUMMARY 85
6 ZUSAMMENFASSUNG 86
7 APPENDIX 88
8 ACKNOWLEDGEMENT 89
9 AUTHOR CONTRIBUTIONS 90
10 ERKLÄRUNG (DECLARATION) 91
11 CURRICULUM VITAE 92

1 INTRODUCTION

"The capacity of DNA to store information vastly exceeds that of any other known system."

Dr. Michael Denton

There are five sensory senses by which individuals are able to obtain cues from the outside world, process and interpret that information in the brain and elicit behavior. Commonly recognized sensory systems are auditory, somatic sensation, vision, gustatory sense (taste) and olfaction (smell). Even though taste and olfaction are separate senses with their own receptors and brain circuits, their perception is often intertwined. The combination of taste and olfaction is most visible in how we perceive the flavors of the food as anyone with bad flu might indicate food tastes different because the sense of smell is impaired.

1.1 OLFACTION

Animals in the natural habitat are surrounded by myriads of odors. These odors constitute a rich source of information, and are perceived by specialized and sensitive olfactory system. The olfactory system helps species to localize food, evade predators, and recognize viable mates. Smell, almost more than any other sense, has the ability to call up memories, and to modify moods. Patients with smell disorder suffer because of a decrease in quality of life, as things become less enjoyable. Moreover, people suffering from smell disorder witness lot of changes in their eating habits, some eat too little and lose weight while others eat too much and gain weight. An impaired sense of smell can be an early signs of depression, Parkinson's disease, Alzheimer's disease, or multiple sclerosis (Lazic et al. 2007, Doty 2008, Doty 2009).

Linda Buck and Richard Axel in 1991 reported ground breaking findings that for the first time shed light on the nature of olfactory receptors and in follow-up work these authors made several seminal contributions to the processing of odor information in the brain. The importance of their work was immense in the field of chemosensation, this earned them the Nobel Prize in Physiology or Medicine in the year 2004. Today, the

field of olfaction is very active as availability of complete sequenced genomes and modern data mining algorithms and molecular techniques pave the way to understand and characterize olfactory receptor gene families, their function and elicited behavior.

1.1.1 OLFACTORY SYSTEM

In vertebrates the olfactory system consists of three major parts, the sensory surface located in the nasal cavity, the target region of the sensory neurons (olfactory bulb (OB) and higher brain centers. Within the sensory surface different cell types are found, including olfactory sensory neurons (OSNs), supporting cells, basal cells and brush cells. OSNs express a single olfactory receptor out of several receptor families (monogenic expression). Neurons expressing the same receptor are scattered throughout the olfactory epithelium (OE), but their axons converge onto a single target region (glomerulus) in the olfactory bulb. Subsequently the odor information is then passed to higher cortical and limibic areas, which are involved in odor perception and emotional and physiological effects of particular odors (Kapur and Haberly 1998).

1.1.1.1 MAMMALIAN OLFACTORY SYSTEM

In higher organisms, the olfactory system controls a wide range of complex and integrative functions such as emotional responses, reproduction, physiological regulation, and social behaviors. To manage these diverse and complex varieties of complex functions, up to five main, discrete and segregated olfactory subsystems are present in rodents (Halpern 1987, Buck 2000, Firestein 2001). Two major subsystem are the main olfactory epithelium (MOE) which detects volatile odorants and the vomeronasal system (VNO) which is specialized in sensing pheromones in mice (Figure 1A) (Buck 2000, Mombaerts 2004). Volatile odorants are largely perceived by a receptor family called odorant receptors (ORs), these ORs are expressed on the cilia and dendritic knob of ciliated OSNs in the MOE that project their axons to the main olfactory bulb (MOB). Other receptors that are expressed in MOE are trace amines-associated receptors (TAARs), and membrane guanylyl cyclase receptor (GC-D) (Fulle et al. 1995, Lindemann et al. 2005). The VNO or the Jacobson's organ expresses three receptor families, vomeronasal receptors type I and type II (V1Rs, V2Rs) and formyl peptide receptors (FPRs) (Figure 1A). The VNO is believed to house receptors involved

in detection of pheromones or disease-related compounds, these receptor families are expressed by microvillous OSNs (Buck 2000, Riviere et al. 2009). Information from the VNO is transmitted to the accessory olfactory bulb (AOB), which further projects towards amygdala and hypothalamus that are involved in aggression and mating behavior (Hasen and Gammie 2009).

1.1.1.2 TELEOST OLFACTORY SYSTEM

Contrary to the mammalian olfactory system, teleost fish have only one olfactory system with a single olfactory organ called OE for olfactory epithelium (Figure 1B). In many teleost fish species, the OE is rosette-shaped, with an inner region containing sensory surface and non-sensory region on the periphery (Figure 1B). To date four types of OSNs are found to be present in the sensory region of the OE. These OSNs (ciliated, microvillous, crypt and kappe) project their axons in the olfactory bulb (OB) (Hansen and Zielinski 2005, Ahuja et al. 2014). Furthermore, ciliated, microvillous, crypt and kappe OSNs can be labeled with specific markers such as, respectively, OMP, S100, TRPC2 and Go (Germana et al. 2004, Sato et al. 2005, Ahuja et al. 2014). Ciliated neurons express large families of *OR* and *TAAR* genes, microvillous neurons express V2R/OlfC receptors, and crypt neurons express a single V1R-related ORA receptor (Hansen and Zielinski 2005, Alioto and Ngai 2006, Hussain et al. 2009, Oka et al. 2012).

1.1.1.3 AMPHIBIAN OLFACTORY SYSTEM

Amphibians embody a transition point in the evolutionary tree, as they are the first species to live on land (as adults). Larval *Xenopus laevis* have two distinct olfactory organs, the main olfactory epithelium (MOE) and the vomeronasal organ (VNO) (Figure 1C). The MOE consists of ciliated and microvillous OSNs, these OSNs can be labeled with tubulin, a marker for ciliated neurons and phalloidin, a marker for microvillous neurons (Hansen et al. 1998, Manzini and Schild 2010). *Xenopus* has a family of several hundred OR genes, and they are shown to be expressed in MOE (Figure 1C) (Mezler et al. 1999, Gliem et al. 2013). In contrast the TAAR family of *Xenopus* is very small, with only 3 TAARs, out of which 2 are expressed in MOE and one is not involved in olfaction (Gliem et al. 2013). *Xenopus* already possess a fully developed VNO, which

has microvillous OSNs expressing V2Rs (Hagino-Yamagishi et al. 2004). However, contrary to mammalian V1Rs that are expressed in VNO, Xenopus V1Rs are reported to be expressed in MOE (Figure 1C) (Date-Ito et al. 2008).

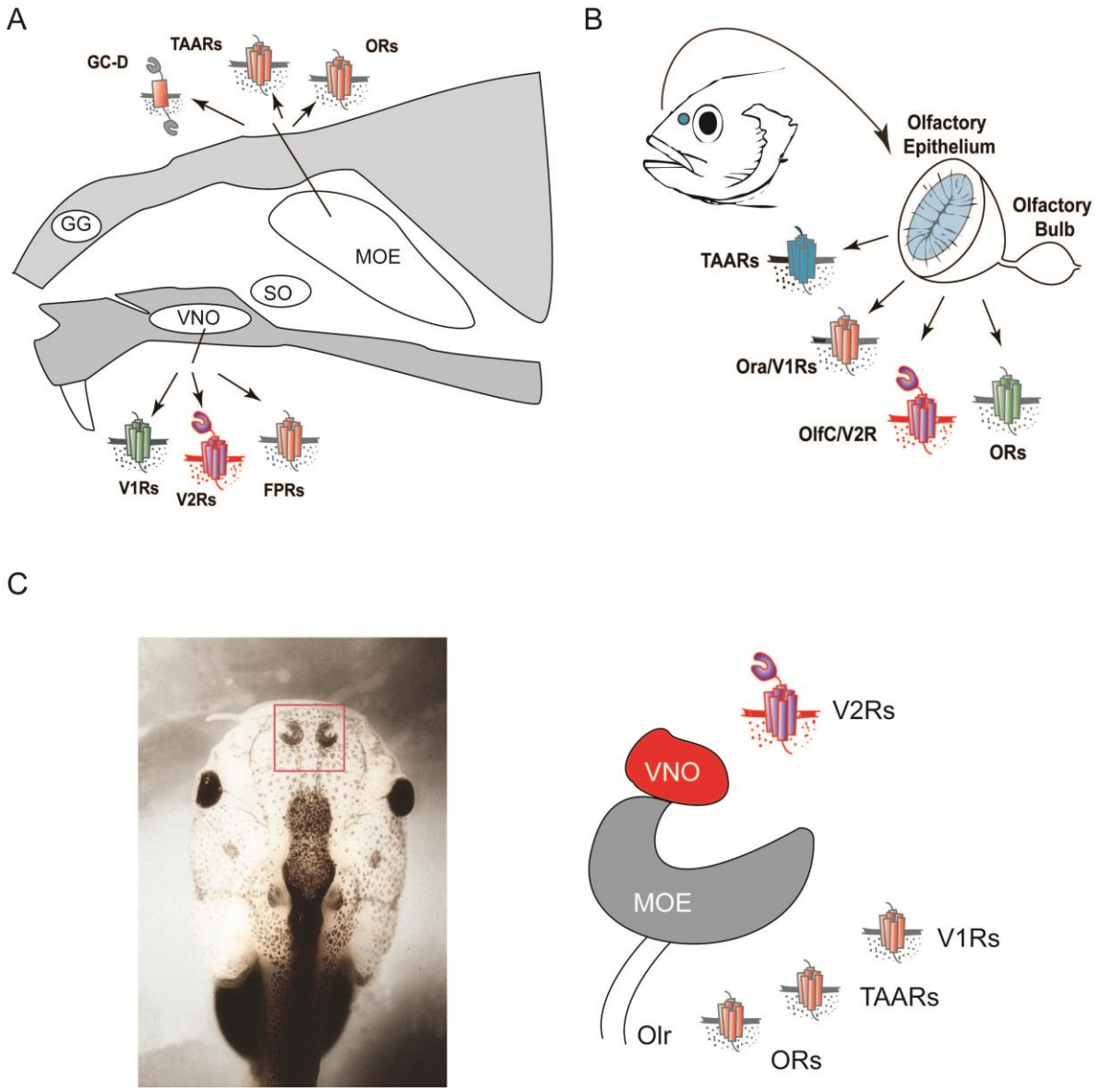

Figure 1: Schematic diagram of olfactory systems in moue, zebrafish and *Xenopus*. Panel A: Main olfactory epithelium (MOE) showing TAARs, Guanylyl cyclase-D and ORs receptors, Grueneberg ganglion (GG), vomeronasal organ (VNO) expressing V2Rs, V1Rs, and FPRs, septal organ of masera (SO). Panel B: Zebrafish olfactory system. Scheme showing olfactory epithelium expressing TAARs, ORA/V1Rs, OlfC/V2Rs and ORs. Panel C: *Xenopus* olfactory system. Showing VNO, MOE and olfactory nerve. Where V2Rs are expressing in VNO, whereas V1Rs, TAARs, ORs expressed in MOE.

1.2 EVOLUTIONARY DYNAMICS of OLFACTORY RECEPTOR GENE REPERTOIRES

Animals in the natural habitat are surrounded by myriads of odors which are a rich source of information and are perceived by specialized olfactory receptor families. During vertebrate evolution a big transition in such repertoires was necessitated by the water to land transition. Study of olfactory receptor repertoires in different species can provide tools to understand this evolutionary transition of the olfactory system.

1.2.1.1 ODORANT RECEPTORS (ORs)

Olfactory receptors are members of class A of GPCRs and can be classified into two distinct groups based on their phylogeny, class I genes have orthologs in fish and class II genes have orthologs in mammals (Freitag et al. 1995, Freitag et al. 1998). *Xenopus* is situated at an important branch point in evolution from aquatic to terrestrial species, and possesses both class I and class II OR genes. This division in OR genes suggested that class I ORs are specialized to recognize water-soluble odorants, whereas class II ORs are used for detecting airborne stimuli. However recent studies show that small number of class I ORs are present in human, mouse and other mammalian species indicating a possible involvement in mammalian olfaction (Glusman et al. 2001, Zhang and Firestein 2002, Niimura and Nei 2007).

OR coding regions are roughly 1000 base pair in length, intron less and found to be expressed in ciliated neurons (Buck and Axel 1991, Mombaerts 2004, Sato et al. 2007). ORs have a dynamic family size in different species, human possess about 350 functional genes, mouse and rat possess in-between 1000 to 1200 and *Xenopus* above 800 OR genes. In teleosts, the OR repertoire is several fold smaller than that of tetrapods, zebrafish are reported to have 147 ORs and pufferfish less than 50 (Figure 2) (Niimura and Nei 2003, Young et al. 2003, Gibbs et al. 2004, Alioto and Ngai 2005). A preliminary study found the OR repertoire size in coelacanths, members of lobe-finned lineage to be similarly small as in ray-finned lineage (Picone et al. 2014).

1.2.1.2 VOMERONASAL RECEPTORS (VRs)

In rodents, there are three distantly related families of GPCR, vomeronasal receptor type1 and type 2 (V1R, V2R) and formyl-peptide receptors (FPRs), all of which

are expressed in the sensory neurons of the accessory olfactory organ named vomeronasal epithelium (Herrada and Dulac 1997, Matsunami and Buck 1997, Dulac 2000, Riviere et al. 2009). The vomeronasal epithelium in mammals is organized in two molecularly distinct layers, an apical layer expressing V1Rs, FPRs and a basal layer expressing V2Rs (Buck 2000, Dulac 2000, Riviere et al. 2009). Interestingly, *Xenopus* already possess a VNO that is anatomically separate from the MOE, but they only express V2Rs in the VNO, and their V1Rs transcripts were found in the MOE (Date-Ito et al. 2008).

Transient receptor potential channel C2 (TRPC2) is reported to be expressed exclusively in mouse VNO, which makes it a very useful marker to study the VNO function during vertebrate evolution. TRPC2 is involved in vomeronasal signal transduction, and interestingly is absent in the species which have lost or significantly reduced ability to detect pheromones (Liman and Innan 2003, Zhang and Webb 2003).

Several earlier derived species exhibit accessory olfactory surfaces, but the morphology is very different from the tetrapod VNO, suggesting that the segregation into accessory olfactory surfaces has occurred independently several times during evolution (e.g. lamprey, shark, lungfish) (Gonzalez et al. 2010, Chang et al. 2013, Meredith et al. 2013). For example, lungfish, one of the very few extant fish species in the lobe-finned lineage possess crypt-like structures at the base of the main olfactory lamellae, which express markers of the vomeronasal receptors like tetrapods (Gonzalez et al. 2010, Nakamuta et al. 2012), and may thus be considered an equivalent structure to tetrapod VNO. In teleost fish with their single olfactory surface, i.e. in the absence of segregation, TRPC2 expression can be used as a marker for microvillous OSN (Sato et al. 2005).

V2Rs, also known as OlfC in fish species, have a multi-exonic structure and belong to class C of GPCRs. As is common for class C receptors, V2Rs possess a large N-terminal extracellular region, which is thought to be the binding domain for pheromones. V2Rs show pronounced species-specific expansion or depletion, and indeed many mammalian species exhibit a complete loss of the V2R gene family (Young and Trask 2007). In mouse the V2R repertoire comprises 121 gene members

(Nei et al. 2008). Phylogenetic studies have revealed a major V2R group (family A+B) and a minor group (family C), which e.g. in mice only contains 7 members (Ishii and Mombaerts 2011). Similarly, these classes can be found in zebrafish and *Xenopus* V2R gene family repertoires; however zebrafish and *Xenopus* possess only 1 member in family C (Alioto and Ngai 2006, Ji et al. 2009). Family C members are broadly expressed and in mouse and fish have been shown to serve as co-receptors for the sparsely expressed family A and B members.

Interestingly, by far the largest V2R repertoire is found in *Xenopus* (Figure 2), although so far the function of such a large repertoire is completely unclear. It has been hypothesized that it may be an evolutionary adaption to their unique living environment (Ji et al. 2009). OlfC/V2R gene repertoires of fish species vary within the range observed for mammals: *Latimeria* which belongs to lobe-finned lineage have 61 V2Rs (Figure 2) (Picone et al. 2014), zebrafish, a ray-finned fish possess 53 and fugu has 18 *olfc* genes (Alioto and Ngai 2006). Potential ligands for V2Rs are thought to be water soluble compounds as many class C GPCRs including two zebrafish OlfC receptors are found to be activated by amino acids (Conigrave et al. 2000, DeMaria et al. 2013). Furthermore, other V2R receptor-ligand studies have also shown peptides (exocrine gland-secreting (ESP) and MHC class I) as ligands (Leinders-Zufall et al. 2004, Kimoto et al. 2005).

V1Rs, also known as ORA in fish species, belong to class A-related GPCRs, span about 1000 basepairs and are intronless (Figure 1B). Like other class A GPCRs the V1Rs possess a small N-terminal extracellular region and similar to OR receptors they exhibit a less conserved sequence in transmembrane domains. V1R gene family sizes vary between 5-6 genes in teleost fishes to around 20 in *Latimeria* and *Xenopus*, and reaching above 300 genes in platypus (Grus et al. 2007, Saraiva and Korsching 2007, Nei et al. 2008), see (Figure 2). V1Rs are highly diverse and often large differences are observed even between closely related species, in contrast to the ortholog ORA family in teleost species. Without exception ortholog ORA genes are closer neighbors within the phylogenetic tree compared to their paralogs in the same species (Saraiva and Korsching 2007). Both V1Rs and ORAs are assumed to function as pheromone receptors. In mouse, V1rb2, a member of V1R family has shown to be

activated by 2-heptanone, a compound found in mouse urine and presumably involved in social signaling (Boschat et al. 2002). Furthermore, ORA1, a member of the zebrafish V1R-related ORA gene family recognizes 4-hydroxyphenylacetic acid, which may function as a pheromone for reproductive behavior (Behrens et al. 2014).

FPRs belong to a class A of GPCRs, and are known to be involved in leukocyte chemotaxis and activation. As known by their name these receptors bind to N-formyl peptides such as N-Formylmethionine, which is a result of bacterial degradation (Yang et al. 2002). These receptors are intronless and consist of roughly 1kb of coding region. Recently, two independent groups have shown that some of these receptors play a role in olfaction and are expressed in the VNO of mice (Liberles et al. 2009, Riviere et al. 2009). VNO-specific FPRs are thought to be activated by disease-related molecules, suggesting that these receptors send alarm signals upon detection of infected conspecifics or contaminated food (Riviere et al. 2009).

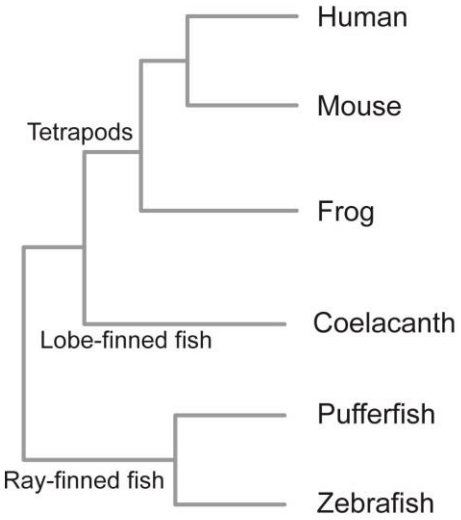

	OR	V1R	V2R	TAAR	T1R	T2R
Human	396	4	0	6	3	24
Mouse	1037	211	121	15	3	33
Frog	824	21	330	3	0	49
Coelacanth	56	15/20	61	4	5	5/58
Pufferfish	47	1	18	18	4	4
Zebrafish	154	6	53	112	4	4

Figure 2: Number of functional chemosensory receptors published in literature. Data collected from (Hussain et al., 2009, Niimura 2009, Dong et al., 2012, Saraiva and Korsching, 2007, Date-ito et al., 2008, Shi and Zhang 2007, Picone et al., 2013, Li and Zhang 2014).

1.2.1.3 TRACE AMINE-ASSOCIATED RECEPTORS (TAARs)

Trace amine-associated receptors (TAARs) belong to class A of GPCRs, they have a coding sequence of roughly 1 kb and are intronless. These receptors were first discovered in 2001 and are thought to be involved in detection of trace amines but not the classical biogenic amines (Borowsky et al. 2001, Bunzow et al. 2001). However, in 2006 TAAR genes were reported to be involved in olfaction and to be expressed in mouse MOE (Liberles and Buck 2006). The TAAR gene repertoire shows similar selective pressure as observed in OR and V1R gene families, in teleost fishes they range from few genes in fugu to above 110 members in zebrafish, much more than observed for tetrapods, 3 in *Xenopus*, and around 15 gene members in mouse (Hashiguchi and Nishida 2007, Hussain et al. 2009), see also (Figure 2). In mouse, TAAR receptors recognize volatile amines found in mouse urine, which suggests their role in detection of social cues (Liberles and Buck 2006). Another study found that Taar13c, a member of the zebrafish TAAR family recognizes cadaverine, which is produced in dead or decaying fish and triggers an aversive behavior in zebrafish (Hussain et al. 2013).

1.2.1.4 MEMBRANE GUANYLYL CYCLASE (GC-D)

Guanylyl cyclases are the only olfactory receptors reported so far that do not belong to the GPCR superfamily. Recently, an orphan receptor GC-D belonging to the family of guanylyl cyclase was found to be expressed in ciliated neurons in the mouse MOE and later shown to be expressed in septal organ (Fulle et al. 1995, Juilfs et al. 1997, Walz et al. 2007). Interestingly, instead of following canonical cAMP odor transduction pathway these neurons are endowed with the cGMP-specific CNG channel subunit, CNGA3, and a cGMP-stimulated phosphodiesterase, PDE2A (Meyer et al. 2000, Hu et al. 2007). In search of the chemosensory role of these receptors, one study showed that the urinary peptides (uroguanylin and guanylin) activate GC-D expressing OSNs, and in another study GC-D neurons are reported to detect carbon dioxide (Hu et al. 2007, Leinders-Zufall et al. 2007, Sun et al. 2009).

1.3 GUSTATORY (TASTE) SYSTEM

Gustatory system (sense of taste) plays a crucial role in identifying food quality. Toxic food sources have to be avoided, and nutritious food has to be identified. Humans and many other vertebrates can recognize five basic tastes: sweet, salty, bitter, sour, and umami. In contrast to fruit flies which have taste receptor cells (TRCs) distributed over head, wings, body and legs, mammals have a tongue and soft palate that houses TRCs clustered in taste buds, which are distributed across the tongue. TRCs are divided into four major subtypes namely TRC I, TRC II, TRC III, and TRC IV, where TRC II cells express receptors involved in taste sensing (Clapp et al. 2001, Breslin and Spector 2008). Recent technical advances in genome sequencing and data-mining techniques made it possible to identify taste receptor repertoires from different species and draw evolutionary conclusions on their functions.

1.3.1 TASTE RECEPTOR GENE FAMILY REPERTOIRES

1.3.1.1 FREQUENT EXPANSION of the BITTER TASTE RECEPTOR GENE REPERTOIRE DURING EVOLUTION of TETRAPODS

Perception of bitter taste is of great importance in animals as it enables them to detect structurally distinct toxic compounds and prevent ingestion of these compounds. In vertebrates, bitter taste is mediated by the receptors known as taste receptor type 2 (T2Rs), which belong to rhodopsin-like class A GPCRs with small N-terminal domains. That T2Rs are crucial for bitter taste was shown in a knockout study in mice, by making a functional knockout of mT2R5, which is candidate cycloheximide receptor, resulting in complete loss of behavioral and nerve responses at concentration that evoked strong responses in wild-type animal (Mueller et al. 2005). Interestingly, *Xenopus* which does not have a tongue uses its oral cavity to detect bitter substances and amino acids (Yoshii et al. 1982). Studies have found that T2Rs fall into two categories, very specific receptors which detect one or a few bitter chemicals, while others respond to a wide variety of bitter chemicals (Behrens and Meyerhof 2009). The T2R gene family shows species-specific expansion (Figure 2), with relatively large families in mice and frogs, whereas teleost fishes only possess a small family of less than 10 receptors (Shi and

Zhang 2006). For *Latimeria chalumnae* there are conflicting reports whether the repertoire is as large as in mammals or small like in teleost fishes (Figure 2) (Li and Zhang 2014, Picone et al. 2014).

1.3.1.2 UMAMI and SWEET TASTE RECEPTORS

Both the taste of sweet (sugar) and of umami (protein-rich) are thought to be detected by a small group of taste receptor type 1 (T1Rs) which belongs to class C GPCRs. These receptors form heterodimers in which T1R3 is combined with either T1R1 (T1R1/T1R3, umami-responsive) or with T1R2 (T1R2/T1R3, sweet-responsive) receptors (Nelson et al. 2001, Nelson et al. 2002, Zhao et al. 2003). In zebrafish, combination of T1R2/T1R3 responds to L-amino acids rather than sweet taste, suggesting a change of function during the transition of vertebrates from water to land (Yasuoka and Abe 2009). Phylogenetic studies have shown T1R orthologs are present in vertebrates but not in any invertebrate species. Furthermore, the small family size of T1Rs stays constant across vertebrate and there is no species-specific expansion (Figure 2) (Shi and Zhang 2006). Interestingly, *Xenopus* which has a large repertoire of T2R receptors lacks T1Rs completely (Shi and Zhang 2006).

1.3.1.3 SALT and SOUR TASTE RECEPTORS

In contrast to other taste receptors that are triggered by large molecules such as sucrose, salt and sour taste detect very simple ions: hydrogen ions (H+) for acidity and sodium ions (Na+) for salt. There have been numerous studies that have reported several receptors responsible for sour taste or describing its pathway including acid-sensing ion channel (ASICs), hyperpolarization-activated cyclic-nucleotide-gated channels (HCNs), K+ channels, and transient receptor potential (TRP) channels PKD2L1 and PKD1L3 (Yarmolinsky et al. 2009). However, knockout studies are needed to determine the role of these candidate receptors.

The taste of salt generates diverse behavior depending on its concentration, low doses of salt are attractive to rodents and high dosage generates repulsive behavior. Amiloride-sensitive epithelial Na+ channel is thought to be responsible for Na+ uptake. Furthermore, it was later confirmed by knocking out epithelial sodium channel (ENaC)

subunit in taste buds as it is strongly inhibited by amiloride, which resulted in the loss of salt taste detection (Chandrashekar et al. 2010).

1.4 EXPERIMENTAL MODEL

A model organism is a species that is extensively studied to understand biological and evolutionary phenomena; findings made in such species can be further extrapolated to include other species in the hope of understanding developmental and biological pathways that are conserved throughout evolution. During my doctoral thesis I have worked with *Xenopus laevis* and *Latimeria chalumnae*, which hold key position in species evolutionary tree.

1.4.1 AFRICAN CLAWED FROG

The amphibian, African clawed frog (*Xenopus laevis)* lives in warm and stagnant water and has a tetraploid genome which means it has four copies of each gene. Its genome is not available, but that of the closely related *Xenopus tropicalis* has been made public, and can be used for bioinformatic searches. *Xenopus* belong to the family of Pipidae and to the order of Anura. *Xenopus laevis* does not possess teeth or tongue therefore it relies heavily on its sensitive fingers and on its sense of smell to search for food (J 1994). *Xenopus* are inexpensive, easy to maintain and are highly accessible. *Xenopus* excels as a model system because it is well positioned between distant metazoans such as Drosophila and C.elegans and the less accessible mammalian models. This makes Xenopus a powerful model system to investigate normal vertebrate development and its deregulation in disease. Study of *Xenopus* provides detailed insight into cellular and molecular mechanisms due to its high degree of conservation in vertebrate species, both within genes and in non-coding elements such as long non-coding RNA and regulatory elements. Moreover oocytes of *Xenopus* are commonly used for gene expression and channel activity for different human diseases. . Furthermore, *Xenopus laevis* unique life style, from being larva (fully aquatic) to adult (semi aquatic) makes it an ideal model to study the evolutionary transition of olfactory systems from water to land.

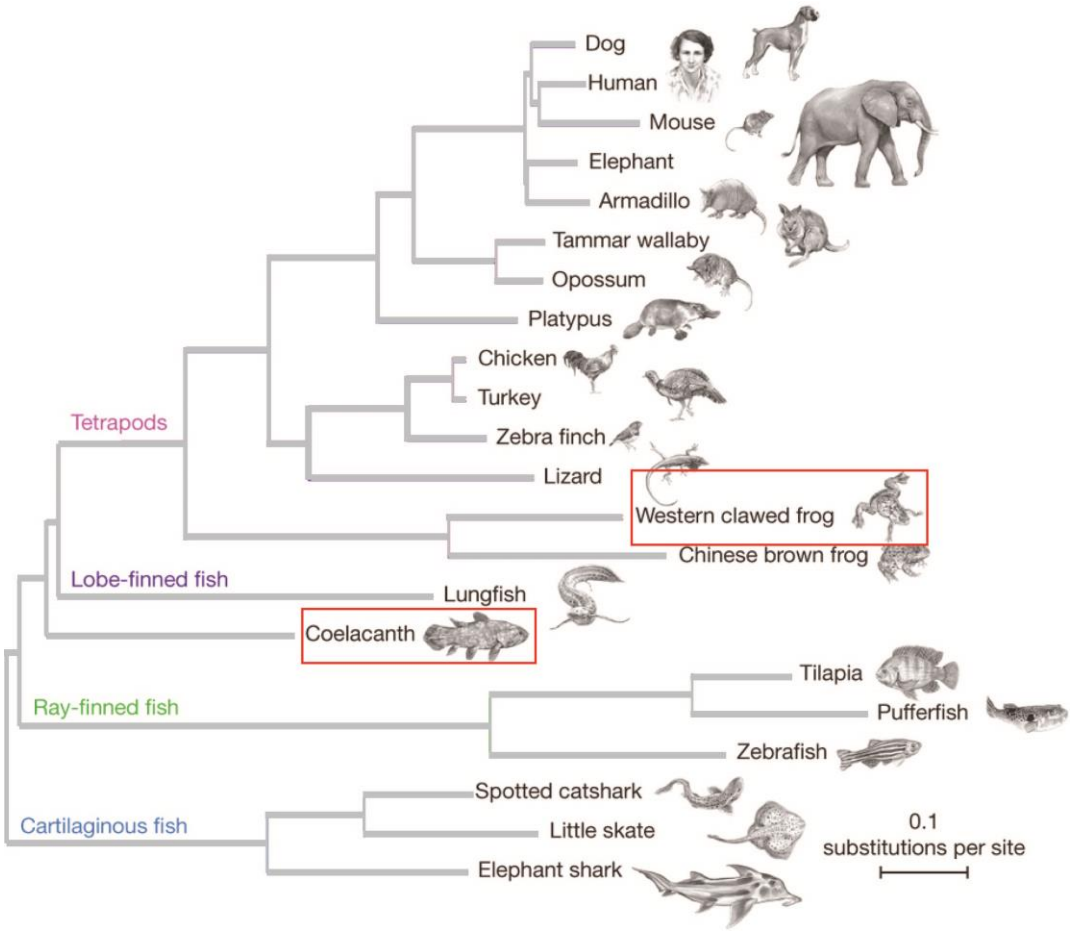

Figure 3: Evolutionary tree of selected jawed vertebrate species: Experimental model organisms are highlighted in rectangle (red). (Figure modified after Amemiya et al 2013)

1.4.2 COELACANTH

Coelacanth and lungfish are the only extant orders of lobe-finned fish, with whom all tetrapods share a common origin. Coelacanth (*Latimeria chalumnae*) is a critically endangered species belonging to the order of *Coelacanthiformes* and the family of *Latimeriidae*. Initially this group of fish was thought to be extinct, until in 1939 Marjorie Countenay-Latimer discovered the species, which later was named after her. *Latimeria chalumnae* holds an important branch point in evolution and is the only living member of the coelacanth order, which was believed to be extinct since the time of dinosaurs (70 million years ago). *Latimeria* lives in deep sea water around 150- 200 meters deep and grows to about 2 meter in length. *Latimeria* diet consists mainly of squids, eels, small

sharks and other animals that are found in the deep sea. Evolutionary biologists have great interest due to its closer phylogenetic relationship to tetrapods than to ray-finned fishes. Recently, the genome of *Latimeria* has been published and is publically available (Amemiya et al. 2013), which has attracted scientists from different fields to data-mine different receptor families and draw evolutionary conclusions.

1.5 AIMS of this DISSERTATION

Olfaction and taste senses are essential for the detection of chemical signals, which allow organisms to detect food, predators, find suitable mates and analyse food quality. The importance of the chemical senses can be gleaned from the large selective pressure required to maintain large gene repertoires throughout evolution. Hence identification and characterization of these chemosensory receptor gene families in different species can help to understand the underlying evolutionary forces shaping these receptor repertoires.

In this study I have focused on two evolutionary relevant animal models, *Latimeria chalumnae* and *Xenopus laevis*. In *Xenopus laevis*, first, I have performed a phylogenetic analysis of the V2R gene family and established the expression pattern of representative genes in the olfactory organs of larval *Xenopus.* Second, I have characterized and examined the localization of TRPC2 in *Xenopus*, which is a known marker for vomeronasal neurons in mammals. Third, I have examined the two-dimensional expression patterns of olfactory receptor gene families in the MOE of *Xenopus* and mapped the odor responses to these receptor families.

In *Latimeria chalumnae,* which are considered the oldest living representatives of the lobe-finned lineage leading to tetrapods, I report here the identification and characterization of two chemosensory receptor gene families, bitter taste receptors (T2Rs), and vomeronasal type-1 receptors (V1Rs).

2 PUBLICATIONS of the DISSERTATION

"Theories come and theories go. The frog remains."

~Jean Rostand

2.1 *XENOPUS laevis* (AFRICAN CLAWED FROG)

2.1.1 EXPRESSION of V2R GENE FAMILY

This section deals with the original research article published in the journal Proceedings of the National Academy of Sciences (Vol. 110, No. 19, Pages 7714-7719, published online on March 2013). Supplementary data associated with this article can be found in the CD attached.

Ancestral amphibian *v2rs* are expressed in the main olfactory epithelium

Adnan S. Syed[a], Alfredo Sansone[b], Walter Nadler[c], Ivan Manzini[b,d], and Sigrun I. Korsching[a,1]

[a]Institute of Genetics, University of Cologne, 50674 Cologne, Germany; [b]Department of Neurophysiology and Cellular Biophysics, University of Göttingen, 37073 Göttingen, Germany; [c]Institute for Advanced Simulation, Juelich Supercomputing Centre, Forschungszentrum Juelich, 52425 Juelich, Germany; and [d]Center for Nanoscale Microscopy and Molecular Physiology of the Brain (CNMPB), 37073 Göttingen, Germany

Edited by John G. Hildebrand, University of Arizona, Tucson, AZ, and approved March 22, 2013 (received for review February 5, 2013)

Mammalian olfactory receptor families are segregated into different olfactory organs, with type 2 vomeronasal receptor (*v2r*) genes expressed in a basal layer of the vomeronasal epithelium. In contrast, teleost fish *v2r* genes are intermingled with all other olfactory receptor genes in a single sensory surface. We report here that, strikingly different from both lineages, the *v2r* gene family of the amphibian *Xenopus laevis* is expressed in the main olfactory as well as the vomeronasal epithelium. Interestingly, late diverging *v2r* genes are expressed exclusively in the vomeronasal epithelium, whereas "ancestral" *v2r* genes, including the single member of *v2r* family C, are restricted to the main olfactory epithelium. Moreover, within the main olfactory epithelium, *v2r* genes are expressed in a basal zone, partially overlapping, but clearly distinct from an apical zone of olfactory marker protein and odorant receptor-expressing cells. These zones are also apparent in the spatial distribution of odor responses, enabling a tentative assignment of odor responses to olfactory receptor gene families. Responses to alcohols, aldehydes, and ketones show an apical localization, consistent with being mediated by odorant receptors, whereas amino acid responses overlap extensively with the basal *v2r*-expressing zone. The unique bimodal *v2r* expression pattern in main and accessory olfactory system of amphibians presents an excellent opportunity to study the transition of *v2r* gene expression during evolution of higher vertebrates.

amino acid odorants | calcium imaging | TAAR | statistical test | spatial pattern

A hallmark of mammalian olfaction is the segregation of the sensory epithelium in several different olfactory organs, each with its own characteristic set of olfactory receptor gene expression, axonal connectivity, and function. However, in teleost fish, all olfactory receptor (OR) families share a common sensory surface. To what extent such differences influence the coding and discrimination abilities of the respective olfactory systems is unclear, and the evolutionary path toward such segregation is unknown. The analysis of amphibians, which are early diverging tetrapods compared with mammals, may shed light on this transition from shared sensory surface to segregated subsystems. Most amphibians already possess an accessory olfactory epithelium (1), the vomeronasal organ (VNO), which has been reported to express type 2 vomeronasal receptors (V2Rs), like the mammalian VNO (2), but in contrast to the latter is missing the type 1 vomeronasal receptors (V1Rs) that are instead expressed in the main olfactory epithelium (MOE) (3). These features suggest an intermediate expression pattern for olfactory receptor gene families in amphibians.

The MOE of both fish and mammalian species exhibits further subdivisions into distinct expression zones and domains (4, 5), and an initial analysis of the amphibian MOE has shown medial-to-lateral gradients of odor responses and corresponding gradients for expression of olfactory receptor genes (6). In that study, however, no candidate genes except one could be uncovered for responses to amino acids, one of the main odor groups for aquatic vertebrates. Because a fish *v2r* ortholog has been shown to respond to amino acids (7), we hypothesized that amphibian *v2r* genes could be candidates for amino acid detection. At first glance this may appear unlikely because all previously analyzed *v2r* genes are almost exclusively expressed in the VNO, with the exception of occasional rare cells in the larval and adult MOE (2). However, the amphibian *v2r* family is exceedingly large, with several hundred members in *Xenopus tropicalis* (8), and analysis of expression patterns has so far not been guided by phylogenetic considerations.

We have cloned several *v2r* genes not previously analyzed and representative of the three major phylogenetic subdivisions of the *v2r* family A as well as the single member of family C. We report here that family C is expressed exclusively in the MOE, together with earlier diverging members of family A, whereas later diverging family A genes are restricted to the VNO. Such a bimodal expression pattern in MOE and VNO has not been described in any species so far, and represents a noteworthy evolutionary intermediate between expression restricted to either the MOE or the VNO. Within the MOE, *Xenopus v2r* genes are expressed in at least two distinct basal expression zones, which overlap extensively with amino acid responses, but are clearly distinguishable from an apical expression domain containing receptors, transduction pathways, and odor responses associated with ciliated olfactory receptor neurons (ORNs) (6).

Results

RT-PCR Analysis Shows Segregation of the Amphibian V2R Family into MOE-Specific and VNO-Specific Genes. Though ~20 *Xenopus laevis v2r* genes have been cloned previously (2), their position in the phylogenetic tree has not been reported, and a systematic analysis of the *X. laevis v2r* family has not been possible due to the absence of a genome project. However, over 330 *v2r* genes have been identified in the genome of the closely related species *X. tropicalis*, the largest known *v2r* family (8). In the phylogenetic analysis using the same data set as Ji et al. (8), the presence of three major subgroups is apparent (Fig. 1), all of which belong to family A. We have selected five representative *v2r* genes (Fig. 1) from two of these groups, as well as Xl-*v2r-C*, the sole member of family C in *Xenopus*, and cloned their *X. laevis* counterparts by RT-PCR using primers derived from the *X. tropicalis* sequence. A gene representative of the third subgroup, x*v2r E-1*, had already been obtained previously (6). In all cases, we obtained *X. laevis* sequences that in BLAST searches (http://blast.ncbi.nlm.nih.gov/) showed the initially considered *X. tropicalis* gene as the closest ortholog. Though we have no way to measure how many *X. laevis v2r*s might cross-react with probes derived from our

Author contributions: A.S.S., I.M., and S.I.K. designed research; A.S.S., A.S., and S.I.K. performed research; W.N. contributed analytic tools; A.S.S., A.S., W.N., I.M., and S.I.K. analyzed data; and A.S.S., I.M., and S.I.K. wrote the paper.

The authors declare no conflict of interest.

This article is a PNAS Direct Submission.

Data deposition: The sequences reported in this paper have been deposited in the European Nucleotide Archive, www.ebi.ac.uk/ena/data/view/HF937211-HF937216 (accession nos. HF937211–HF937216).

[1]To whom correspondence should be addressed. E-mail: sigrun.korsching@uni-koeln.de.

This article contains supporting information online at www.pnas.org/lookup/suppl/doi:10.1073/pnas.1302088110/-/DCSupplemental.

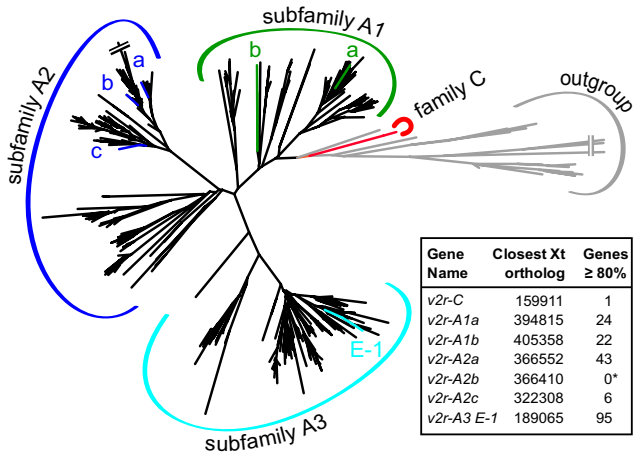

Gene Name	Closest Xt ortholog	Genes ≥ 80%
v2r-C	159911	1
v2r-A1a	394815	24
v2r-A1b	405358	22
v2r-A2a	366552	43
v2r-A2b	366410	0*
v2r-A2c	322308	6
v2r-A3 E-1	189065	95

Fig. 1. A phylogenetic tree of the *X. tropicalis* V2R repertoire was generated by a modified maximum-likelihood method (aLRT-ML). Colored branches refer to the nearest *X. tropicalis* orthologs of cloned *X. laevis* genes analyzed here. Note that amphibian *v2r-C* is a single gene, orthologous to the mammalian V2R-C family (8). (*Inset*) *X. laevis* genes analyzed here, as well as their closest orthologs in *X. tropicalis* and an estimate for the number of cross-reacting *v2r* genes (≥80% amino acid sequence identity to the *X. laevis* clones). *No close ortholog of *v2r-A2b* in *X. tropicalis*. Accession numbers have been deposited with the European Nucleotide Archive.

clones, we estimate from the sequence comparison with the *X. tropicalis v2r* repertoire that between 1 and 95 genes show ≥80% identity to our probes (Fig. 1). In total we expect our probes to sample the expression of at least half of the *X. laevis v2r* gene repertoire.

We performed RT-PCR of larval *X. laevis* tissues to analyze the tissue specificity of expression for the six representative *v2r* genes described above. As control for dissection accuracy of the closely neighboring VNO and MOE tissues, we examined the distribution of olfactory marker protein 2 (*omp2*), which in larval *X. laevis* is expressed exclusively in the MOE (9). An *omp2* band was absent from the VNO and only observed in the MOE (Fig. 2*A*), confirming the accuracy of the dissection. Three of the six genes were expressed in the VNO, with clear RT-PCR signals reproducibly found in the VNO, and signals absent from the MOE and other organs, such as brain and heart (Fig. 2*A*). Occasionally, weak or very weak bands were observed in other organs. This expression pattern is consistent with expectations from previous analysis for other *v2r* genes (2, 6).

For three other *v2r* genes, however, we found a highly unexpected result. We observed strong bands for the MOE, but none or occasionally very faint bands for the other tissues (Fig. 2*A*). Thus, *v2r* genes *v2r-C*, *v2r-A1a*, and *v2r-A1b* (and those genes cross-reacting with the corresponding probes) show a highly specific expression in the MOE, and are absent from the VNO and other organs. To the best of our knowledge, it is without precedent that major groups of a large olfactory receptor family are expressed in two different olfactory organs such as the VNO and the MOE. We therefore decided to analyze this highly unusual expression pattern at the cellular level by performing in situ hybridization.

Receptor Neurons in the MOE Express Early Diverging *v2r* Genes, but Vomeronasal Neurons Express Late Diverging *v2r* Genes. Expression of all *v2r* genes was examined by in situ hybridization of larval *X. laevis* tissue sections encompassing both VNO and MOE. Three of the genes, *v2r-A2a*, *v2r-A2b*, and *v2r-A2c*, are expressed exclusively in the VNO (Fig. 2), confirming results obtained by RT-PCR. These probes label sparse populations of cells, consistent with limited cross-reactivity to only a handful of other genes for each probe (Fig. 1). Of several hundred cells examined, a single labeled cell was detected in the MOE (Fig. 2), making the restriction of these genes to the VNO as stringent as that of the previously analyzed x*v2r E-1* (2, 6), which we include here for comparison (Fig. 2).

However, the three other *v2r* genes, *v2r-C*, *v2r-A1a*, and *v2r-A1b*, exhibit a strikingly different pattern of expression. We could not detect a single cell in the VNO for any of the three genes (Fig. 2). In contrast, all three genes show a strong expression in the MOE (Figs. 2 and 3), confirming our results obtained by RT-

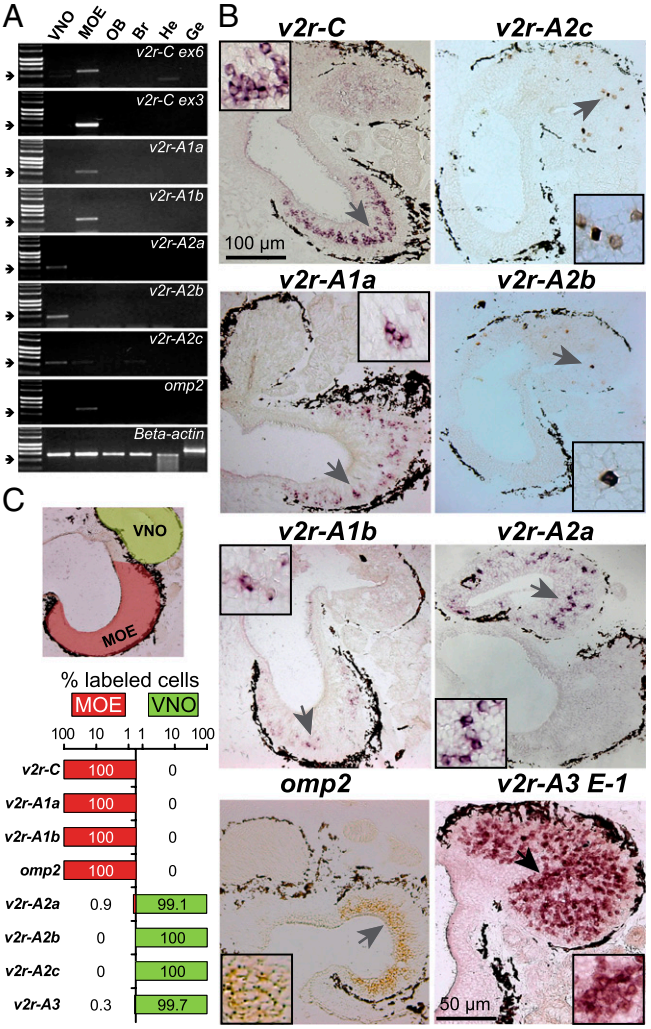

Fig. 2. Bimodal expression for the V2R family in MOE and VNO. (*A*) RT-PCR (40 cycles) was performed under stringent conditions; specificity does not change at higher cycle numbers. Lanes from left to right: VNO, MOE, olfactory bulb, brain, heart, and genomic DNA (in *Bottom* panel only). A β-actin intron-spanning probe was used as control for absence of genomic DNA contamination (*Bottom*). Arrows, 400-bp bands of molecular weight marker. (*B*) Cryosections of larval *X. laevis* were hybridized with antisense probes for seven *v2r* genes and *omp2* as depicted. Note the bimodal expression of *v2r* genes in either MOE (*Left*) or VNO (*Right*). Micrographs shown are from ventral horizontal sections of larval head tissue, which contain both VNO and MOE. VNO is above and/or to the right of the MOE, see also the colored overlay in *C*. Most probes cross-react with several to many other genes (Fig. 1), resulting in higher abundance of labeled cells. Scale bar for *v2r-C* valid for all panels except *v2r-A3 E1*. (*C*) Percentage of *v2r*-expressing cells in MOE (red bars) and VNO (green bars). Axis is shown on top; note the logarithmic scale. Over 100 to 350 cells (corresponding to 1–10 tissue sections) were analyzed per gene. For MOE-specific *v2r* genes, not a single cell was observed in the VNO, whereas very rare exceptions (2 of 677 cells) were seen for VNO-specific *v2r* genes.

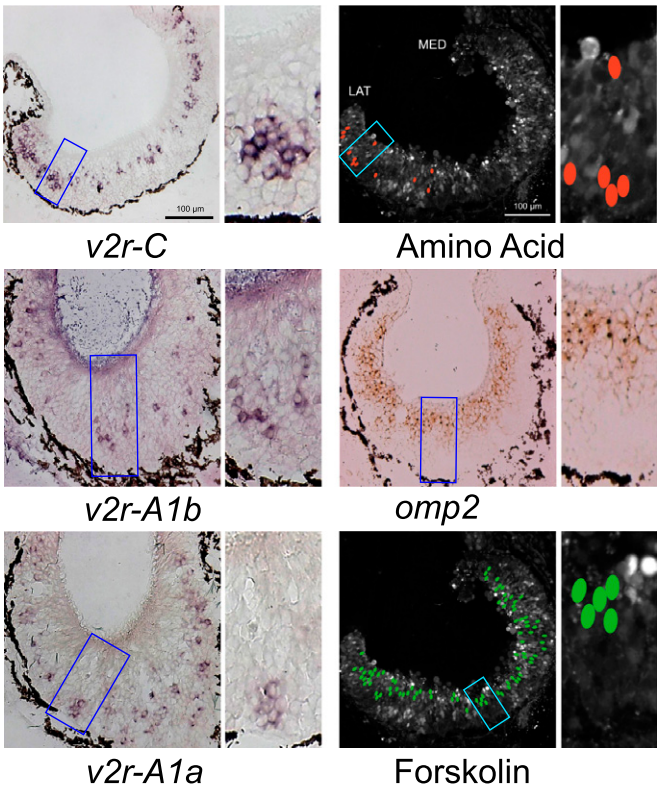

Fig. 3. A basal zone of the MOE is dedicated to *v2r* gene expression. In situ hybridization was performed for the three MOE-specific *v2r* genes and *omp2* using dorsal horizontal sections of larval head tissue. Enlargements from regions delineated by blue or cyan rectangles are shown to the right of each complete section. A ring of dark brown melanophores delineates the basal border of the epithelium; apical is toward the lumen. All *v2r* genes are enriched basally, whereas *omp2*-expressing cells are preferentially localized in an apical region. Forskolin- and amino acid-responsive cells were identified by calcium imaging (green and red ovals, respectively). Forskolin-responsive cells are apically enriched, very similar to *omp2*-expressing cells, whereas amino acid-responsive cells show a preferentially basal location.

PCR (Fig. 2*A*). Cell numbers for *v2r-A1a* and *v2r-A1b* are well above those expected for a single gene, but roughly consistent with our estimate of over 20 cross-reacting *v2r* genes for each (Fig. 1). The *v2r-C* probe is not expected to cross-react with other genes, but nevertheless labels an even larger population of cells (Fig. 2), similar to the broad expression of genes in the orthologous mammalian family (10). Thus, the MOE-specific *v2r* genes constitute a sizable group of the V2R repertoire and are expressed in a major neuronal population of the MOE.

For all seven *v2r* genes analyzed, a strong correlation is found between ancestrality in the phylogenetic tree and ancestrality in the mode of expression. All *v2r* genes with MOE-restricted expression reside in the earlier diverging subgroup A1 of family A or in family C (*v2r*-C), which is even less derived than the V2R-A1 subgroup (Fig. 1). In contrast, all *v2r* genes belonging to the later diverging subgroups A2 or A3 of family A (Figs. 1 and 2) are expressed exclusively in the VNO. In other words, more ancestral (earlier diverging) *v2r* genes of *X. laevis* are expressed in the more ancestral mode (in the MOE), like all the *v2r* genes of earlier diverging vertebrates, such as teleost fish. Complementarily, the more modern expression mode for *v2r* genes (expression in the VNO), is found for the more modern (later diverging) *v2r* genes among the amphibian *v2r* gene repertoire. This surprising correlation of phylogenetic position with expression mode is consistent with the notion that the transition from ancestral to derived mode of expression is a characteristic feature of later diverging *X. laevis v2r* genes.

MOE-Specific *v2r* Genes Are Expressed in a Basal Crescent. When examining results of in situ hybridization we noticed that the distribution of v2r-expressing cells within the MOE did not appear to be homogeneous. Both the apical and the basal region of the MOE are mostly devoid of labeled cells, and this feature of the distribution is constant over a wide range of dorsal/ventral locations, as seen by the comparison of more ventral (Fig. 2) with more dorsal sections (Fig. 3), although the latter contain up to 10-fold more cells. It is known that the basal layer contains progenitor cells and immature neurons (11), which could explain the dearth of *v2r*-expressing cells in this region. However, no such argument can be made for the near absence in apical regions, because nonneuronal supporting cells constitute just the outermost monolayer of cells (11, 12). Indeed, *omp2* expression is prominent in the apical region, and cells expressing trace amine-associated receptor 4a are also found in apical positions (Figs. 2 and 4). Albeit very distinct, V2R and OMP distributions are partially overlapping. Therefore, we performed quantitative analysis to examine the significance of the observed differences in the distributions.

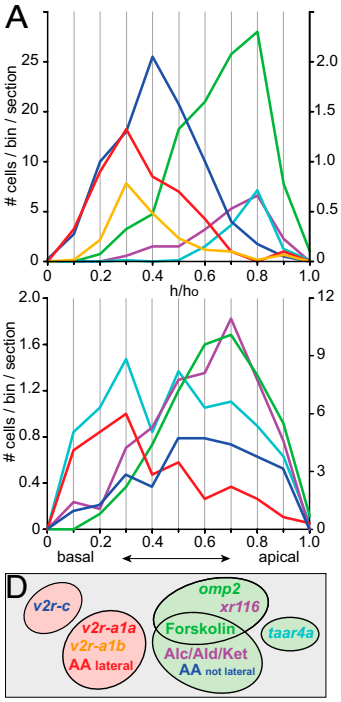

B Gene / odor	peak (h/ho)	half-width	median (h/ho)	skewness
v2r-A1a	0.3	0.216	0.333	0.885
v2r-A1b	0.3	0.182	0.353	1.277
v2r-C	0.4	0.233	0.418	0.209
omp2	0.8	0.224	0.688	-0.527
xr116	0.8	0.201	0.710	-0.778
taar4a	0.8	0.099	0.774	-1.343
AA	0.3, 0.5	0.433	0.483	0.143
AA lateral	0.3	0.325	0.315	0.716
AA not lateral	0.6	0.300	0.590	-0.257
Alc/Ald/Ket	0.7	0.271	0.629	-0.460
Forskolin	0.7	0.280	0.652	-0.300

C Gene/odor	gene/odor	p value
v2r-A1a	*v2r-A1b*	0.039
v2r-A1a	*v2r-C*	0.00002
v2r-A1b	*v2r-C*	0.0033
v2r-C	*omp2*	<0.00001
omp2	*xr116*	0.37
omp2	*taar4a*	<0.000001
Forskolin	Alc/Ald/Ket	0.0235
AA	Alc/Ald/Ket	0.00017
AA lateral	AA not lateral	0.000002
Forskolin	AA not lateral	0.041
AA lateral	*v2r-A1a*	0.132
AA lateral	*v2r-C*	0.00052
AA not lateral	*omp2*	0.001
Forskolin	*omp2*	0.0301
Alc/Ald/Ket	*omp2*	0.0016

Fig. 4. Basal-to-apical distributions were quantified for olfactory receptor genes and odor responses. (*A*) Receptor gene (*Upper*) and odor response (*Lower*) distributions are shown as histogram of relative height (0, most basal; 1, most apical position; bin size 0.1, bin center is shown). (*Upper*) *v2r-A1a* (red) and *v2r-A1b* (yellow) are centered basally; *v2r-C* (blue) encompasses both *v2r*-A1 receptors. *Omp2* (green), *xr116* (magenta, an *or* gene), and *taar4a* (cyan) are centered apically. Right *y* axis, *xr116*, and *taar4a*; left *y* axis, all others. (*Lower*) Forskolin (green), alcohol, aldehydes, and ketone responses (magenta) are centered apically, whereas amino acid responses (cyan) show a bimodal distribution (lateral, red; nonlateral, blue; Fig. S1). Right *y* axis, forskolin responses; left *y* axis, all others. (*B*) Characteristic parameters for the distributions shown in *A*. (*C*) Pairwise comparisons of different genes and/or odor responses were performed using the Kolmogorov–Smirnov test of the unbinned distributions. Distributions were considered significantly different for $P < 0.01$. (*D*) Venn diagram of differences between distributions. Entries within one circle share the same distribution; circles not overlapping correspond to different distributions. Note that the colors in *B*, *C*, and *D* correspond to those in *A* for receptors and odor responses, respectively.

Basal Expression Zone of MOE-Specific *v2r* Genes Is Significantly Different from an Apical Expression Zone for OMP2, OR, and Trace Amine-Associated Receptors. We used relative height (Fig. S1) as measure for the basal-to-apical dimension and evaluated 100–400 cells per gene. All three *v2r* genes showed a basal peak of expression, and their distributions appeared roughly similar to each other, as judged by peak position, median value, and skewness (Fig. 4 *A* and *B*). In contrast, the distribution of *omp2*-expressing cells was centered apically, had a much higher median value, and opposite sign skewness (Fig. 4 *A* and *B*). These features were shared by the distributions of two olfactory receptor genes, *xr116* (OR class I) and *taar4a*, albeit their cell density was only 1–2% of that of *omp2*.

In pairwise comparisons using the Kolmogorov–Smirnov test (13) we found that the apical-centered distribution of class I OR XR116 is highly similar to that of OMP2, whereas the apical-centered *taar4a* distribution is significantly different (Fig. 4*C*), suggesting further subdivisions within an apical expression zone defined by *omp2* expression.

Distributions of the basal-centered three MOE-specific *v2r* genes (*v2r-C*, *v2r-A1a*, and *v2r-A1b*) were significantly different from the apical-centered *omp2* (Fig. 4*C*; Table S1) and thus define a basal expression zone. Distributions for the two members of subgroup A1 are very similar to each other (Fig. 4*C*), but both are different from the V2R-C distribution (Fig. 4*C*; $P < 0.01$), which is slightly more broad, and whose median and peak values lie somewhat more apical (Fig. 4*B*). Thus, the expression zone defined by *v2r-C* may enclose *v2r-A1a* and *v2r-A1b* expression at its basal side, and other yet-to-be-identified *v2r* genes at its apical side. Together, the three MOE-specific *v2r* genes constitute a basal expression zone in the MOE, distinct from the apical expression zone of *omp2*-expressing neurons (Fig. 4 *A*–*D*).

A medial-to-lateral gradient perpendicular to the apical-to-basal gradient described here (Fig. 5) was identified in a previous study (6) for several genes and odor responses. Preferred positions in both dimensions do not appear to be correlated (apical and lateral preference for TAAR4a vs. apical and medial for XR116). To analyze a possible interdependence between preferred positions on both axes more rigorously, we compared for all genes height distributions for medial, intermediate, and lateral segments. We report that height distributions in all three segments are indistinguishable for each of the three *v2r* genes, as well as for *omp2*, *xr116*, and *taar4a* (Fig. S1; Table S2). Furthermore, all three *v2r* genes and *omp2* do not show enrichment or depletion along the medial-to-lateral axis (Table S3; Fig. 5), unlike *xr116* and *taar4a* (6). Taken together, these data are consistent with the hypothesis that preferred positions in each dimension are specified independently.

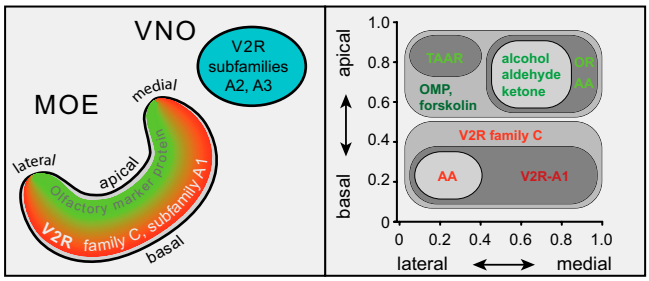

Fig. 5. Bimodal and zonal topology of *v2r* gene expression and odor responses. (*Left*) Complementary expression of two groups of *v2r* genes in MOE (*v2r-C* and two *v2r-A1* genes) and VNO (*v2r-A2* and *v2r-A3* genes). Within the MOE, gradients of expression frequency are observed. A basal zone (red) contains the *v2r* genes, whereas an apical zone (green) contains OMP2 as well as an odorant receptor; forskolin; and alcohol, aldehyde, and ketone responses (not depicted). (*Right*) A 2D schematic representation of the center region of each odor response and gene expression analyzed. Amino acid responses are heterogeneous, basal in the lateral segment, but apical in the intermediate and medial regions. In all, multiple subdivisions are observed, resulting in a highly complex pattern.

Amino Acid Responses Show a Bimodal (Apical and Basal) Distribution, Whereas Forskolin Responses Are Restricted to an Apical Zone. This independence of preferred positions in the two dimensions allows us to test the tentative assignment of receptor gene families to odor responses, which we derived from the correlations between receptor expression and odor responses in the medial-to-lateral dimension (6). We had concluded that ciliated receptor neurons may express class II *or* and some class I *or* genes and respond to alcohols, aldehydes, and ketones, and had found a single gene, *taar4a*, with an expression pattern correlating to amino acid responses. These two odor responses segregate nearly completely (6), thus defining the medial and lateral stream of odor processing, and were chosen here together with forskolin, an activator of adenylate cyclase (6), for analysis of basal-to-apical distribution.

Responses were measured as calcium signals using a previously established imaging method (14). Forskolin-responding cells were situated preferentially apically (Fig. 3), very similar to responses to alcohols, aldehydes, and ketones. Indeed, these two distributions did not differ significantly in the basal-to-apical dimension (Fig. 4*C*), suggesting that responses to these odors may be carried mostly by forskolin-responsive ORNs, i.e., ciliated neurons (15). Interestingly, responses to the mixture of alcohols, aldehydes, and ketones are more restricted than those to forskolin in the other, the medial-to-lateral, dimension (Fig. S1; Table S3), suggesting that the former may represent a spatially restricted subpopulation of the latter.

Unexpectedly, amino acid stimuli evoked responses in basal as well as apical cells, resulting in a broad and bimodal distribution (Fig. 4 *A* and *B*; Tables S1 and S2), significantly different from all other genes and odor responses (Fig. 4*C*; Tables S1 and S2). This finding might be explainable by a heterogeneous population of amino acid-responsive cells, because the sum over two different distributions would result in two peaks and increased half-width. To test this assumption, we examined the apical-to-basal distribution of amino acid responses separately for the three subregions (medial, intermediate, and lateral) defined previously (6). Lateral cells show a basal distribution, whereas nonlateral (intermediate and medial) cells exhibit a preferentially apical localization (Figs. 4 *A* and *B* and 5; Fig. S1), significantly different from the distribution of basal cells, but very similar to forskolin responses (Fig. 4*C*). Moreover, median values are distinctly different for the lateral and the nonlateral population, and in particular half-width for both is much smaller than for the total population (Fig. 4*B*). These data provide evidence for two distinct amino acid response systems of similar abundance (Fig. 4*A*; Table S3) (6), one centered basolaterally, the other one apical and nonlateral. In comparison, the apical-to-basal distributions of forskolin responses in medial, intermediate, and lateral segments are very similar in all quantitative parameters (Fig. S1; Table S2), consistent with cells in all three segments belonging to the same population.

Two *v2r*-A Genes Define Subregions in the V2R Expression Zone Similar to Those of Lateral Amino Acid-Responsive Cells. Amino acids constitute one of the main classes of odor stimuli for aquatic vertebrates (16). TAAR4a emerged as a candidate receptor in a previous study (6) due to the remarkable similarity of its medial-to-lateral distribution to that of amino acid-responsive cells. However, in the apical-to-basal dimension the correlation of TAAR4a expression with amino acid responses breaks down, because TAAR4a is found in the apical expression zone throughout medial, intermediate, and lateral segments, whereas amino acid responses are localized basally in the lateral zone and apically in the nonlateral segments (see above). These results directly exclude an involvement of TAAR4a in the basolateral amino acid response, and also make an involvement in the apical and nonlateral amino acid response unlikely, because the TAAR4a expression zone is

CELL BIOLOGY

not restricted in the medial-to-lateral dimension in contrast to the laterally depleted apical amino acid response. Because the spatial distribution of a receptor is not expected to be broader than that of an odor response based on that receptor, we conclude that TAAR4a does not seem to be involved in either the basal or the apical amino acid response.

For comparison, the distribution of forskolin responses is similar to that of *xr116*, a *class I or* gene, in the medial-to-lateral dimension (6) as well as the apical-to-basal dimension (Fig. 4). Here the analysis of height supports the hypothesis formed by analysis of the medial-to-lateral distributions.

We show in this study the expression of a major population of *v2r* genes in the MOE. The large size of this receptor repertoire and the response of a fish V2R homolog to amino acids (7) as well as the expression of *v2r* genes in fish microvillous receptor neurons, which do respond to amino acids (17), led us to hypothesize that amphibian V2Rs could be candidates for amino acid detection. Indeed the apical-to-basal distribution of amino acid responses in the lateral region (Fig. 4) is very similar to that of *v2r-A1a* and *v2r-A1b* gene expression (Fig. 4; Table S2). However, *v2r-A1a* and *v2r-A1b* show no lateral enrichment (Fig. S1 and Table S3) and are therefore unlikely to be involved in the basolateral amino acid response. Other members of the V2R-A1 subfamily would appear to be the best candidates for mediating *Xenopus* amino acid responses.

Discussion

The most striking property of *Xenopus v2r* gene expression is the segregation of the family in MOE-expressing and VNO-expressing members, with the segregation apparently occurring according to phylogenetic distance. Earlier-diverging (more ancestral) genes are expressed exclusively in the MOE and later-diverging (more modern) genes are restricted to the VNO. This segregated expression pattern might be rather ancestral in the lineage of tetrapods, because lungfish express the V2R-correlated G protein Go both in their MOE and their vomeronasal primordia (18). However, a salamander, a later-diverging amphibian species compared with *Xenopus*, shows already the mammalian-like VNO-specific V2R and associated marker gene expression (19). Thus, VNO-restricted expression may have arisen more than once in later-diverging tetrapods, possibly each time during the transition to a terrestrial lifestyle and reflecting the concomitant restricted access of nonvolatile odors to the VNO in these species.

The three v2r genes analyzed here, *v2r*-C, *v2r-A1a*, and *v2r-A1b*, represent a major population of *v2r*-expressing olfactory neurons and a sizable part of the total *Xenopus v2r* repertoire, due to cross-reactivity. Moreover, MOE-specific expression was found in a large percentage (50%) of the *v2r* genes analyzed here. This pattern of expression is very different from the ectopic or broad expression of sporadic mammalian *or* and *v1r* genes (20, 21) and diametrically opposite to the very rare cells occasionally seen for more modern *v2r* genes of subgroup A2 and A3 both in larval MOE [this study and results by Hagino-Yamagish et al. (2)] and adult middle cavity (2), a subdivision of the MOE arising during metamorphosis (22). In fact, the restriction of the more ancestral *v2r* genes to the MOE is even stricter than that of the more modern *v2r* genes to the VNO, because we did not find a single exception in over 400 counted cells.

Furthermore, we show in the present study that within the MOE of *X. laevis*, *v2r* genes are expressed in a basal zone. In a quantitative analysis of the *v2r* distribution, it becomes obvious that there are no sharp borders of this basal zone. Instead, toward the apical region, a gradual decrease in frequency of expression is observed. This distinct, albeit broad distribution, is very reminiscent of similar distributions observed in the olfactory epithelium of teleost fish (4) and for some mammalian OR receptor genes (5).

The basal expression zone is defined by expression of *v2r-C* and is subdivided by the expression of *v2r-A1* genes. Such subdivisions have been reported for the expression of *v2r* genes in the mammalian VNO (23). It is remarkable that this vertical arrangement of zones and subzones may have survived the migration of *v2r* expression from the MOE to the VNO during the evolution of tetrapods. The mammalian *v2r-C*-orthologous family is coexpressed with other *v2r* genes (10, 24), and the *v2r-C* localization described here is consistent with an analogous role of the *Xenopus* V2R-C.

Within the apical zone, the *omp2* distribution is indistinguishable from the forskolin distribution, and an individual *or* gene (*xr116*) exhibits a scaled-down version of the same distribution. In contrast, the *taar4a* distribution, albeit apical as well, is significantly different and much narrower; it is unclear whether this is related to the diminutive size of the *taar* gene family in *Xenopus* (25). Thus, the apical domain, as well as the basal domain, appears to have further subdivisions, resulting in a complex picture of spatial regulation of olfactory receptor gene expression.

Interestingly, the apical-to-basal distribution of lateral amino acid-responsive cells fits closely to the *v2r-A1a* distribution, whereas the apical-to-basal distribution of intermediate and medial regions resembles the *omp2* distribution. Thus, amino acid-responsive cells appear to form a heterogeneous population. Amino acid-responsive ORNs are laterally enriched, as are markers for microvillous receptor neurons (6), and so the simplest explanation for the observed distributions would be that the observed amino acid responses are the sum of a lateral population of microvillous, *V2R*-expressing ORNs combined with a nonlateral population of ciliated, *omp2*-expressing ORNs; this would parallel previous observations of ciliated ORNs responding to amino acids in some fish species (26).

Combining all spatial expression patterns obtained in this and a preceding analysis (6) leads us to hypothesize two dimensions of gene segregation: a medial-to-lateral dimension (6) and an apical-to-basal dimension transversing the epithelial layer (this study). The coordinates in these two dimensions appear to be specified independently, because many different combinations of preferred positions are observed (Fig. 5). In both dimensions, distributions are broadly overlapping, but nevertheless distinctly identifiable by parameters such as half-width, median, and skewness, as well as by statistical tests (13, 27).

In sum, we identified a unique expression pattern for the amphibian *v2r* family in both MOE and VNO and found a particular domain of the MOE dedicated to *v2r* expression. Further study is required to elucidate the molecular mechanisms underlying the ontogenesis of such restricted expression patterns, which could involve either directed migration or regiospecific determination of neuronal cell fate within the MOE. Foremost, it will be exciting to reveal the differences between VNO-residing V2Rs and those expressed in the MOE, in terms of function and of expression regulation. The *Xenopus* olfactory system appears uniquely suited to analyze such questions.

Materials and Methods

Phylogenetic Analysis. The complete set of *X. tropicalis v2r* sequences (8) was aligned using MAFFT, version 6, and E-INS-i strategy with default parameters (http://align.bmr.kyushu-u.ac.jp/mafft/online/server/). Phylogenetic trees were constructed using a modified maximum-likelihood method, aLRT-PhyML (28), as implemented on the Phylemon2 Web server (http://phylemon.bioinfo.cipf.es/index.html). For the visualization of the phylogenetic tree, Phylodendron was used (http://iubio.bio.indiana.edu/treeapp/treeprint-form.html).

Animal Handling. All procedures for animal handling were carried out according to the guidelines of the Göttingen University Committee for Ethics in Animal Experimentation. Larval *X. laevis*, stages 50–54, staged after ref. 29, were cooled to produce complete immobility and killed by transection of the brain at its transition to the spinal cord.

Cloning. Nonambiguous primers were designed based on published sequence information or homologous sequences in *X. tropicalis* (Table S4). Conserved regions among mouse, fish, and frog *v2r-C* sequences were used to guide the choice of primers for *v2r-C*. For genes from the *v2r-A1* and *v2r-A2* subfamilies,

regions conserved within their respective subfamilies were chosen. Annealing temperatures between 55 °C and 58 °C were used with genomic DNA as template. Resulting fragment lengths varied from 200 to 500 bp. All fragments were cloned into pGEM-T (Promega) and later confirmed by sequencing.

RT-PCR. Total RNA was extracted from *X. laevis* tissues using the innuPREP DNA/RNA Mini Kit (Analytik Jena) and Omniscript Reverse Transcriptase (Qiagen) for first-strand cDNA synthesis. PCR primer and PCR conditions were as stated above.

In Situ Hybridization. Digoxigenin-labeled (DIG; Roche Molecular Biochemicals) RNA probes for in situ hybridization were prepared from the cloned DNA by using the same forward primers and reverse primers with a T3 promoter site attached to their 5′ end. For in situ hybridization, tissue blocks containing MOE and VNO were cut horizontally, fixed in 4% formaldehyde solution for 2 h at room temperature, equilibrated in 30% saccharose, and embedded in Jung tissue-freezing medium (Leica). Cryostat sections of 10–12 μm (Leica CM1900) were dried at 55 °C and postfixed in 4% (wt/vol) paraformaldehyde for 10–15 min at room temperature. Hybridizations were performed overnight at 60 °C using standard protocols [50% (vol/vol) formamide]. Anti-DIG primary antibody coupled to alkaline phosphatase and NBT (4-nitro blue tetrazolium chloride), BCIP (5-bromo-4-chloro-3-indolyl-phosphate) (NBT-BCIP) (both from Roche Molecular Biochemicals) were used for signal detection.

Calcium Imaging. Odor responses were measured as changes of intracellular calcium concentrations of individual ORNs in Vibratome slices of the olfactory organs using Fluo-4/AM as calcium indicator dye, essentially as described (12). Odorant stimuli [an amino acid mixture and a mixture of alcohols, aldehydes, and ketones (6)], and forskolin, an activator of adenylate cyclase and therefore the cAMP signaling pathway, were applied by gravity feed and used at 100 μM final concentration per compound (50 μM for forskolin). Minimum interstimulus interval was 2 min to avoid adaptation, and reproducibility of ORN responses was verified by repeating the application of each stimulus at least twice.

Fluorescence images of the whole MOE were acquired at 1 Hz (excitation at 488 nm; emission above 505 nm) using a laser-scanning confocal microscope (LSM 510/Axiovert 100 M; Zeiss) and analyzed using custom programs written in MATLAB (MathWorks). Active ORNs were identified as regions of high cross-correlation between the fluorescence signals of neighboring pixels (30). The diameter of such regions was typically 6–10 μm, consistent with these signals emanating from the somata of individual ORNs (14). Optical section thickness was chosen to ensure that observed signals originated from single cells. Ten images before the onset of stimulus application were taken as control (F_0). A response was considered significant if the first two fluorescence values after stimulus arrival at the mucosa, F_1 and F_2, were larger than the maximum of the F_0 values, and if F_2 was larger than F_1 (12).

Analysis of Spatial Distribution. The position of cells was evaluated in two dimensions perpendicular to each other, medial-to-lateral and basal-to-apical. Position in the first dimension was determined according to ref. 6, and in the second dimension by measuring the relative height of the cell, defined as distance of the cell soma center from the basal border of the epithelium divided by total thickness of the epithelial layer at the position of the cell ($h_{rel} = h_{cell}/h_{layer}$; Fig. S1). Cell positions were measured using ImageJ (http://rsbweb.nih.gov/ij/) and/or manually on printouts.

Median, skewness, and half-width of the resulting spatial distributions were calculated from unbinned values using Open Office (version 3.2; www.openoffice.org/). Half-width of a height distribution was defined as difference between the values for the upper quartile and the lower quartile. The peak value was taken from the graphical representation of the histograms. To estimate whether two spatial distributions were significantly different, we performed Kolmogorov–Smirnov tests on the unbinned distributions as described in ref. 13. This test is particularly suitable for continuous distributions and makes no assumptions about the nature of the distributions investigated, which is essential because the skewness of the observed distributions showed that these are not Gaussian. Due to the sensitive nature of the test on large distributions ($n > 100$), we selected $P < 0.01$ as cutoff criterion for significant difference. Results of the Kolmogorov–Smirnov test were confirmed by permutation analysis (27) without exception.

ACKNOWLEDGMENTS. Mehmet Saltürk and Shahrzad Bozorgnia kindly provided clones for two *v2r*. We are grateful to Evangelia Tantalaki for DNA and RNA extraction and cDNA synthesis. This work was supported by Deutsche Forschungsgemeinschaft (DFG) Schwerpunktprogramm 1392 (to I.M. and S.I.K.), and Cluster of Excellence and DFG Research Center Nanoscale Microscopy and Molecular Physiology of the Brain (I.M.).

1. Eisthen HL (1992) Phylogeny of the vomeronasal system and of receptor cell types in the olfactory and vomeronasal epithelia of vertebrates. *Microsc Res Tech* 23(1):1–21.
2. Hagino-Yamagishi K, et al. (2004) Expression of vomeronasal receptor genes in *Xenopus laevis*. *J Comp Neurol* 472(2):246–256.
3. Date-Ito A, Ohara H, Ichikawa M, Mori Y, Hagino-Yamagishi K (2008) *Xenopus* V1R vomeronasal receptor family is expressed in the main olfactory system. *Chem Senses* 33(4):339–346.
4. Weth F, Nadler W, Korsching S (1996) Nested expression domains for odorant receptors in zebrafish olfactory epithelium. *Proc Natl Acad Sci USA* 93(23):13321–13326.
5. Mori K, Sakano H (2011) How is the olfactory map formed and interpreted in the mammalian brain? *Annu Rev Neurosci* 34:467–499.
6. Gliem S, et al. (2012) Bimodal processing of olfactory information in an amphibian nose: Odor responses segregate into a medial and a lateral stream. *Cell Mol Life Sci*, 10.1007/s00018-012-1226-8.
7. Luu P, Acher F, Bertrand HO, Fan J, Ngai J (2004) Molecular determinants of ligand selectivity in a vertebrate odorant receptor. *J Neurosci* 24(45):10128–10137.
8. Ji Y, Zhang Z, Hu Y (2009) The repertoire of G-protein-coupled receptors in *Xenopus tropicalis*. *BMC Genomics* 10:263.
9. Kashiwagi A, et al. (2006) Stable knock-down of vomeronasal receptor genes in transgenic *Xenopus* tadpoles. *Biochem Biophys Res Commun* 345(1):140–147.
10. Martini S, Silvotti L, Shirazi A, Ryba NJ, Tirindelli R (2001) Co-expression of putative pheromone receptors in the sensory neurons of the vomeronasal organ. *J Neurosci* 21(3):843–848.
11. Hassenklöver T, Schwartz P, Schild D, Manzini I (2009) Purinergic signaling regulates cell proliferation of olfactory epithelium progenitors. *Stem Cells* 27(8):2022–2031.
12. Hassenklöver T, et al. (2008) Nucleotide-induced Ca2+ signaling in sustentacular supporting cells of the olfactory epithelium. *Glia* 56(15):1614–1624.
13. Press WH, Teukolsky SA, Vetterling WT, Flannery BP (1992) *Numerical Recipes in C: The Art of Scientific Computing* (Cambridge Univ Press, Cambridge, UK), Vol 2.
14. Manzini I, Schild D (2004) Classes and narrowing selectivity of olfactory receptor neurons of *Xenopus laevis* tadpoles. *J Gen Physiol* 123(2):99–107.
15. Munger SD, Leinders-Zufall T, Zufall F (2009) Subsystem organization of the mammalian sense of smell. *Annu Rev Physiol* 71:115–140.
16. Caprio J, Byrd RP, Jr. (1984) Electrophysiological evidence for acidic, basic, and neutral amino acid olfactory receptor sites in the catfish. *J Gen Physiol* 84(3):403–422.
17. Koide T, et al. (2009) Olfactory neural circuitry for attraction to amino acids revealed by transposon-mediated gene trap approach in zebrafish. *Proc Natl Acad Sci USA* 106(24):9884–9889.
18. Nakamuta S, Nakamuta N, Taniguchi K, Taniguchi K (2012) Histological and ultrastructural characteristics of the primordial vomeronasal organ in lungfish. *Anat Rec (Hoboken)* 295(3):481–491.
19. Kiemnec-Tyburczy KM, Woodley SK, Watts RA, Arnold SJ, Houck LD (2012) Expression of vomeronasal receptors and related signaling molecules in the nasal cavity of a caudate amphibian (*Plethodon shermani*). *Chem Senses* 37(4):335–346.
20. Feldmesser E, et al. (2006) Widespread ectopic expression of olfactory receptor genes. *BMC Genomics* 7:121.
21. Fleischer J, Breer H, Strotmann J (2009) Mammalian olfactory receptors. *Front Cell Neurosci* 3:9.
22. Hansen A, Reiss JO, Gentry CL, Burd GD (1998) Ultrastructure of the olfactory organ in the clawed frog, *Xenopus laevis*, during larval development and metamorphosis. *J Comp Neurol* 398(2):273–288.
23. Herrada G, Dulac C (1997) A novel family of putative pheromone receptors in mammals with a topographically organized and sexually dimorphic distribution. *Cell* 90(4):763–773.
24. Ishii T, Mombaerts P (2011) Coordinated coexpression of two vomeronasal receptor V2R genes per neuron in the mouse. *Mol Cell Neurosci* 46(2):397–408.
25. Hussain A, Saraiva LR, Korsching SI (2009) Positive Darwinian selection and the birth of an olfactory receptor clade in teleosts. *Proc Natl Acad Sci USA* 106(11):4313–4318.
26. Hansen A, et al. (2003) Correlation between olfactory receptor cell type and function in the channel catfish. *J Neurosci* 23(28):9328–9339.
27. Manly BFJ (1997) *Randomization, Bootstrap and Monte Carlo Methods in Biology* (Chapman & Hall/CRC, London).
28. Anisimova M, Gascuel O (2006) Approximate likelihood-ratio test for branches: A fast, accurate, and powerful alternative. *Syst Biol* 55(4):539–552.
29. Nieuwkoop PD, Faber J (1994) *Normal Table of Xenopus laevis (Daudin)* (Garland, New York).
30. Junek S, Chen TW, Alevra M, Schild D (2009) Activity correlation imaging: Visualizing function and structure of neuronal populations. *Biophys J* 96(9):3801–3809.

2.1.2 TRPC2 is EXPRESSED in TWO OLFACTORY SUBSYSTEMS

This section deals with the original research article published in the journal of Experimental Biology (Vol. 217, Pages 2235-2238, published online on April, 2014). Supplementary data associated with this article can be found in the CD attached.

© 2014. Published by The Company of Biologists Ltd | The Journal of Experimental Biology (2014) 217, 2235-2238 doi:10.1242/jeb.103465

SHORT COMMUNICATION

Trpc2 is expressed in two olfactory subsystems, the main and the vomeronasal system of larval *Xenopus laevis*

Alfredo Sansone[1,*], Adnan S. Syed[2,*], Evangelia Tantalaki[1,3], Sigrun I. Korsching[2] and Ivan Manzini[1,3,‡]

ABSTRACT

Complete segregation of the main olfactory epithelium (MOE) and the vomeronasal epithelium is first observed in amphibians. In contrast, teleost fishes possess a single olfactory surface, in which genetic components of the main and vomeronasal olfactory systems are intermingled. The transient receptor potential channel TRPC2, a marker of vomeronasal neurons, is present in the single fish sensory surface, but is already restricted to the vomeronasal epithelium in a terrestrial amphibian, the red-legged salamander (*Plethodon shermani*). Here we examined the localization of TRPC2 in an aquatic amphibian and cloned the *Xenopus laevis trpc2* gene. We show that it is expressed in both the MOE and the vomeronasal epithelium. This is the first description of a broad *trpc2* expression in the MOE of a tetrapod. The expression pattern of *trpc2* in the MOE is virtually undistinguishable from that of MOE-specific *v2rs*, indicating that they are co-expressed in the same neuronal subpopulation.

KEY WORDS: Amphibians, Olfactory organ, RT-PCR, *In situ* hybridization

INTRODUCTION

The organization of olfactory organs varies considerably across vertebrate species. Fishes generally possess a single olfactory organ (Hamdani and Døving, 2007). Clearly anatomically segregated main and vomeronasal olfactory systems first appeared in amphibians (Taniguchi et al., 2011), and persisted in most later diverging terrestrial vertebrates including rodents (Liberles, 2014). In rodents, the main and vomeronasal systems are separated anatomically, morphologically and molecularly. Their main olfactory epithelium (MOE) contains ciliated olfactory receptor neurons (ORNs) generally expressing OR-type olfactory receptors that are endowed with the canonical cAMP-mediated transduction pathway (Liberles, 2014). Their vomeronasal organ (VNO) contains two subpopulations of microvillous receptor neurons, either expressing vomeronasal type-1 receptors (V1Rs) and $G\alpha_i$, or vomeronasal type-2 receptors (V2Rs) and $G\alpha_o$. Recently, an additional subpopulation of sensory neurons expressing formyl peptide receptors has been identified (for a review, see Liberles, 2014). V1R- and V2R-expressing sensory neurons depend on a phospholipase C- and diacylglycerol-mediated transduction pathway that leads to activation of canonical transient receptor potential channel 2 (TRPC2), a cation channel crucial for signal transduction in the rodent VNO. In addition, some TRPC2-independent signaling pathways are also present in the rodent VNO (for a detailed review, see Liberles, 2014; and references therein). These VNO-specific genes were first identified in rodents, but later were also found in the olfactory system of teleost fishes (for a review, see Hamdani and Døving, 2007). VR-type olfactory receptors and TRPC2 are also present in earlier diverging fishes such as sharks and lampreys (Grus and Zhang, 2009), indicating that molecular components of the rodent VNO already existed in the common ancestor of all living vertebrates. Amphibians are early diverging tetrapods compared with rodents, represent a transitional stage in the evolution of the vomeronasal system, and may thus be crucial for understanding of the evolution of the vomeronasal system and its genetic components. On the one hand, they have an anatomically segregated vomeronasal system; on the other hand, at least in the mostly aquatic *Xenopus*, expression of vomeronasal receptors is not limited to the VNO. *V1rs* (Gliem et al., 2013) and more 'ancient', earlier diverging, *v2rs* (Syed et al., 2013) are exclusively expressed in the MOE. Also, the cellular composition of the *Xenopus* MOE is very similar to that of the single sensory epithelium of teleost fishes (Hamdani and Døving, 2007), as it contains ciliated as well as microvillous ORNs (Gliem et al., 2013). However, the *Xenopus* VNO is already very similar to that of rodents, in the sense that it is made up solely of microvillous receptor neurons, and that its cells express *v2rs*, $G\alpha_i$ and/or $G\alpha_o$ (Gliem et al., 2013). In the terrestrial salamander *Plethodon shermani*, a later diverging amphibian compared with *Xenopus*, all V2Rs and TRPC2 are already confined to the VNO (Kiemnec-Tyburczy et al., 2012).

Here we identified the *trpc2* gene of *Xenopus laevis* (Daudin 1802), and found that it is expressed in cells of both the larval MOE and VNO. This is the first description of a widespread *trpc2* expression in the MOE of a vertebrate also possessing a VNO. Furthermore, we show that the expression pattern of *trpc2* in the *Xenopus* MOE is virtually undistinguishable from that of a broadly expressed *v2r* gene, *v2r-C*, suggesting a co-expression in the same subset of cells.

RESULTS AND DISCUSSION

Trpc2 expression has so far not been reported in any anuran species, so we used RT-PCR to test whether the *trpc2* transcript is present in the olfactory organ of *X. laevis*. The *X. laevis* genome sequence is not available, and the *trpc2* gene sequence was not known. Therefore, we designed degenerate primers based on the *trpc2* sequence of *Xenopus tropicalis*, a species closely related to *X. laevis*. The primers were designed to target a highly conserved region among different vertebrate species (Fig. 1A). We then performed RT-PCR on the olfactory organ (MOE and VNO) of larval *X. laevis*

[1]Institute of Neurophysiology and Cellular Biophysics, University of Göttingen, Humboldtallee 23, 37073 Göttingen, Germany. [2]Institute of Genetics, University of Cologne, Zülpicher Strasse 47a, 50674 Cologne, Germany. [3]Center for Nanoscale Microscopy and Molecular Physiology of the Brain (CNMPB), 37073 Göttingen, Germany.
*Shared first authors

‡Author for correspondence (imanzin@gwdg.de)

Received 4 February 2014; Accepted 2 April 2014

The Journal of Experimental Biology (2014) doi:10.1242/jeb.103465

List of abbreviations

DIG	digoxigenin
MOE	main olfactory epithelium
ORN	olfactory receptor neuron
TRPC2	transient receptor potential channel 2
V1R	vomeronasal type-1 receptor
V2R	vomeronasal type-2 receptor
VNO	vomeronasal organ

and a 1402 bp fragment was isolated and sequenced (Fig. 1B). In BLAST searches, the obtained sequence (accession no. HG326501, European Nucleotide Archive) showed the *X. tropicalis* gene as the closest ortholog (90% nucleotide identity). A multi-species alignment (see supplementary material Fig. S1) showed a high degree of similarity between the *X. laevis trpc2* fragment and the sequence of diverse vertebrate species (identity: *Plethodon shermani* 78%, *Danio rerio* 72%, *Mus musculus* 72%, *Macropus eugenii* 72%). Next we analyzed the tissue specificity of the *trpc2* gene expression by performing RT-PCR with a second set of primers specific for the *X. laevis* sequence (see Materials and methods). Amplified products of the expected size were reproducibly found in the larval MOE and the VNO, whereas no signals were detected from the olfactory bulb and other organs, such as the brain, heart and eye (Fig. 1C). In a next step, the expression of *trpc2* was examined by *in situ* hybridization of larval *X. laevis* tissue sections encompassing both MOE and VNO. Numerous *trpc2*-positive cells were observed in the epithelia of both the MOE and the VNO (Fig. 2A). This bimodal expression in the two main olfactory organs is different from the situation in all other tetrapods examined so far. *Trpc2* expression in salamander (*Plethodon shermani*), the only non-mammalian tetrapod examined, is limited to the VNO (Kiemnec-Tyburczy et al., 2012), as in all mammals investigated so far (Liberles, 2014).

Xenopus laevis is also peculiar in that some *v2rs* are expressed in the MOE, whereas other *v2rs* are expressed in the VNO (Gliem et al., 2013; Syed et al., 2013). Thus, the TRPC2 distribution we report here parallels the distribution of V2Rs. In a terrestrial salamander, *v2r* expression is confined to the VNO, in other words, it again parallels the *trpc2* expression, which is also restricted to the VNO in this species (Kiemnec-Tyburczy et al., 2012). Such co-localization supports the hypothesis that TRPC2 is involved in V2R signal transduction.

To obtain a more stringent criterion of co-localization, we examined the relative height (in basal-to-apical direction) of cells expressing *trpc2*. This parameter shows a distinct, non-random distribution for cells expressing *v2rs* in the MOE of *Xenopus laevis* (Syed et al., 2013) (see also Fig. 2B). Evaluation of more than 300 *trpc2*-expressing cells showed that the *trpc2* gene is expressed in a distinct zone of the MOE that closely resembles the expression zone of *v2r* genes, particularly *v2r-C* (Fig. 2C,D), determined in earlier work of our group (Syed et al., 2013). In fact, the epithelial distribution of *trpc2* and *v2r-C* is almost identical, as judged by peak position, half-width, median value and skewness (Fig. 2D). Similar to *v2rs* (Syed et al., 2013), the medial-to-lateral distribution of *trpc2*-positive cells within the MOE was uniform with no tendency for lateralization (not shown). Together, these results lead to the hypothesis that in *Xenopus*, TRPC2 and V2Rs might be present in the same subpopulation of cells.

Recent work of our group showed that a large subpopulation of amino acid odor-sensitive microvillous ORNs of the *Xenopus* MOE has a phospholipase C- and diacylglycerol-mediated transduction pathway that may couple to TRPC2 (Gliem et al., 2013; Sansone et al., 2014). Microvillous ORNs in the single sensory surface of fishes are also known to be sensitive to amino acid odors and to express *v2rs* and *trpc2* (Sato et al., 2005). In fact, two fish V2Rs, OlfCa1 and OlfCc1, have been shown to be sensitive to amino acid odors (DeMaria et al., 2013; and references therein). Together, these data suggest that in *Xenopus*, TRPC2 could be involved in mediating the amino acid response of V2Rs, similar to the situation in fishes. Further investigations will be necessary to substantiate this hypothesis.

Our results strengthen the general concept that sensory neurons expressing *v2rs* and *trpc2* may be connected to the detection of non-volatile odors. In fully terrestrial vertebrates (Liberles, 2014), including a terrestrial salamander (Kiemnec-Tyburczy et al., 2012), vomeronasal receptors and *trpc2* are solely expressed in the sensory neurons of the VNO, mainly specialized for the detection of large non-volatile molecules. In contrast, in teleost fishes, vomeronasal receptors and *trpc2* are expressed in the single sensory epithelium (Sato et al., 2005; Hamdani and Døving, 2007). In the fully aquatic larvae of *X. laevis*, vomeronasal receptors (Gliem et al., 2013; Syed et al., 2013) and *trpc2* (present study) are expressed in both the MOE and VNO. It will be interesting to see whether the correlation of sensory neurons expressing vomeronasal receptors and *trpc2* for non-volatile odors holds up in adult *X. laevis*, in which the larval MOE has metamorphosed into an air nose and a new adult water nose has emerged.

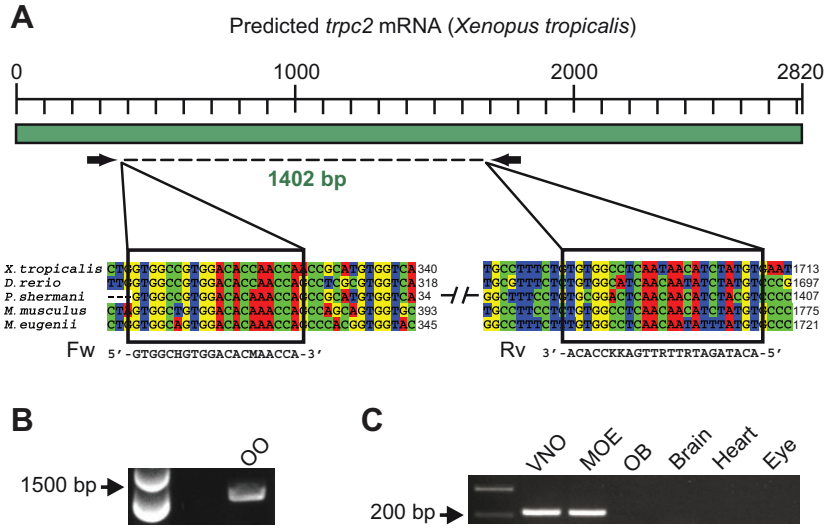

Fig. 1. Cloning of *trpc2* and analysis of tissue-specific expression. (A) Schematic representation of the predicted *trpc2* transcript of *Xenopus tropicalis* and degenerate primers used for the PCR shown in B. Two fragments of the *trpc2* multi-species alignment are shown below. The black boxes highlight the conserved regions chosen to design the degenerate primers. (B) Touchdown RT-PCR with degenerate primers (see A). An amplification product of 1402 bp was detected in the olfactory organ (OO) including both the main olfactory epithelium (MOE) and the vomeronasal organ (VNO). The obtained fragment was sequenced, and in BLAST searches (http://blast.ncbi.nlm.nih.gov/) gave the best score with the predicted *X. tropicalis trpc2* sequence (90% nucleotide identity). (C) For analysis of tissue specificity, an RT-PCR (35 cycles) for *trpc2* was performed with specific primers (see Materials and methods) under stringent conditions. OB, olfactory bulb. An amplification product of the expected size was detected in the VNO and MOE, whereas no signal was detected from other organs.

The Journal of Experimental Biology (2014) doi:10.1242/jeb.103465

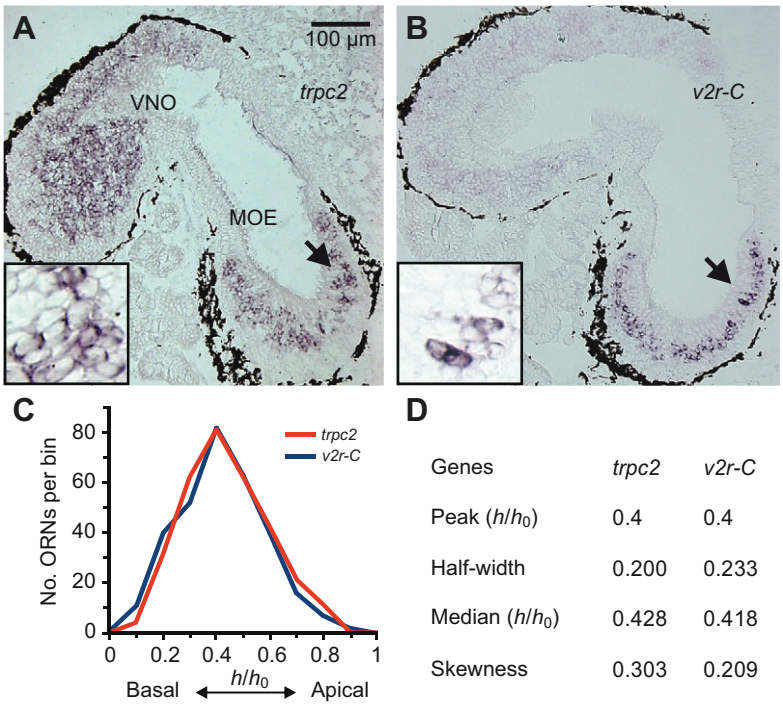

Fig. 2. Distribution of *trpc2*-positive cells closely mimics that of *v2r-C*-expressing cells in the MOE. (A) Cryosections of larval *Xenopus laevis* were hybridized with antisense probes for the *trpc2* gene. The micrograph shown is from a horizontal section of larval head tissue, which contains both the MOE and the VNO. A zone of *trpc2*-positive cells was detected in the MOE and widespread labeling was visible in the VNO. The arrow is pointing at the region enlarged in the inset. (B) Cryosections of larval head tissue were hybridized with antisense probes for the *v2r-C* gene. Orientation and region as explained in A. Consistent with previous results (see Syed et al., 2013), *v2r-C*-positive cells were only found in the MOE, and occupy a discrete zone there. The arrow is pointing at the region enlarged in the inset. (C) Basal-to-apical distribution (0, most basal; 1, most apical position) of *trpc2* (314 cells, 5 sections) and *v2r-C*-expressing cells [data taken from Syed et al. (Syed et al., 2013) and shown here for comparison]. Data are given as mid-bin values (0.1 bin size); *y*-axis shows total number of cells per bin. (D) Characteristic parameters for the distribution of *trpc2*-expressing cells; values for *v2r-C* taken from our earlier work (Syed et al., 2013) are shown for comparison.

Certainly the results of the present study add to growing evidence that the olfactory regionalization in *X. laevis*, and very likely also in other aquatic amphibians, is still incomplete. They possess an anatomically segregated vomeronasal system, but their main olfactory system is still very similar to that of teleost fishes, including cellular and genetic components that are already confined to the VNO in fully terrestrial vertebrates. This intermediate segregation of the *Xenopus* olfactory system results in an excellent model system to study the molecular driving forces governing the evolution of the vertebrate olfactory system.

MATERIALS AND METHODS

cDNA synthesis and PCR

Larvae of *X. laevis* (of either sex, stages 50 to 54) were cooled in iced water to produce complete immobility and killed by transection of the brain at its transition to the spinal cord, as approved by the Göttingen University Committee for Ethics in Animal Experimentation. Tissue samples from the VNO, MOE, olfactory bulb, brain, heart and eye were isolated and flash frozen until nucleic acid extraction. Genomic DNA and total RNA were extracted using the innuPREP DNA/RNA Mini Kit (Analytik Jena, Jena, Germany). Purity and quantity of RNA were measured using a NanoPhotometer (Implen, Munich, Germany) and integrity of RNA was evaluated using 1% agarose gel electrophoresis. cDNA synthesis was performed using the Omniscript Reverse Transcriptase Kit (Qiagen, Hilden, Germany) according to the manufacturer's protocol. Amplification of a partial sequence of the *X. laevis trpc2* gene was performed using degenerate PCR. Design of primers [5′-GTGGCHGTGGACACMAACCA-3′, 5′-ACATAGATRTTRTTGAKKCCACA-3′; modified from Kiemnec-Tyburczy et al. (Kiemnec-Tyburczy et al., 2012)] was based on multi-species alignment (ClustalW2, http://www.clustal.org/) of the *trpc2* gene sequences of *Plethodon shermani* (accession no.: JN805769), *Danio rerio* (NM_001030166), *Mus musculus* (NM_001109897), *Macropus eugenii* (GQ860951) and *Xenopus tropicalis* (predicted by automated computational analysis; XM_002941188). A touchdown PCR protocol was performed using the Phusion High-Fidelity DNA Polymerase (New England Biolabs, London, UK). The touchdown PCR parameters were: 98°C for 2 min; 20 cycles of 98°C for 1 min, 58°C for 30 s, 72°C for 1 min; 20 cycles of 98°C for 1 min, 51.4°C for 30 s, 72°C for 1 min; and 72°C for 10 min. The amplified product was then extracted from the agarose gel (QIAEXII, Qiagen), purified (QIAquick PCR Purification Kit, Qiagen) and re-amplified with the same set of primers under the same conditions. The purified product was sequenced (Seqlab, Göttingen, Germany). The sequence has been deposited in the European Nucleotide Archive (accession no. HG326501). For analysis of tissue specificity, we used the same cDNAs and a second primer pair targeting a shorter region of the *trpc2* transcript. The second primer pair was also used for producing an *in situ* hybridization probe (see below).

In situ hybridization

A *trpc2* fragment of 265 bp was obtained by PCR using genomic DNA of *X. laevis* as template and 5′-AAGGGATTAAGATGGACATCAA-3′ and 5′-GCAATGCCCTTGTAGGTGTT-3′ as primers, cloned into pGEMT (Promega, Mannheim, Germany) and confirmed by sequencing. Digoxigenin (DIG) probes were synthesized according to the DIG RNA labeling kit supplier protocol (Roche Molecular Biochemicals, Mannheim, Germany) using the same forward and reverse primers with a T3 promoter site attached to their 5′ end. Tissue blocks containing VNO and MOE were fixed in 4% formaldehyde solution for 2 h at room temperature, equilibrated in 30% saccharose, and embedded in Jung tissue freezing medium (Leica, Bensheim, Germany). Sections of 8–12 µm were cut horizontally using a cryostat (CM1900, Leica). Cryostat sections were then dried at 55°C and postfixed in 4% paraformaldehyde for 10–15 min at room temperature. Hybridizations were performed overnight at 60°C using standard protocols. Anti-DIG primary antibodies coupled to alkaline phosphatase (Roche Molecular Biochemicals) and NBT-BCIP (Roche Molecular Biochemicals) were used for signal detection.

Analysis of spatial distribution

The basal-to-apical position of *trpc2*-positive cells within the MOE was calculated by measuring the relative height of the cell, defined as distance of the center of the cell soma from the basal border of the MOE divided by total thickness of the epithelial layer at the position of the cell ($h_{rel}=h_{cell}/h_{layer}$). The medial-to-lateral distribution of *trpc2*-positive cells within the MOE was determined by subdividing the epithelium into three parts and counting positive cells in each of the three subdivisions [for more information, see Gliem et al. (Gliem et al., 2013)]. Cell positions were measured using ImageJ (http://rsbweb.nih.gov/ij/). Median, skewness and half-width of the resulting spatial distribution were calculated from unbinned values using Open Office (http://www.openoffice.org; for more information,

see Syed et al. (Syed et al., 2013)]. The epithelial position of ORNs expressing vomeronasal receptors used for comparison was determined in a previous study using identical methods (Syed et al., 2013).

Acknowledgements
We are grateful to Dr Thomas Hassenklöver for valuable discussions and comments on earlier versions of the manuscript.

Competing interests
The authors declare no competing financial interests.

Author contributions
A.S. and A.S.S. contributed equally to this work. I.M. and S.I.K., designed the study. I.M., S.I.K., A.S., A.S.S. and E.T. interpreted the results. A.S., A.S.S. and E.T. performed the experiments. I.M. and S.I.K. wrote the paper. All authors revised and approved the paper.

Funding
This work was supported by the German Research Foundation (DFG) Schwerpunktprogramm 1392 (to I.M. and S.I.K.) and Cluster of Excellence and DFG Research Center Nanoscale Microscopy and Molecular Physiology of the Brain (to I.M.). Deposited in PMC for immediate release.

Supplementary material
Supplementary material available online at
http://jeb.biologists.org/lookup/suppl/doi:10.1242/jeb.103465/-/DC1

References

DeMaria, S., Berke, A. P., Van Name, E., Heravian, A., Ferreira, T. and Ngai, J. (2013). Role of a ubiquitously expressed receptor in the vertebrate olfactory system. *J. Neurosci.* **33**, 15235-15247.

Gliem, S., Syed, A. S., Sansone, A., Kludt, E., Tantalaki, E., Hassenklöver, T., Korsching, S. I. and Manzini, I. (2013). Bimodal processing of olfactory information in an amphibian nose: odor responses segregate into a medial and a lateral stream. *Cell. Mol. Life Sci.* **70**, 1965-1984.

Grus, W. E. and Zhang, J. (2009). Origin of the genetic components of the vomeronasal system in the common ancestor of all extant vertebrates. *Mol. Biol. Evol.* **26**, 407-419.

Hamdani, H. and Døving, K. B. (2007). The functional organization of the fish olfactory system. *Prog. Neurobiol.* **82**, 80-86.

Kiemnec-Tyburczy, K. M., Woodley, S. K., Watts, R. A., Arnold, S. J. and Houck, L. D. (2012). Expression of vomeronasal receptors and related signaling molecules in the nasal cavity of a caudate amphibian (*Plethodon shermani*). *Chem. Senses* **37**, 335-346.

Liberles, S. D. (2014). Mammalian pheromones. *Annu. Rev. Physiol.* **76**, 151-175.

Sansone, A., Hassenklöver, T., Syed, A. S., Korsching, S. I. and Manzini, I. (2014). Phospholipase C and diacylglycerol mediate olfactory responses to amino acids in the main olfactory epithelium of an amphibian. *PLoS ONE* **9**, e87721.

Sato, Y., Miyasaka, N. and Yoshihara, Y. (2005). Mutually exclusive glomerular innervation by two distinct types of olfactory sensory neurons revealed in transgenic zebrafish. *J. Neurosci.* **25**, 4889-4897.

Syed, A. S., Sansone, A., Nadler, W., Manzini, I. and Korsching, S. I. (2013). Ancestral amphibian v2rs are expressed in the main olfactory epithelium. *Proc. Natl. Acad. Sci. USA* **110**, 7714-7719.

Taniguchi, K., Saito, S. and Taniguchi, K. (2011). Phylogenic outline of the olfactory system in vertebrates. *J. Vet. Med. Sci.* **73**, 139-147.

2.1.3 ODOR MAPPING to the OLFACTORY RECEPTORS EXPRESSION in MOE

This section deals with the original research article published in the journal Cellular and Molecular Life Sciences (Vol. 70, No. 11, Pages 1965-1984, published online on December, 2012).

Cell. Mol. Life Sci. (2013) 70:1965–1984
DOI 10.1007/s00018-012-1226-8

Cellular and Molecular Life Sciences

RESEARCH ARTICLE

Bimodal processing of olfactory information in an amphibian nose: odor responses segregate into a medial and a lateral stream

Sebastian Gliem · Adnan S. Syed · Alfredo Sansone · Eugen Kludt · Evangelia Tantalaki · Thomas Hassenklöver · Sigrun I. Korsching · Ivan Manzini

Received: 5 October 2012 / Revised: 26 November 2012 / Accepted: 27 November 2012 / Published online: 27 December 2012

Abstract In contrast to the single sensory surface present in teleost fishes, several spatially segregated subsystems with distinct molecular and functional characteristics define the mammalian olfactory system. However, the evolutionary steps of that transition remain unknown. Here we analyzed the olfactory system of an early diverging tetrapod, the amphibian *Xenopus laevis*, and report for the first time the existence of two odor-processing streams, sharply segregated in the main olfactory bulb and partially segregated in the olfactory epithelium of pre-metamorphic larvae. A lateral odor-processing stream is formed by microvillous receptor neurons and is characterized by amino acid responses and $G\alpha_o/G\alpha_i$ as probable signal transducers, whereas a medial stream formed by ciliated receptor neurons is characterized by responses to alcohols, aldehydes, and ketones, and $G\alpha_{olf}$/cAMP as probable signal transducers. To reveal candidates for the olfactory receptors underlying these two streams, the spatial distribution of 12 genes from four olfactory receptor gene families was determined. Several class II and some class I odorant receptors (ORs) mimic the spatial distribution observed for the medial stream, whereas a trace amine-associated receptor closely parallels the spatial pattern of the lateral odor-processing stream. Other olfactory receptors (some class I odorant receptors and vomeronasal type 1 receptors) and odor responses (to bile acids, amines) were not lateralized, the latter not even in the olfactory bulb, suggesting an incomplete segregation. Thus, the olfactory system of *X. laevis* exhibits an intermediate stage of segregation and as such appears well suited to investigate the molecular driving forces behind olfactory regionalization.

Keywords *Xenopus laevis* · Olfactory receptor neurons · *taar* genes · *v1r* genes · *or* class I and class II genes · G proteins

Abbreviations

MOE	Main olfactory epithelium
VNO	Vomeronasal organ
ORs	Odorant receptors
V1Rs	Vomeronasal receptors of type 1
V2Rs	Vomeronasal receptors of type 2
AOB	Accessory olfactory bulb
MOB	Main olfactory bulb
TAARs	Trace amine-associated receptors
ORNs	Olfactory receptor neurons

Introduction

The neuronal representation of odors in mammals generally relies heavily on segregation in subsystems that differ anatomically, functionally, and molecularly [1–3]. The two largest subsystems are the main olfactory epithelium (MOE) and the vomeronasal organ (VNO). The MOE contains

S. Gliem and A. S. Syed are shared first authors, S. I. Korsching and I. Manzini are shared senior authors.

S. Gliem · A. Sansone · E. Kludt
Department of Neurophysiology and Cellular Biophysics, University of Göttingen, Humboldtallee 23, 37073 Göttingen, Germany

A. S. Syed · S. I. Korsching
Department of Genetics, University of Cologne, Zülpicher Strasse 47a, 50674 Köln, Germany

E. Tantalaki · T. Hassenklöver · I. Manzini (✉)
Cluster of Excellence "Nanoscale Microscopy and Molecular Physiology of the Brain (CNMPB)", Department of Neurophysiology and Cellular Biophysics, University of Göttingen, Humboldtallee 23, 37073 Göttingen, Germany
e-mail: imanzin@gwdg.de

mostly ciliated neurons expressing the G protein $G\alpha_{olf}$ and odorant receptors (ORs) that segregate in several distinct expression zones, with class I odorant receptors stringently restricted to one of these zones. The VNO contains two sharply delineated populations of microvillous neurons, a basal layer expressing vomeronasal receptors of type 2 (V2Rs) and $G\alpha_o$, and an apical layer expressing vomeronasal receptors of type 1 (V1Rs) and $G\alpha_i$. The Grüneberg ganglion and the septal organ of Masera constitute two additional olfactory organs [4]. All these sensory surfaces have discrete target areas, the VNO in the accessory olfactory bulb (AOB) and all others within the main olfactory bulb (MOB). Interestingly, lungfish, the closest living relatives of tetrapods, possess several vomeronasal primordia, which share a target region in the olfactory bulb [5, 6]. It is not known whether these primordia are derived from a common ancestral structure in lobe-finned fishes or whether they represent lineage-specific specializations.

In contrast, ray-finned fishes including macrosmatic species [7] possess a single olfactory sensory surface and a common olfactory bulb. Nevertheless, the two main sensory neuron populations, ciliated and microvillous neurons, as well as the main olfactory receptor families and corresponding G proteins all are found in the teleost fish olfactory system intermingled in the shared sensory surface [8–10]. Within the olfactory bulb, the target regions of ciliated and microvillous neurons are somewhat segregated, but are still massively intertwined [11, 12].

Xenopus laevis, as an early diverging tetrapod, is evolutionarily much closer to mammals than lungfish, and this also holds true for the structural design of its MOE and VNO. However, *Xenopus* larvae still exhibit a fully aquatic life style. The transition from aquatic to airborne olfaction within the tetrapod lineage likely required a major reconstruction of the olfactory system. The inverse transition necessitated by the secondarily aquatic life style of whales and dolphins did not succeed well, as cetaceans are by and large anosmic species [13]. It is unclear whether the segregation in different subsystems was required by the evolutionary transition to airborne olfaction. Alternatively, the tendency to segregate olfactory functions may long precede this transition. In this case, one would expect evidence of segregation at the molecular and functional level already in the larval olfactory system of *X. laevis*. Some physiological aspects of the larval *Xenopus* olfactory system have already been examined (for a review see [14]). Preliminary information about the larval expression of one vomeronasal and some odorant receptors is available ([15, 16], respectively), and the olfactory receptor gene repertoires of a closely related species, *X. tropicalis*, have been established [17]. However, there has been no attempt so far to correlate molecular analysis and physiological function. Here we examined the spatial distribution of olfactory receptor molecules, associated G proteins, and odor responsiveness in the main sensory surface and the olfactory bulb as well as the nose–brain connections at the same defined stage in *Xenopus* larval development shortly before the onset of metamorphosis. We identified a lateral stream of odor-processing characterized by responses to amino acids, the presence of $G\alpha_o$/$G\alpha_i$ and the expression of trace amine-associated receptors (TAARs), which is segregated from a medial stream of odor processing, characterized by expression of class II ORs, responses to alcohols, aldehydes, and ketones and presence of $G\alpha_{olf}$. We report that significant spatial segregation of odor processing occurs already in the sensory surface and that segregation of these two odor streams is enhanced in the olfactory bulb.

Materials and methods

Tracing of neuronal processes

For visualization of glomerular clusters (see also [18]) in the MOB of larval *X. laevis*, axons of olfactory receptor neurons (ORNs) were labeled using biocytin (ε-biotinoyl-L-lysine, Molecular Probes, Leiden, The Netherlands). All procedures for animal handling and tissue dissections were carried out according to the guidelines of the Göttingen University Committee for Ethics in Animal Experimentation. Briefly, animals (stages 50–54; staged after [19]) were anesthetized with 0.02 % MS-222 (Sigma, Deisenhofen, Germany) for at least 1 min to produce complete immobility. Subsequently, small crystals of biocytin were placed into both nasal cavities, platinum electrodes (0.22 mm in diameter) were inserted into the cavities and square pulses with alternating polarity (30 V, 20 ms, 12 pulses at 1 Hz) were applied to facilitate biocytin intake into ORNs. To allow anterograde axonal transport of the dye, the animals were then kept in water tanks at low light levels for approximately 1 day. The animals were then cooled to produce complete immobility, killed by transection of the brain at its transition to the spinal cord, and fixed in 4 % formaldehyde solution for 2 h at room temperature. A block of tissue containing the olfactory organs, olfactory nerves, and the forebrain was then excised and processed as described below.

To visualize the epithelial location of ORNs that project to the lateral or medial glomerular clusters, ORN axons of the lateral and medial axonal tracts were labeled by electroporation of biocytin. Briefly, a block of tissue (see above) was excised, and all tissue ventral to the olfactory bulb was cut off to get access to the axonal sorting zone. The olfactory nerve and the olfactory organs were left intact. The explant was subsequently transferred to a recording chamber filled with bath solution and a patch pipette (resistance 5–8 MΩ) filled with bath solution saturated with biocytin (Molecular

Probes) was carefully inserted into the axonal tract close to its glomerular target region. Lateral and medial axonal tracts of the left and right MOB were, respectively, labeled. Electroporation was performed by application of square pulses (100 V, 20 ms, 12 pulses at 1 Hz). The tissue block was then kept in bath solution for 4 h to allow retrograde axonal transport of biocytin and was subsequently fixed in 4 % formaldehyde solution for 2 h at room temperature.

The formaldehyde-fixed preparations were washed in PBS, embedded in 5 % low-melting point agarose (Sigma) and sectioned at 70 μm on a vibratome (Leica VT 1200S, Bensheim, Germany). The sections were then washed with PBS containing 0.2 % Triton X-100 (PBS-TX) for 15 min and incubated with Alexa Fluor 488 conjugated avidin (100 μg/ml in PBS-TX; MoBiTec, Göttingen, Germany) for 2 h at room temperature. The sections were then washed in PBS for 15 min, transferred to slides, and mounted in mounting medium (Dako, Hamburg, Germany). All tissue sections were viewed using a confocal laser-scanning microscope (LSM 510/Axiovert 100 M, Zeiss, Jena, Germany).

Preparations of acute slices of the MOE and nose–brain preparations

Larval *X. laevis* (stages 50–54) were killed as described above. For slices of the MOE, a block of tissue containing the olfactory organs, the olfactory nerves, and the forebrain was cut. The tissue was then glued onto the stage of the vibroslicer, cut horizontally into a 150-μm-thick slice, and kept in bath solution. For low magnification imaging of axon terminals in whole olfactory bulbs, tadpoles were anesthetized and ORNs were stained with Fluo-4 10 kDa dextran (Molecular Probes) via electroporation (as described above for biocytin). At least 24 h later, the animals were killed and tissue blocks containing the olfactory systems were excised. The connective tissue covering the ventral side of the telencephalon was removed prior to confocal microscopy. For imaging individual glomeruli, we used nose–brain preparations with the dorsal surface of the olfactory bulbs removed using the vibroslicer. The olfactory organs and the olfactory nerves were left intact. For a more detailed description of these preparations, see earlier work of our lab [20, 21].

Solutions, staining protocol, and stimulus application

The bath solution consisted of (in mM): 98 NaCl, 2 KCl, 1 $CaCl_2$, 2 $MgCl_2$, 5 glucose, 5 Na-pyruvate, 10 HEPES, 230 mOsmol/l, pH 7.8. All bath solution chemicals were purchased from Merck (Darmstadt, Germany) or Sigma and were of the highest purity available. Tissue preparations (see above) were transferred to a recording chamber, and bath solution containing 50 μM Fluo-4/AM (Molecular Probes) was added. Fluo-4/AM was dissolved in DMSO (Sigma) and Pluronic F-127 (Molecular Probes). The final concentrations of DMSO and Pluronic F-127 did not exceed 0.5 and 0.1 %, respectively. Cells of the MOE and the olfactory bulb of larval *X. laevis* express multidrug transporters [22, 23] with a wide substrate spectrum, including calcium-indicator dyes. To avoid transporter-mediated destaining of the slices, 50 μM MK571 (Alexis Biochemicals, Grünberg, Germany), an inhibitor of multidrug transporters, was added to the incubation solution. The preparations were incubated on a shaker at room temperature for 35 min. As odorants, we used a mixture of alcohols, aldehydes, and ketones, and mixtures of amines, bile acids (obtained from crude ox bile), and amino acids, all purchased from Sigma (listed in Table 1). Furthermore, we used forskolin (Sigma) as an activator of adenylate cyclase. The odorant mixtures were dissolved in bath solution (stocks of 10–50 mM) and used at a final concentration of 100–200 μM. Forskolin was dissolved in DMSO (stock of 10 mM) and used at a final concentration of 50 μM. In all experiments, the odorant mixtures were repeatedly applied in random order at a minimal interstimulus interval of 2 min. Bath solution was applied

Table 1 Components of odorant mixtures

Odorant mixture	Components[a]
Amino acids (AA) (nose–brain prep)	L-Proline, L-valine, L-leucine, L-isoleucine, L-methionine, glycine, L-alanine, L-serine, L-threonine, L-cysteine, L-arginine, L-lysine, L-histidine, L-tryptophan, L-phenylalanine
Amino acids (AA) (MOE acute slices)	L-Proline, L-valine, L-leucine, L-isoleucine, L-methionine, glycine, L-alanine, L-serine, L-threonine, L-cysteine, L-asparagine, L-glutamine, L-arginine, L-lysine, L-histidine, L-glutamate, L-aspartate, L-tryptophane, L-phenylalanine
Bile acids (BA) (main components)	Taurocholic acid, glycocholic acid, cholic acid, deoxycholic acid
Amines (AM)	2-Phenylethylamine, tyramine, butylamine, cyclohexylamine, hexylamine, 3-methylbutylamine, *N*,*N*-dimethylethylamine, 2-methylbutylamine, 1-formylpiperidine, 2-methylpiperidine, *N*-ethylcyclohexylamine, 1-ethylpiperidine, piperidine
Mixture of alcohols, ketones and aldehydes (AL)	α-Terpineol, β-ionone, β-phenylethylalcohol, γ-phenylpropylalcohol, Citral

[a] All components used at a final concentration of 100–200 μM

by gravity feed from a storage syringe through a funnel drug applicator to the recording chamber. The tip of the applicator was placed directly above the MOE. The odorants and forskolin were applied into the funnel without stopping the flow. Outflow was through a syringe needle placed close to the MOE.

Ca^{2+} imaging and data evaluation

Changes of intracellular calcium concentrations of individual ORNs or glomeruli were monitored using a laser-scanning confocal microscope (LSM 510/Axiovert 100 M, Zeiss). Fluorescence images (excitation at 488 nm; emission >505 nm) of the MOE (acute slice of the MOE) or the olfactory bulb (nose–brain preparations) were acquired at 1.27 Hz and 786-ms exposure time per image with ten images taken as control images before the onset of stimulus application. The thickness of the optical slices excluded fluorescence detection from more than one cell layer or glomerulus. Image analysis was performed using custom programs written in MATLAB (MathWorks, Natick, MA, USA). To facilitate selection of regions of interest, a "pixel correlation map" was obtained by calculating the cross-correlation between the fluorescence signals of a pixel to that of its immediate neighbors and by then displaying the resulting value as a grayscale map [24]. The fluorescence changes for individual regions of interest (ORNs or glomeruli) are given as $\Delta F/F$ values. For more detailed information, see our previous work [25]. For whole olfactory bulb imaging, low-resolution $\Delta F/F$ data was processed using a Gaussian filter and is presented as a semi-transparent overlay of the peak response onto the olfactory bulb structure.

In order to quantify the spatial distribution of ORNs responding to amino acids or forskolin, the MOE was subdivided into three parts with equal length of the enclosing borders (see Fig. 3a) using the image-processing and analysis tool ImageJ (http://rsbweb.nih.gov/ij/). Cells with particular response specificities were counted in each of the three MOE subdivisions.

Immunohistochemistry

The following antibodies were used: $G\alpha_{olf/s}$ (Santa Cruz Biotech, cat-no. sc-383, lot H1409); $G\alpha_{i3}$ (Santa Cruz Biotech, cat-no. sc-262, lot E0710, also cross-reacting with other $G\alpha_i$ proteins according to manufacturer information); $G\alpha_o$ (Abcam, Ab35150, lot GR39385-1); $G\alpha_{q/11}$ (Santa Cruz Biotech, cat-no. sc-46972, lot A0208); $G\alpha_q$ (Santa Cruz Biotech, cat-no. sc-393, lot D0510); anti-tubulin (acetyl K40, Abcam, Ab11323, lot 6-11B-1); Alexa Fluor 488 goat anti-mouse (MoBiTec, cat-no. AZA11001); Alexa Fluor 546 goat anti-mouse (MoBiTec, cat-no. AZA11003); Alexa Fluor 488 goat anti-rabbit (MoBiTec, cat-no. AZA11008); Alexa Fluor 546 goat anti-rabbit (MoBiTec, cat-no. AZA11010); Alexa Fluor 488 rabbit anti-goat (MoBiTec, cat-no. A11078).

Antisera directed against the G protein α-subunits $G\alpha_{olf/s}$, $G\alpha_o$ and $G\alpha_i$ were used to localize different subsets of receptor neurons (see [15, 26, 27]) in the olfactory organ of larval *X. laevis* and to determine their projection pattern into the olfactory bulb. In some cases, ORNs were visualized by retrograde biocytin labeling (see [28]). $G\alpha_{q/11}$ and $G\alpha_q$ only stained non-sensory supporting cells (data not shown).

Larval *X. laevis* (stages 50–54) were killed as described above. Tissue blocks (see above) were fixed in 4 % formaldehyde solution for 2 h at room temperature, equilibrated in 30 % saccharose, and embedded in Jung tissue freezing medium (Leica) for cryosectioning (10–20 µm sections). Sections were washed in PBS-TX, and non-specific binding was blocked with 3 % normal goat serum (ICN, Aurora, OH, USA) for $G\alpha_i$ stainings, or 3 % bovine serum albumin (Sigma) for $G\alpha_{olf/s}$ and $G\alpha_{q/11}$ stainings, or 2 % bovine serum albumin for $G\alpha_o$ and $G\alpha_q$, in PBS-TX for 1 h. The sections were then incubated overnight at 4 °C with the primary antibodies (1:200) diluted in the respective blocking solution/PBS. Primary antibodies were washed off with PBS and the respective fluorophore-coupled secondary antibodies were applied at a dilution of 1:500 in 1 % blocking solution/PBS for 2 h at room temperature. The secondary antibodies were then washed off in several changes of PBS. To allocate signaling molecule expression to either ciliated or microvillous ORNs, we performed double-labeling experiments with antibodies against $G\alpha_{olf/s}$, $G\alpha_i$ and $G\alpha_o$ together with antibodies against tubulin (ciliary marker; 1:2,000) or fluorophore-coupled phalloidin (marker for microvilli; 1:250; Alexa Fluor 488 coupled to phalloidin, MoBiTec, cat-no. AZA12379; Alexa Fluor 546 coupled to phalloidin, MoBiTec, cat-no. AZA22283). All preparations were then transferred to slides, mounted in mounting medium (Dako) and viewed using a confocal laser-scanning microscope (LSM 780/upright Axio Examiner Z1, Zeiss). Optical sections were processed using ZEN software (Zeiss) and displayed as maximum intensity projections.

In order to quantify the spatial distribution of G protein-like immunoreactivity, we subdivided the MOE as described in the section above, and summed up the G protein-related fluorescence intensity values of the entire area of each subdivision of the MOE.

Western-blot analysis

Western blots were performed to test the specificity of antibodies directed against mammalian G alpha protein subunits $G\alpha_{olf/s}$, $G\alpha_o$ and $G\alpha_i$ in larval *X. laevis*. Tissue from the olfactory organs and the olfactory bulb from larval *X. laevis* (stages 43–45, 52–54 and 64–66) was collected and immediately conserved in liquid nitrogen. The frozen

tissue samples were then homogenized using a glass homogenizer in lysis buffer containing 10 mM Tris/HCl, pH 7.4, 0.1 % SDS, 1 mM EDTA pH 8.0, 1 % Triton X100, and a protease inhibitor mixture (Sigma). The lysate was centrifuged at 10,000 × *g* for 1 min, and the protein content in the supernatant was quantified by BCA assay (Thermo Scientific, Rockford, USA). Equal amounts of protein (30 µg per lane) were separated in 10 % SDS-PAGE gels under reducing conditions and then transferred to Amersham Hybond-ECL nitrocellulose membranes (GE Healthcare, Little Chalfont, England) for Western-blot analysis. The membranes were blocked with 5 % non-fat dry milk in PBS-Tween 20 (137 mM NaCl, 2.7 mM KCl, 8 mM Na_2HPO_4, 1.46 mM KH_2PO_4, 0.05 % Tween 20, pH 7.4) and incubated overnight at 4 °C with 1:1,000 dilution of the primary antibodies (anti-$G\alpha_{olf/s}$, anti-$G\alpha_o$ and anti-$G\alpha_i$, for details see above). Blots were washed three times with PBS Tween 20 and probed with horseradish peroxidase (HRP)-conjugated secondary antibodies (Dianova, anti-rabbit) for 1 h at a concentration of 1:2,000 at room temperature. The blots were washed again three times with PBS Tween 20, developed using ACE-Glow *chemiluminescence substrate* (peqlab, Erlangen, Germany) and analyzed by Bio1D software (Vilber Lourmat, Eberhardzell, Germany). The experiments revealed bands in the range of the appropriate molecular weight.

In situ hybridization

Xenopus laevis genomic DNA was extracted using standard protocols and used for PCR-mediated cloning. For this study, 12 genes from four olfactory receptor families were used. Primers were designed using published sequence information for the OR class l (*xb242, xr116, or52d1*) and OR class ll *(xb180, xb177, xgen147*) receptor genes, ([16, 29]; Mezler and Breer, GenBank entries). Primers were designed for two *v1r* genes (*v1r10, v1r11*) reported in [27], and one *v1r* gene (*v1r6*) was cloned using the homology approach with *v1r6* in *X. tropicalis*. The *X. laevis v1r6* turned out to share 92 % amino acid sequence identity with its ortholog in *X. tropicalis*. For two TAAR (*taar1, taar4a*) and one *v2r* gene (*xv2r E-1*), we used the primer set described in [30] and [15], respectively. The primer sequences we used were: *xr116* (5′-GTGACTCTCCTCTGCTACTT-3′, 5′-AGTAAAAACCGTCCGTCTTG-3′), *xb242* (5′-ACCAATGCAGTGGTATTAGTG-3′, 5′-TGGGTACTAGATTTGTGCTCG-3′), *or52d1* (5′-GAYTCYTTCATCMTYATGCTGATG-3′, 5′-CHAWTARRTGRGTGGTACAGGT-3′), *xb180* (5′-AATGAAGGAGCCACAATGTAC-3′, 5′-GCAATAATGAGTACGCCAATG-3′), *xb177* (5′-TTACCTTCTGATAATCTGGGAG-3′, 5′-AGCAACAATGGACAATACAAC-3′), *xgen147* (5′-CAGTRATGTCCTWTGACAG-3′, 5′-TCCCGGTATTGGACACTATC-3′), *v1r11* (5′-AGYCAACCTCATACTCTACC-3′, 5′-TCTGTCTGTGCTCCTTTTGC-3′), *v1r10* (5′-CAGTTTGCTCAGCTGTTATCAG-3′, 5′-GTSAGATAGTCCRTGTCACAG-3′), *v1r6* (5′-TCATTCTCAATGCCCGTACA-3′, 5′-CCAAAACCATTAGCCCAACA-3′), *taar1* (5′-GCCTTCACAATGGTATTTCTGG-3′, 5′-CCTATCTCTGCTTCGGGACAC-3′), *taar4a* (ACTTGGTCTGTTTCCTGTGTGTTTT-3′, 5′-TGGAAACTATGGTGGTTATGTACAAG-3′), *xv2r E-1* (5′-TGAGCTTCCTCCTCCTTGTC-3′, 5′-GGTAATGTCCGAGCTAAAAATGC-3′).

Resulting fragment lengths varied from 200 to 500 bp. All the genes were cloned into pDrive (Qiagen, Hilden, Germany) and later confirmed by sequencing. Antisense probes for in situ hybridization were derived from the cloned DNA by PCR, using the same primer sequences, but one of them with a T3 (TATTAACCCTCACTAAAGGGAA) promoter site attached to the 5′-end. Digoxigenin (DIG) was incorporated into the probes according to the DIG RNA labeling kit supplier protocol (Roche Molecular Biochemicals, Mannheim, Germany). Olfactory organ tissue blocks were prepared as described for immunohistochemistry. Cryostat sections of 10–12 µm were obtained and postfixed in 4 % paraformaldehyde for 10–15 min at room temperature.

Hybridizations were performed overnight at 60 °C using standard protocols. Anti-DIG primary antibodies coupled to alkaline phosphatase (Roche Molecular Biochemicals) and NBT-BCIP (Roche Molecular Biochemicals) were used for signal detection.

In order to quantify the spatial distribution of olfactory receptor genes, the MOE was subdivided into three parts as described above. Areas were nearly identical for the subregion close to the VNO (medial region) and the intermediate region (36 and 35 %, respectively), but somewhat less for the lateral region, most distant from the VNO (29 %). Half of the in situ experiments were randomized and cell count was done blindly with respect to the genes involved. No difference in the results from non-randomized evaluation was seen.

Results

The lateral and medial glomerular cluster exhibit distinctly different odor-response profiles

We analyzed the medial-to-lateral spatial distribution of olfactory bulb responses to four main odor groups of aquatic animals, amino acids (feeding stimulants, [31, 32]), amines (also food signals, [32, 33]), bile acids (social interactions, [31, 32, 34]) and alcohols, aldehydes, and ketones [35]. In addition, we analyzed olfactory bulb responses upon mucosal application of forskolin, an activator of the cAMP-dependent transduction pathway of ORNs.

In low magnification views of the whole olfactory bulb (Fig. 1a), application of amino acids and forskolin to the

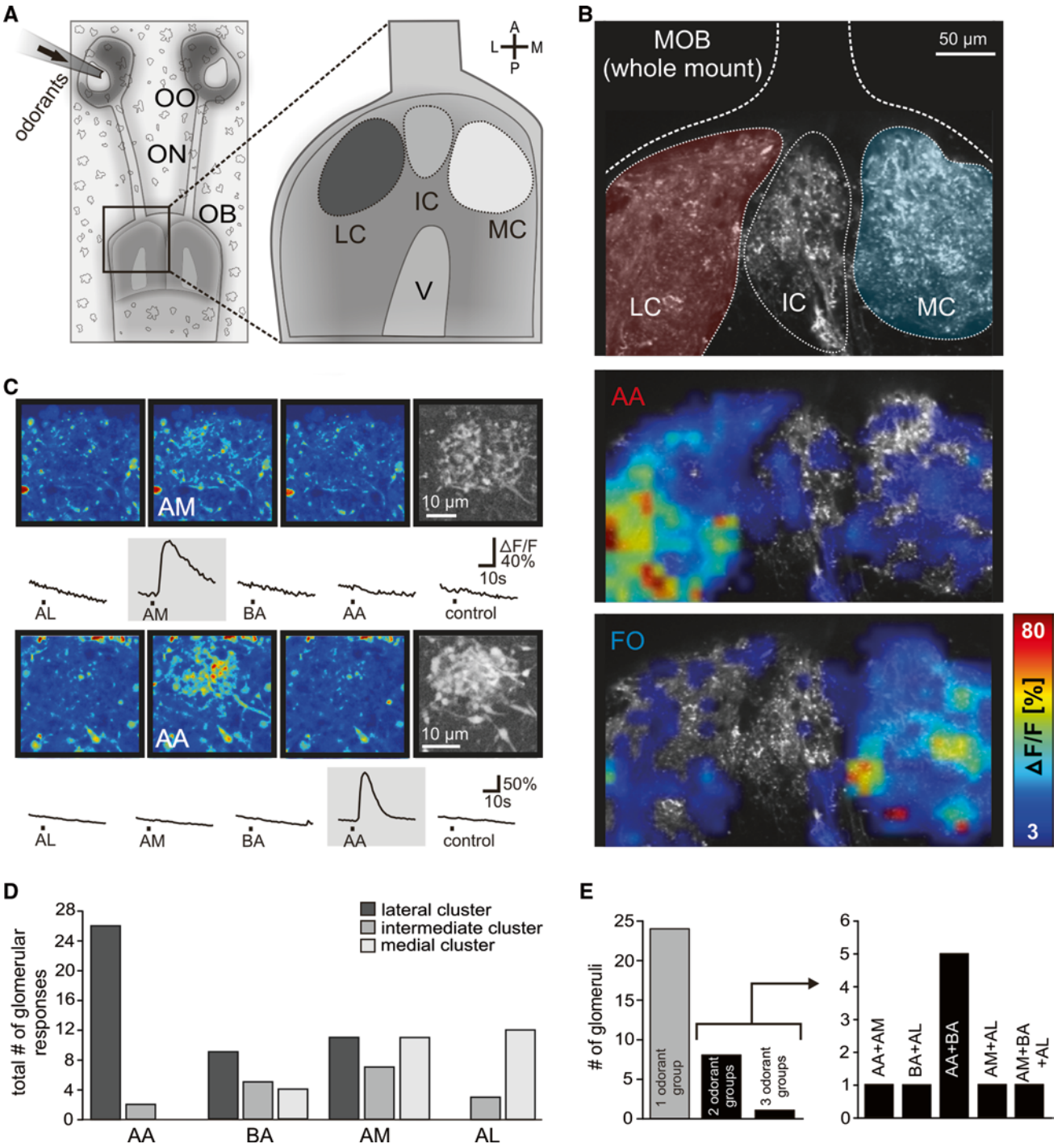

intact olfactory organ induced transient increases of Ca^{2+}-dependent fluorescence of Fluo-4 in the neuropil of the glomerular layer (Fig. 1b). Amino acids preferentially induced responses in the lateral cluster, whereas forskolin elicited activity predominantly in the medial cluster. For analysis of individual glomeruli, we used nose–brain preparations with the surface of the olfactory bulbs removed. Odor-responsive structures were first allocated to one of the known glomerular clusters of the MOB (see Fig. 1a). We then focused on the responding neuropil and repeated the odorant application to verify that the responding spots were individual, clearly delineated glomeruli with the typical fine structure (Fig. 1c, pseudocolored and grayscale images). The reproducibility of glomerular responses was verified in nearly all cases by repeating the odorant application at least twice. The signals were odor-specific, since application of bath solution alone never evoked a comparable response (see Fig. 1c).

◀**Fig. 1** Odorant responses in the glomerular layer of the main olfactory bulb. **a** Schematical representation of the nose–brain preparation (*left panel*) and the three main glomerular clusters of the MOB (*right panel*). **b** Whole-mount olfactory bulb preparation stained with Fluo-4 dextran showing the three main clusters of the MOB (*upper panel*; LC *red*, MC *blue*). Application of amino acids preferentially induced an increase in Ca^{2+}-dependent fluorescence in the lateral cluster (*intermediate panel*), whereas forskolin elicited activity predominantly in the medial cluster (*lower panel*). A representative example of seven separate experiments is shown. **c** Sequence of three pseudocolored images showing calcium transients of an individual glomerulus situated in the medial cluster upon application of amines. The images were taken before stimulus application, at the peak of the response and after return to the baseline fluorescence (from *left* to *right*). The fine glomerular structure of the activated glomerulus was visualized by a grayscale correlation map (*rightmost image*; see "Materials and methods" for details). The time courses of the $[Ca^{2+}]_i$ transients of the glomerulus, evoked by mucosal application of the different odorant groups are given below the images. The lower group of pictures shows an individual glomerulus, situated in the lateral cluster, responsive solely to amino acids (same explanation as above). **d** Histogram showing the location of odorant-responsive glomeruli ($n = 80$ glomeruli from 32 nose–brain preparations). **e** Out of 33 glomeruli tested for their responsiveness to all four odorant groups, 24 responded to one odorant group, eight responded to two odorant groups, and one glomerulus to three odorant groups (*left panel*). Odorant profiles of multiresponsive glomeruli are shown in the *right panel*. All odorants were applied at a final concentration of 200 μM, forskolin was applied at a final concentration of 50 μM. *A* anterior, *P* posterior, *L* lateral, *M* medial, *OO* olfactory organ, *ON* olfactory nerve, *OB* olfactory bulb, *AA* amino acids, *AL* alcohols, ketones, and aldehydes, *AM* amines, *BA* bile acids, *FO* forskolin, *LC* lateral glomerular cluster, *IC* intermediate glomerular cluster, *MC* medial glomerular cluster, *V* lateral ventricle, *control* application of bath solution

As representative examples, we show the response characteristics of two glomeruli to all four odor groups (Fig. 1c). The first glomerulus, a component of the medial cluster, reacts only to amines, the second glomerulus, situated in the lateral cluster, only to amino acids. In total, we analyzed odor responses of 80 glomeruli that could be clearly allocated to a glomerular cluster ($n = 32$, nose–brain preparations; 42, 15, and 23 glomeruli for lateral, intermediate, and medial cluster, respectively; Fig. 1d). Thirty-three glomeruli were tested with all four odor groups, and of these, the large majority reacted only to a single of the four odor groups (Fig. 1e). Of the 24 monoresponsive glomeruli, seven reacted to the mixture of amino acids, six to bile acids, seven to amines, and four to the mixture of alcohols, aldehydes, and ketones. With one exception, the odor responses of the remaining nine glomeruli were restricted to two out of four odor groups. Amine responses were found to co-exist with all three other odor groups, likewise for bile acids, however we never found a glomerulus that reacted to both amino acids and alcohols, aldehydes, and ketones (Fig. 1e).

Clear positional preferences were seen already in the overview of the whole olfactory bulb for amino acid and forskolin responses: amino acid responses were nearly exclusively found in the lateral cluster, while forskolin responses showed a complementary restriction to the medial cluster (Fig. 1b). This result was confirmed by the examination of single glomeruli at higher magnification, where we found an almost exclusive location of amino acid-responsive glomeruli in the lateral cluster (Fig. 1d), consistent with previous observations [18, 36]. Moreover, the glomeruli responsive to alcohols, aldehydes, and ketones were almost exclusively located in the other large cluster, the medial glomerular cluster (Fig. 1d). In contrast, bile acid- and amine-responsive glomeruli were more broadly distributed, and were found in all three cluster regions, lateral, intermediate and medial (Fig. 1d).

Lateral and medial glomerular cluster in the olfactory bulb are innervated by spatially segregated populations of receptor neurons

To what extent is the functional segregation apparent in the glomerular response patterns in the olfactory bulb already present in the sensory surface? To analyze this question we used retrograde tracing of biocytin from the axonal tracts emerging from the lateral and medial cluster (Fig. 2a) at very lateral and very medial positions, respectively. For lateral injections, the large majority of biocytin-labeled somata were situated in the lateral part of the MOE, but occasionally cells were also found in the medial region (Fig. 2b). For medial injections, the distribution of labeled somata was the inverse, i.e., the vast majority were positioned in the medial part of the MOE and only rarely were cells found in the lateral region (Fig. 2b). These findings show that the segregation apparent in the olfactory bulb is already present in the olfactory epithelium, some overlap of the two subsystems notwithstanding. These two spatially segregated ORN projection paths will be named lateral and medial stream throughout the manuscript.

The existence of these two subsystems suggests that the receptor neuron sub-populations projecting to the lateral and the medial cluster of glomeruli should have distinct response properties, reflecting that of the respective glomerular clusters. Thus we proceeded to measure calcium responses of individual ORNs in situ using acute slices of the MOE stained with the calcium-indicator dye Fluo-4.

Most receptor neurons are specific for one of the four odor groups

We detected sparse populations of responsive receptor neurons for all four odor groups tested for glomerular responses (Fig. 3a, b). For amino acids and amines, this corroborates earlier observations [28, 30], whereas responses to bile acids and the mixture of alcohols, aldehydes, and ketones had not been examined so far. Representative traces obtained

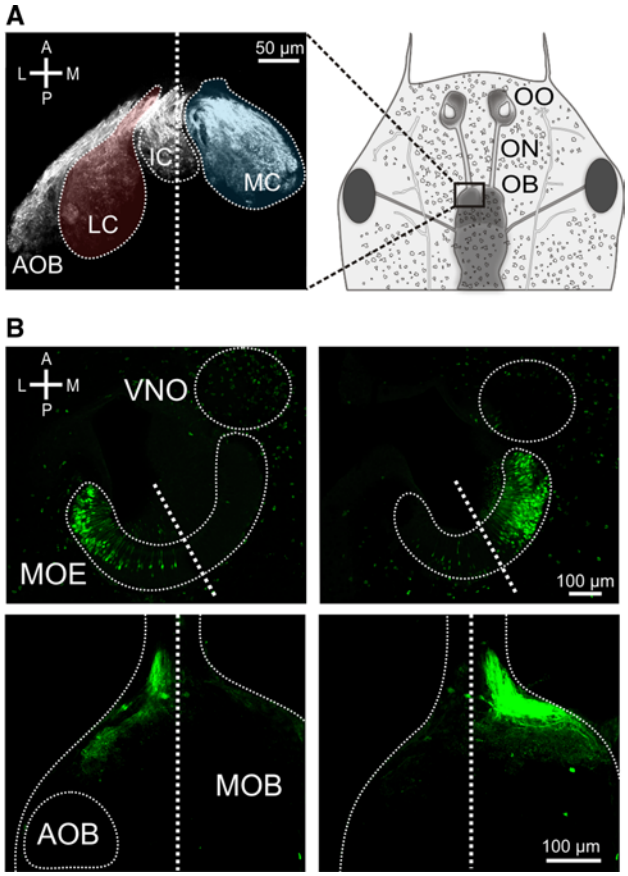

Fig. 2 Visualization of spatially segregated streams within the main olfactory system. **a** Glomerular clusters are visualized by anterograde transport of biocytin (*left panel*). The three main glomerular cluster (LC *red*, MC *blue*) as well as the AOB are distinctly visible. The schematic drawing (*right panel*) shows the location of the *left panel* in larval *Xenopus laevis*. **b** Retrograde labeling of ORNs by biocytin electroporation into the lateral (*lower left-hand panel*) and medial (*lower right-hand panel*) axonal tracts at the level of the MOB. *Thick dotted lines* indicate midlines and *thin dotted lines* trace organ outlines. Electroporation into the lateral axonal tract predominantly labeled lateral ORNs (*upper left-hand panel*), whereas electroporation into the medial axonal tract predominantly labeled medial ORNs (*upper right-hand panel*). *A* anterior, *P* posterior, *L* lateral, *M* medial, *OO* olfactory organ, *ON* olfactory nerve, *OB* olfactory bulb, *LC* lateral glomerular cluster, *IC* intermediate glomerular cluster, *MC* medial glomerular cluster

for individual neurons (Fig. 3c) show fast calcium transients for all odor groups, typical for ORN responses (see [37]). As a positive control, we applied the adenylate cyclase activator forskolin, which increases cAMP levels, i.e., activates the cAMP-dependent ciliated receptor neurons (Fig. 3a–d). Application of bath solution by itself never evoked any comparable response (Fig. 3c). The reproducibility of ORN responses was verified by regularly repeating the application of most of the odorants at least twice. In total, we analyzed the odorant responses of 340 ORNs out of 17 MOE slices (Fig. 3b–d).

Amino acid responses were observed much more frequently than those to each of the other three odor classes, with 188 versus 46, 70, and 65 responsive cells for amino acids, bile acids, amines, and the mixture of alcohols, aldehydes, and ketones, respectively. Over 90 % of ORNs responded only to one odor group (Fig. 3d), showing that the vast majority is narrowly tuned to individual groups of odorants, similar to the high tuning specificity described above for individual glomeruli (Fig. 1e). The remaining cells mostly responded to two of the four odor groups and only three cells responded to three odor groups. An example of a mixed odor response is shown in Fig. 3c (top row), whereas the other three cells depicted in Fig. 3c only react to a single odor group each. Amine responses were found to co-exist with all three other odor groups, likewise for bile acids, however we never found a cell that reacted to both amino acids and the mixture of alcohols, aldehydes, and ketones (Fig. 3d). This parallels exactly our observations for glomeruli (see Fig. 1), consistent with a clearly segregated pathway for amino acids versus alcohols, aldehydes, and ketones.

Amino acid-responsive cells were notably more specific than the other three groups, as <5 % of amino acid-responsive cells, but about one-third of amine, bile acid-responsive cells, and cells responsive to the mixture of alcohols, aldehydes, and ketones reacted to other odor groups (Fig. 3d, bottom left panel). We therefore went ahead to measure the spatial distribution of amino acid-responsive neurons.

Amino acids activate lateral ORNs, while odors signaling via cAMP preferentially elicit responses in medial ORNs

In previous work, we have shown that the MOE of larval *X. laevis* comprises two large subsets of ORNs with differing transduction cascades and a differential sensitivity to amino acid odorants [21, 38]. Here, we have analyzed the spatial distribution of such cells. From the tracing results described above, we expected the tripartite organization of the olfactory bulb in three major glomerular clusters to be somewhat reflected in the sensory surface. We have therefore quantified the number of odor-responsive cells in the lateral, intermediate, and medial third of the olfactory epithelium separately. We find that amino-acid responsive cells were strongly enriched in the lateral third of the olfactory epithelium (Fig. 3a), with about 60 % of all amino acid-responsive cells restricted to the lateral third of the MOE, and the remaining 40 % evenly distributed between intermediate and medial region. This lateral preference corresponds to the spatial pattern for amino acid responsive glomeruli in the olfactory bulb and thus provides functional evidence for the existence of at least two segregated subsystems suggested by our tracing experiments reported above. Interestingly, the lateral-to-medial gradient is steeper in the olfactory bulb,

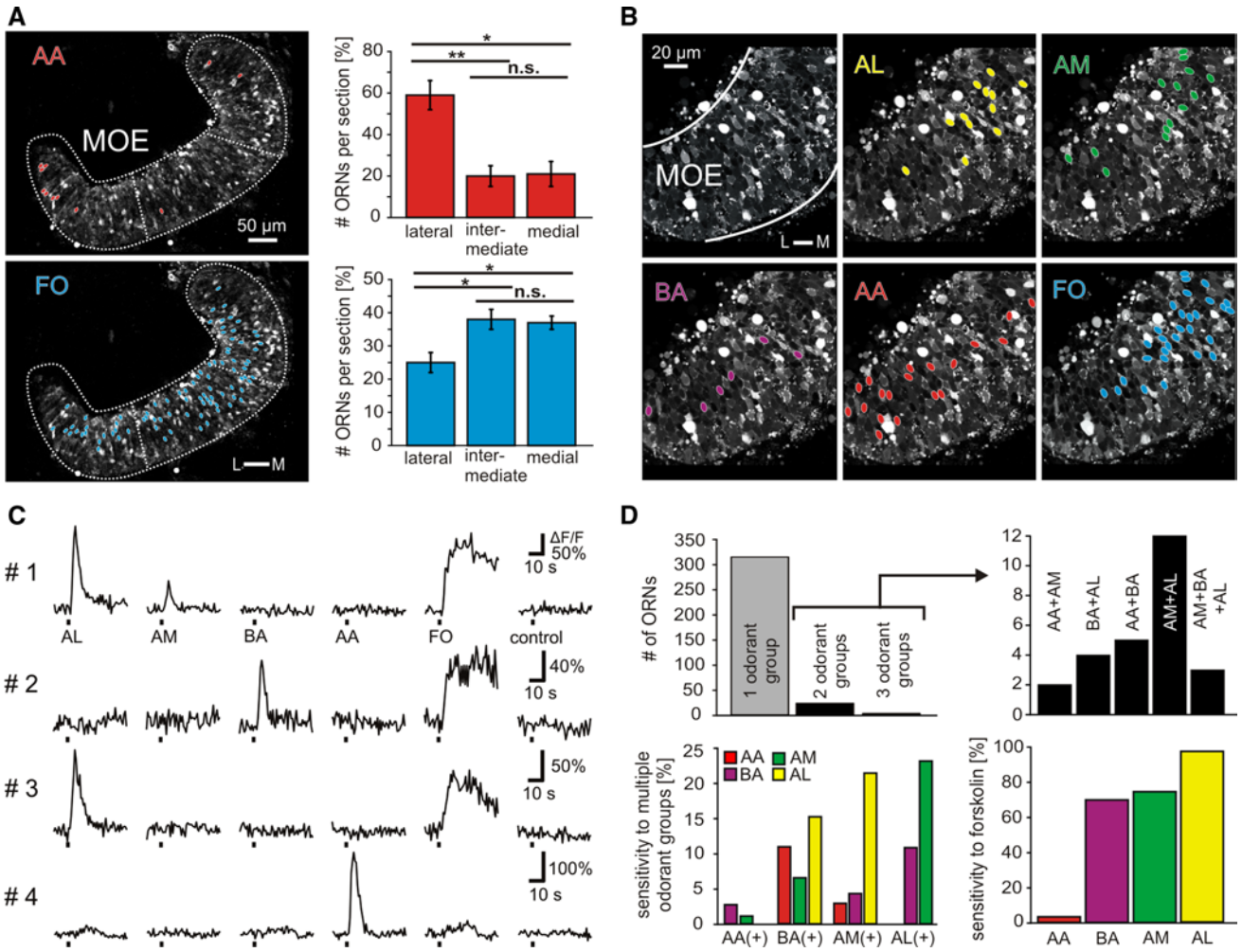

Fig. 3 Odorant responses at the level of the main olfactory epithelium. **a** Acute slice preparation of the whole MOE stained with Fluo-4 (image acquired at rest). The *red ovals* indicate somata of individual ORNs that responded to the mixture of amino acids (100 µM). Quantitative evaluation (*right panel*) shows more amino acid-responsive cells in the lateral third of the MOE compared to intermediate and medial segments ($n = 116$ ORNs from 13 acute slices of the MOE). The *blue ovals* indicate somata of forskolin-responsive cells (50 µM) of the same slice preparation. Significantly more forskolin-responsive cells were located in the medial and intermediate third of the MOE compared to its lateral third ($n = 600$ ORNs from 14 acute slices of the olfactory epithelium). Statistical analysis was performed using a *t* test; $*p < 0.05$, $**p < 0.01$; *error bars* show SEM. **b** Acute slice preparation of the MOE stained with Fluo-4 (image acquired at rest). Field of view does not cover the whole MOE. The *colored ovals* indicate somata of individual ORNs that responded to the mixture of alcohols, aldehydes, and ketones (*yellow*), amines (*green*), bile acids (*magenta*), amino acids (*red*) or to forskolin (*blue*). All odorants were applied at a final concentration of 200 µM, forskolin at a final concentration of 50 µM. **c** Time courses of $[Ca^{2+}]_i$ transients of four responsive ORNs of this slice. **d** Out of 340 ORNs tested ($n = 17$ acute slices), 314 responded to only one odorant group whereas 23 responded to two odorant groups and three to three odorant groups (*upper left panel*). The exact odorant profile of multiresponsive cells is shown in the *upper right panel*. The *histogram* in the *lower left-hand panel* gives the frequencies of correlated responses to the tested odorant groups. The *lower right-hand panel* gives the correlation of odorant- and forskolin-sensitivity of individual ORNs. *L* lateral, *M* medial, *AA* amino acids, *AL* alcohols, ketones, and aldehydes, *AM* mixture of amines, *BA* mixture of bile acids, *FO* forskolin, *control* application of bath solution

where not a single amino acid-responsive glomerulus was observed in the medial cluster (Fig. 1d), pointing to further sorting-out within the olfactory nerve connecting MOE and olfactory bulb.

Cells responding to the mixture of alcohols, aldehydes, and ketones appeared to exhibit a preferentially medial location, while responses to bile acids as well as amines seemed more evenly distributed through all regions of the olfactory epithelium (data not shown). However, due to low cell numbers, quantification was not reliably possible in these cases. We have therefore chosen to analyze the spatial distribution of cells responding to forskolin, as a summary measure for neurons transducing odor signals via cAMP. From our olfactory bulb responses (see Fig. 1) and from comparison with other species, these may be expected to include three of the four odor groups tested here, amines, bile acids, and

alcohols, aldehydes, ketones [12, 39, 40]. Amino acids are expected to mostly signal via a cAMP-independent mechanism [12, 41]; but see [11].

We found forskolin-responsive cells to be moderately depleted in the lateral segment, with no difference between intermediate and medial segments (Fig. 3a). Thus, the forskolin response was inversely distributed to the amino acid response. In terms of absolute numbers of cells counted, the lateral depletion of forskolin is very similar to the lateral enrichment of amino acid-responsive cells, consistent with the notion that these two pathways are strictly segregated and may amount to most or all of olfactory signaling in the MOE.

The analysis of traces originating from individual cells confirms this prediction of exclusivity between amino acid response and forskolin response (Fig. 3c, d). Virtually all amino acid-sensitive ORNs did not respond to forskolin and virtually all ORNs responsive to the mixture of alcohols, aldehydes, and ketones were sensitive to forskolin (Fig. 3d, bottom right panel). Interestingly, while the large majority of bile acid- and amine-responsive cells were activated by forskolin, about one-fourth were not, suggesting that bile acid- as well as amine-responsive cell groups are not homogeneous, but contain cells signaling via cAMP as well as via a cAMP-independent pathway. This heterogeneity of bile acid- and amine-responsive receptor neurons may explain their broader spatial distribution and less narrow chemical tuning compared to the two other groups.

The lateral sensory surface contains microvillous neurons that express $G\alpha_i$ and $G\alpha_o$, whereas the medial region contains ciliated neurons that express $G\alpha_{olf/s}$

In the mammalian olfactory system, two main signal transduction pathways are known. One is the so-called canonical pathway, which uses $G\alpha_{olf}$ and cAMP, and is found in ciliated receptor neurons; the other uses $G\alpha_i$ or $G\alpha_o$ and is found in microvillous neurons [2]. Our results with forskolin, detailed above, suggest that the medial subsystem, which is responsive to alcohols, aldehydes, and ketones, signals via cAMP and therefore might be in ciliated receptor neurons, whereas the amino acid-responsive lateral subsystem may be expected to reside in microvillous receptor neurons. To test these hypotheses, we have analyzed the spatial distribution of G proteins both in the olfactory epithelium and the olfactory bulb, alone and in combination with markers for cilia and microvilli (Figs. 4, 5). The latter was necessary, because in larval *X. laevis* the processes of microvillous and ciliated receptor neurons are not much different in length and can therefore not be distinguished unequivocally by morphology (data not shown; see also [42]).

For immunohistochemical localization, we employed antibodies against $G\alpha_i$, $G\alpha_o$ and $G\alpha_{olf/s}$, whose specificity was confirmed in Western blots of olfactory bulb and olfactory organ (Fig. 5). All three antibodies stain the apical surface, i.e., the apical endings of ORNs, as well as axons in the olfactory nerve and olfactory bulb (Fig. 5a, d and g), but not the cell somata.

$G\alpha_i$-like and $G\alpha_o$-like immunoreactivity showed a graded distribution, decreasing from the lateral to medial area of the MOE (Fig. 5a, c, d, f). A drastically different distribution was observed for $G\alpha_{olf/s}$-like immunoreactivity, which was strongly enriched in the medial and intermediate part of the MOE, but very minor in the lateral part (Fig. 5g, i). The distributions in the olfactory bulb are even more sharply delineated, with $G\alpha_i$ and $G\alpha_o$ nearly exclusively restricted to the lateral glomerular cluster (and the AOB), and $G\alpha_{olf/s}$ restricted to glomeruli of the medial and intermediate glomerular cluster (Fig. 5a, d, g; bottom panels). A similar segregation is already seen in the olfactory nerve layer of the olfactory bulb, with the $G\alpha_i$ and $G\alpha_o$ containing fibers preferentially located in the lateral part and the $G\alpha_{olf/s}$ containing fibers preferentially located in the medial part (Fig. 5a, d, g; bottom panels). Thus, considerable sorting out occurs en route to the olfactory bulb, consistent with the sorting out seen for amino acid-responsive and forskolin-responsive neurons (Figs. 1, 2, 3). These data suggest that the lateral stream signals via $G\alpha_i$ and $G\alpha_o$ and the medial stream may signal via $G\alpha_{olf/s}$.

To establish the cell types expressing the respective G proteins, we used phalloidin, a marker for f-actin that is abundant in microvilli [43] and antibodies against tubulin as a ciliary marker [44]. Both markers label the whole sensory as well as non-sensory epithelium (Fig. 4), due to the presence of microvilli and cilia also in supporting and non-sensory cells [42]. Double-labeling experiments with G protein antibodies revealed that both $G\alpha_i$-like and $G\alpha_o$-like immunoreactivity are restricted to the apical endings of microvillous ORNs (Fig. 5a, d, upper panel), whereas $G\alpha_{olf/s}$-labeled structures could be identified as cilia of ORNs (Fig. 5g, upper panel).

Our data suggest the medial olfactory stream to be composed of ciliated receptor neurons and the lateral stream to consist of microvillous receptor neurons.

Microvillous and ciliated receptor neuron populations are expected to express different receptor families. As a first step in linking such molecular features to the two streams, we cloned 12 genes from the four olfactory receptor gene families of *X. laevis* and investigated their spatial distribution within the olfactory epithelium by in situ hybridization.

Sparse expression patterns of *or* class I, *or* class II, *v1r* and *taar* genes in the larval MOE

We performed in situ hybridizations with members of *or* class I and II, *v1r*, *v2r*, and *taar* olfactory receptor gene

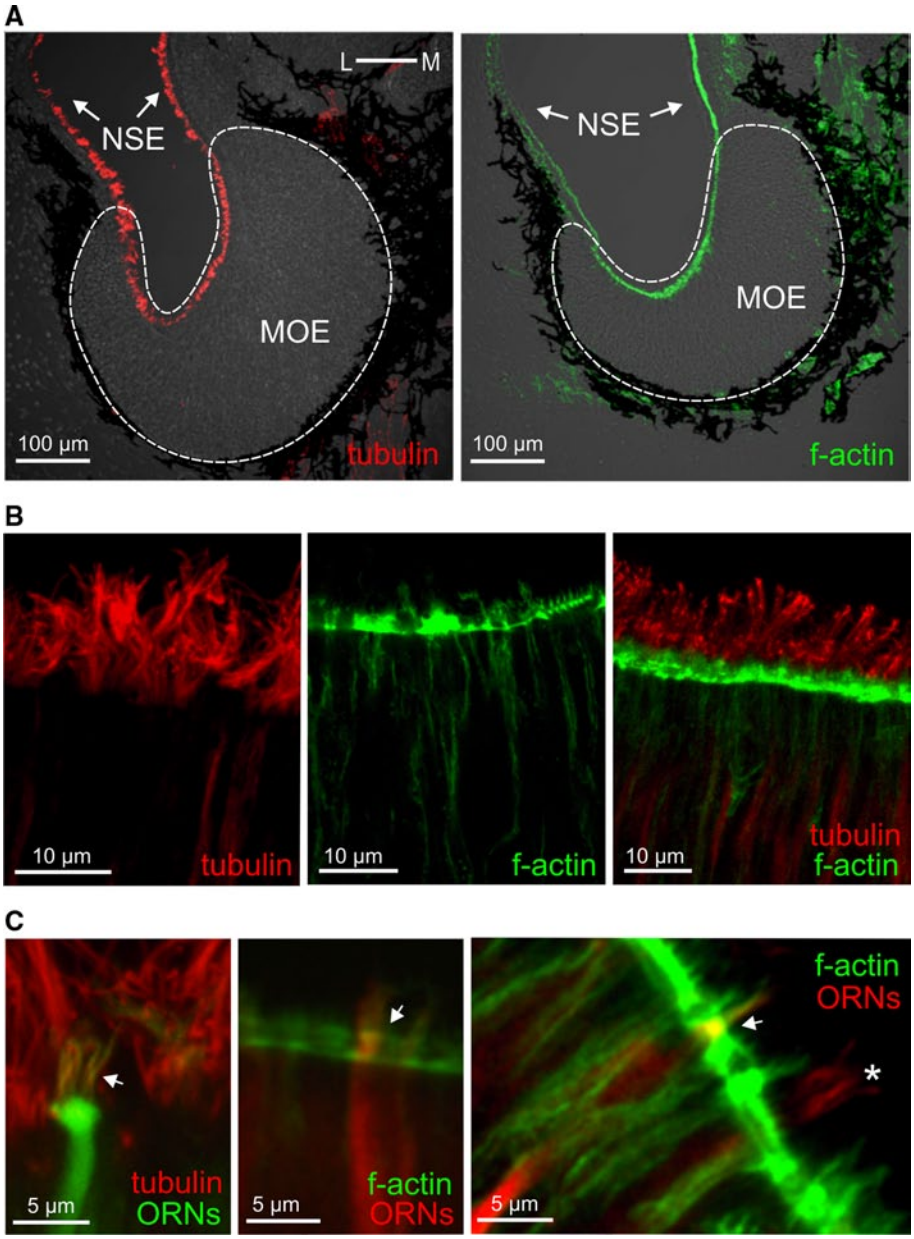

Fig. 4 Tubulin and actin identify cilia and microvilli, respectively. **a** Antibodies against tubulin and a marker of f-actin (phalloidin) both labeled structures in the whole MOE and in the adjacent non-sensory epithelium (NSE; tubulin, *left-hand panel*; f-actin, *right-hand panel*). **b** Higher magnifications of the apical MOE show cilia labeled with antibodies against tubulin (*left-hand panel*), microvilli labeled with phalloidin (*middle panel*), and a double-labeled MOE (*right-hand panel*). **c** ORNs and their processes were visualized by nerve backfills with biocytin and double labeled with antibodies against tubulin (*left panel*, ciliated neuron, the *arrow* points to cilia), and phalloidin (*middle and right panels*, microvillous neurons, *arrows* point to olfactory knobs). Another backfilled neuron with somewhat longer processes (*asterisk*) was not labeled by phalloidin, i.e., it is a ciliated neuron

families, using RNA probes for a total of 12 different genes. We show that *taar1* was not expressed in the sensory surface (Fig. 6j), and thus may have a non-olfactory role in *Xenopus*, as has been reported for mammalian and fish orthologs of *taar1* [45, 46].

The *v2r* probe was chosen for its extensive crossreactivity with many closely related *v2r* genes. The probe covers a highly conserved region of the *v2r* gene and a MSA (Multiple Sequence Alignment) search in the *X. tropicalis* V2R repertoire finds 75 family members with sequence identity 94 % and above (data not shown). This probe labels a dense population of cells in the VNO (Fig. 6l), presumably due to extended cross-reactivity. However, expression is nearly absent from the MOE, and only occasionally a labeled cell was observed (data not shown, see also [15], well below the expression frequency observed for single receptor genes of about 1–2 cells/section. Due to this near absence in the MOE, genes detected by this probe are not candidates for mediating odor responses in the MOE. In contrast, all *v1r*, class I and II *or* genes and one *taar* gene examined were absent from the VNO and found exclusively within the MOE (Fig. 6), exhibiting sparse expression patterns characteristic of individual olfactory receptor genes [47] and similar to adult, post-metamorphic expression patterns, which have been reported for some of these genes [16, 27, 29]. For *or* and *taar* genes, an expression in the MOE is expected, as both fish and mammals show this pattern. The MOE-specific V1R expression parallels the situation in

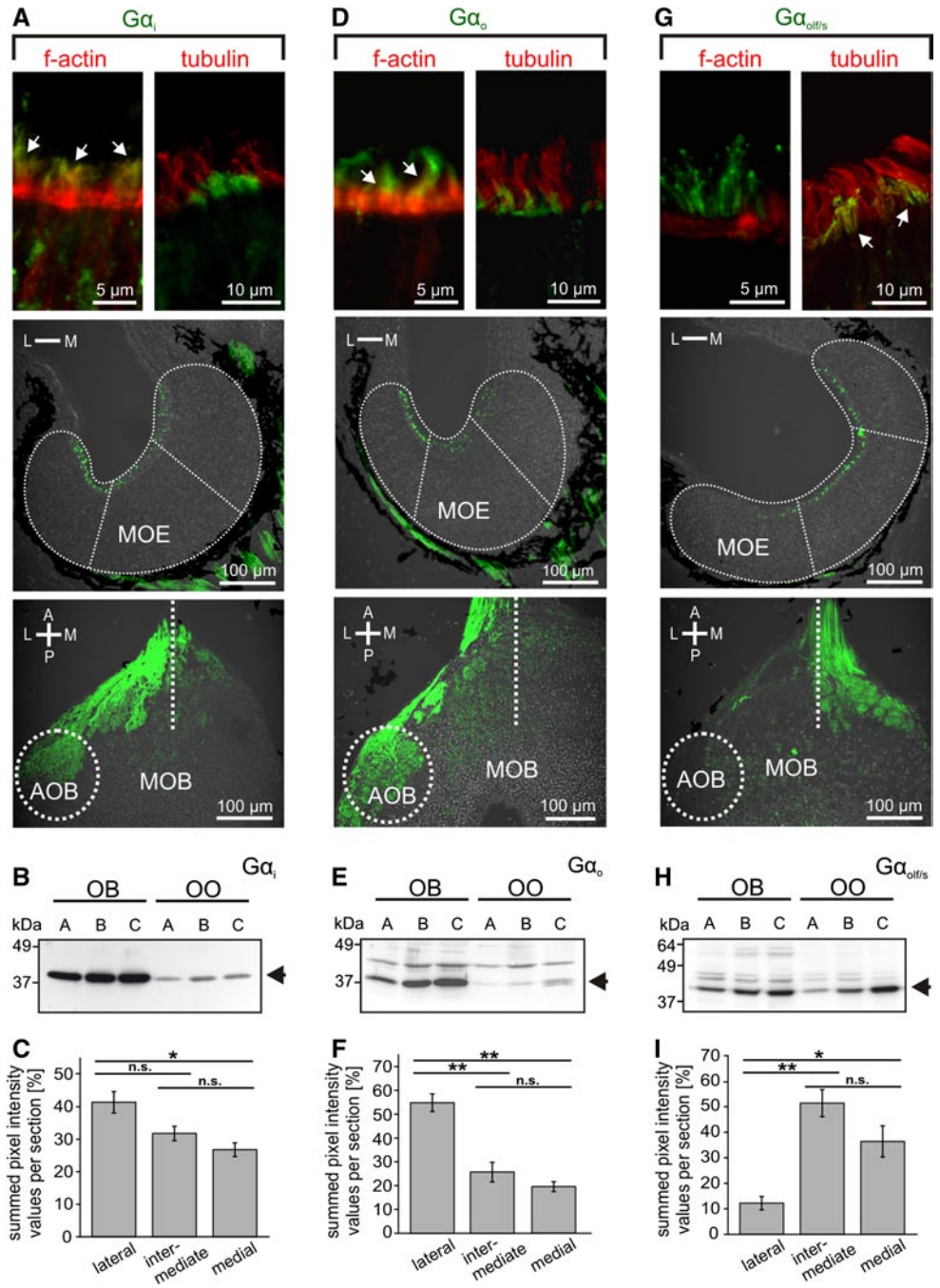

Fig. 5 G-protein immunohistochemistry in the main olfactory epithelium and the main olfactory bulb. Antibodies against $G\alpha_i$ (**a**) and $G\alpha_o$ (**d**) preferentially labeled apical structures of ORNs located in the lateral and intermediate part of the MOE (*middle row*) and axon bundles of the olfactory nerve and glomeruli of the lateral and intermediate glomerular clusters of the MOB, as well as glomeruli in the AOB (*lower row*). *Dotted lines* indicate the approximate borders and subdivisions of MOE and olfactory bulb. $G\alpha_i$ and $G\alpha_o$ immunoreactivity was localized in apical endings of phalloidin-positive (*arrows*) and tubulin-negative microvillous olfactory receptor neurons (*upper row*). $G\alpha_{olf/s}$ (**g**) immunoreactivity showed a complementary distribution, preferentially localized in ORNs and glomeruli of the medial and intermediate regions of MOE and MOB (*middle* and *lower row*, respectively). $G\alpha_{olf/s}$ in apical endings of ORNs co-localized with the ciliary marker tubulin, but not with f-actin (*upper row*, *arrows*). Western-blot analysis of $G\alpha_i$ (**b**), $G\alpha_o$ (**e**) and $G\alpha_{olf/s}$ (**h**) antibodies using tissue samples of olfactory organ and olfactory bulb of larval *Xenopus laevis* (**a** stages 43–45, **b** 52–54, and **c** 64–66, respectively). *Arrows* indicate bands corresponding to the predicted molecular weights of $G\alpha_i$ and $G\alpha_o$ (~40 kDa) and $G\alpha_{olf/s}$ (~44 kDa). The $G\alpha_i$ antibody is highly specific, whereas $G\alpha_o$ and $G\alpha_{olf/s}$ antibodies show minor crossreactivity to other proteins. Quantification of fluorescence intensity of G protein labeling for $G\alpha_i$ (**c** $n = 9$ MOEs), Gαo (**f** $n = 7$ MOEs) and $G\alpha_{olf/s}$ (**i** $n = 5$ MOEs). $G\alpha_i$ and Gαo are enriched laterally, whereas $G\alpha_{olf/s}$ shows clear depletion in the lateral segment. Significance was evaluated by *t* test (*$p < 0.05$, **$p < 0.01$; *error bars* show SEM). *A* anterior, *P* posterior, *L* lateral, *M* medial, *OO* olfactory organ, *OB* olfactory bulb

teleost fish, but not in mammals, which express *v1r* genes generally in the VNO, with few exceptions [48–50]. Thus, the amphibian VNO appears to represent a transition state, morphologically clearly a distinct organ like the mammalian one, but molecularly in an intermediate stage compared to the mammalian VNO.

Spatial distribution of several *or* genes parallels that of the medial odor processing stream

To compare the spatial expression patterns of olfactory receptor genes in the MOE with the previously identified lateral and medial odor processing streams, we quantified the expression frequency for ten different genes by in situ hybridization, applying the previously used subdivision into medial, intermediate, and lateral regions (Fig. 7). About 100 tissue sections were evaluated per gene, resulting in counts of over 100–200 labeled cells per gene. These experiments showed clear and highly significant differences in the spatial distribution of individual olfactory receptor genes.

Notable was a group of genes showing strong and significant depletion in the lateral third of the MOE ($p < 0.01$, Fig. 7). This group encompasses all three class II *or* genes examined and one of the class I *or* genes. Another class I *or* gene shows the same tendency, which, however, does not reach significance. This expression pattern is very similar to the spatial patterns observed for the medial odor processing stream described above, consistent with class II and at least some class I ORs underlying the odor responses associated with the medial stream.

At least one class I *or* and one *v1r* gene are distributed rather evenly between the three subdivisions of the MOE. Such expression patterns could be part of either the lateral or the medial stream, due to the broad and partly overlapping nature of both streams, and therefore no tentative assignment to either of these streams is possible. Interestingly, another *v1r* gene, *v1r6*, shows a distribution not encountered for any of the odor responses and G proteins examined, namely a pronounced depletion in the intermediate region, highly significant in comparison to both the lateral and the medial region. The third *v1r* gene, *v1r11*, exhibits a similar pattern, which however, only reaches significance in the intermediate-to-medial comparison.

The spatial distribution of the *taar* gene parallels that of the lateral odor processing stream

Somewhat unexpectedly, the *taar* gene investigated showed a very pronounced lateral enrichment (Fig. 7), very similar to the spatial distribution of amino acid responses (Fig. 3). Thus, the *taar* gene might be a candidate for mediating amino acid responses. However, the *taar* gene family in *Xenopus* comprises just three genes [46], one of which is not expressed in the olfactory system (Fig. 6j), which is much less than expected judging from the frequency and diversity of reported amino acid responses [28].

Since a fish V2R has been shown to bind amino acids [51, 52], this large family appeared to be a good candidate for additional receptors with a lateral enrichment.

However, the V2R subclade examined here using a broadly cross-reactive probe very rarely shows any expression in the MOE (data not shown). Furthermore, expression patterns for several genes from other V2R subclades also do not parallel the amino acid response pattern (A.S., S.I.K., unpublished observation).

Taken together, the medial olfactory stream is characterized by expression of class II *or* and at least some class I *or* genes in ciliated ORNs that are activated by, among others, alcohols, aldehydes and ketones and signal via $G\alpha_{olf/s}$ (Fig. 8, blue hues). The lateral olfactory stream responds, among others, to amino acids, and signals via $G\alpha_i$ and $G\alpha_o$ (Fig. 8, red hues). Its olfactory receptors could include *taar* genes. Interestingly, neuronal responses to bile acids and amines may be carried by both streams (Fig. 8, green hues).

Discussion

The building principles structuring the olfactory sense of teleost fishes are very different from that of terrestrial mammals. Spatial segregation into different olfactory subsystems and distinct segregation even within such subsystems are a hallmark of mammals [2], whereas a single sensory surface with little segregation is observed in the olfactory system of teleost fishes [53]. It is not known how this major reorganization of the olfactory system took place during evolution of terrestrial vertebrates. The presence of an accessory olfactory system in lungfish [5, 6], a close relative of tetrapods, might indicate that this structure arose early in the evolution of lobe-finned fishes. However, the vomeronasal primordia of lungfish are morphologically very different from the VNO of mammals and may well have arisen as lineage-specific specializations. The pronounced topography of the projection from MOE to olfactory bulb observed in some cartilaginous fish [54] appears to be an example of such lineage-specific specialization, since neither mammals nor teleost fish exhibit this feature.

Here we have examined the olfactory system of the amphibian *X. laevis*, an early diverging tetrapod. We focused this analysis on the larval olfactory system, since adults have undergone complex restructuring during metamorphosis, making them less suitable for comparison to the mammalian (and teleost) olfactory system. Furthermore, *Xenopus* larvae are fully aquatic, allowing the comparison of aquatic with terrestrial tetrapods. Their olfactory epithelium shows clear morphological separation into two subsystems, the

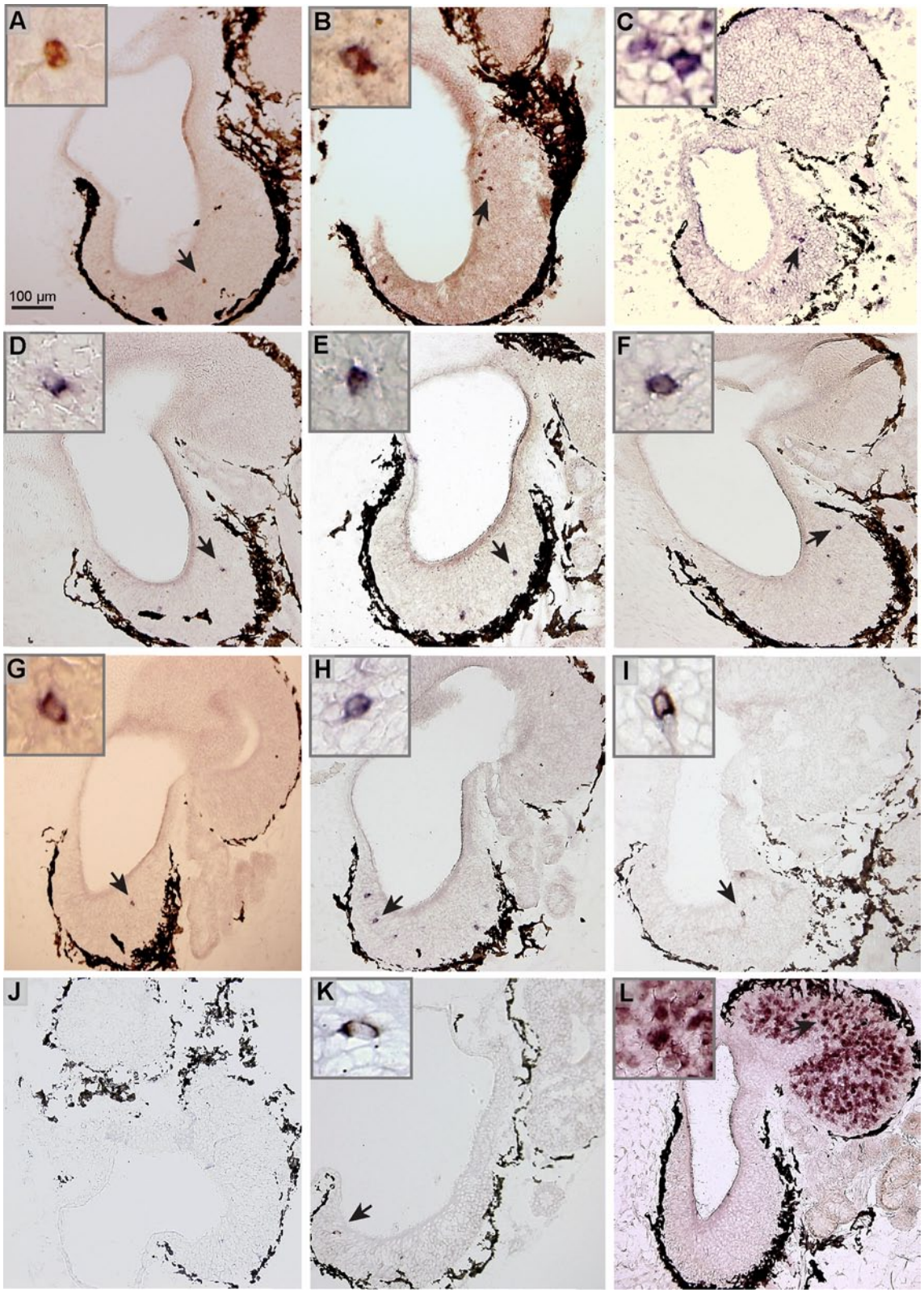

MOE and the VNO [42, 55], but the MOE still appears to be much more heterogeneous than the MOE of mammals [15, 27]. We have quantitatively analyzed several molecular and functional parameters within the MOE and olfactory bulb of *X. laevis* to establish the degree of segregation in this olfactory subsystem.

◀ **Fig. 6** Spatial expression patterns of olfactory receptor genes from the different families. Twelve genes from four olfactory receptor families were cloned by PCR using either the published *Xenopus laevis* sequence information for the primer or degenerated primer based on the *Xenopus tropicalis* sequence. The clones were confirmed by sequencing and riboprobes were prepared. In situ hybridization (**a**–**l**) was performed under stringent conditions, using cryostat sections of larval *Xenopus* nose tissue, which encompassed both the MOE and the VNO. *Insets* show enlargements of cells marked by *arrow*. Class I *or* genes (**a** *xr116*, **b** *xb242*, **c** *or52d1*); class II *or* genes (**d** *xb180*, **e** xb177, **f** *xgen147*); *v1r* genes (**g** *v1r10*, **h** *v1r11*, **i** *v1r6*); *taar* genes (**j** *taar1*, **k** *taar4a*); **l** *v2r* gene *xv2r E-1*. Results for *xr116* and *xgen147* are consistent with in situ hybridization results obtained by Mezler and coworkers [16] for similar larval stages, and the result for *xv2r E-1* is consistent with reports by Hagino-Yamagishi and coworkers [15]

Incomplete segregation of the vomeronasal system from the main sensory system

Most amphibian species, including *Xenopus*, have both a MOE and a VNO [42, 56]. We have used a broadly crossreactive probe hybridizing with at least 75 different *v2r* genes and find nearly exclusive expression in the VNO. The occasional labeled cells in the MOE most likely represent fuzzy targeting of these *v2r* genes since the frequency of MOE expression is well below that of other individual receptor genes. The expression pattern we observed is similar to the one observed for some *v2r* genes in larval and adult *X. laevis* [15]. We estimate that our probe samples roughly one-fifth of the *Xenopus* V2R repertoire [57]. Several other *v2r* genes we have examined show VNO-specific expression as well (A.S. and S.I.K., unpublished observation). In contrast, we found the *v1r*-like receptor genes to be expressed exclusively in the MOE, like their teleost counterparts (*ora* genes, [58]), and unlike the mammalian *v1r* genes, which are mostly restricted to the VNO ([2], for exceptions see [48, 49]). This expression is retained during the complex morphological reorganization taking place during metamorphosis (cf. [27]).

Taken together, the vomeronasal system appears to have originated as a segregated system for V2R-expressing neurons only. This opens the fascinating possibility that some time after the divergence of amphibians from the tetrapod lineage V1R-expressing neurons may have been reprogrammed for targeting the VNO.

G proteins in the MOB define the medial and lateral streams

Anatomically, three large and one small ventromedial glomerular cluster can be distinguished in the larval *X. laevis* olfactory bulb [18, 59]. Such glomerular clusters also have been described in other lower vertebrates (see [12, 60–62]). We have shown that the lateral and medial cluster are distinguished by their exclusive and complementary expression of G proteins, non-overlapping afferent pattern at extreme lateral and medial positions, as well as exclusive and complementary responses to two odor groups, amino acids and alcohols, aldehydes and ketones. The intermediate cluster appears to be a transition zone, with mixed identity. These results confirm and extend earlier results by some of the authors [18].

The sharp segregation of $G\alpha_{olf/s}$ and $G\alpha_i/G\alpha_o$ protein expression into a medial and a lateral half of the MOB shows that these G proteins demarcate the medial and the lateral olfactory stream, respectively. The co-expression of $G\alpha_{olf/s}$ with tubulin, a marker of ciliated neurons, shows the medial stream to be composed of ciliated ORNs. Correspondingly, the co-expression of $G\alpha_i$ and $G\alpha_o$ with phalloidin, a marker for f-actin, shows microvillous ORNs as a main component of the lateral odor processing stream. This is reminiscent of similar G protein spatial patterns in the lamprey and goldfish olfactory system [62, 63], although the segregation is less strict for the fish olfactory system.

Odor responses to amino acids and alcohols, aldehydes, and ketones are strictly segregated to the lateral and the medial stream, respectively

The complete absence of amino acid-responding glomeruli in the medial olfactory bulb, and the complementary total absence of alcohol, aldehyde, and ketone-responding glomeruli in the lateral olfactory bulb show that there are clear-cut functional differences between the medial and lateral olfactory processing stream. It is worth pointing out that this is not valid for all odor groups, as amines and bile acids are represented in both streams and indeed we find both forskolin-sensitive (cAMP-dependent) and forskolin-insensitive neurons in these two odor groups. Nevertheless, we can conclude that responses to amino acids in *X. laevis* are carried exclusively by microvillous receptor neurons and that responses to alcohols, ketones, and aldehydes are carried exclusively by ciliated receptor neurons. For amino acids, this corresponds to the situation in fishes ([12, 41] but see [11, 32, 33, 64, 65]) and for alcohols, aldehydes, and ketones it is very reminiscent of the mammalian situation [66]. The distribution of amine and bile acid responses to both streams appears to be less specific than in fish (catfish: [11]; zebrafish: [33]; goldfish: [32], but see salmon: [67]), but has some parallels in the mammalian system, where, e.g., amines have been found to elicit responses both in the main and the accessory olfactory system [68].

The lateral and medial olfactory streams are partially segregated already in the sensory surface

We observe $G\alpha_{olf/s}$, the marker of the medial stream to be strongly depleted, but not absent in the lateral region of

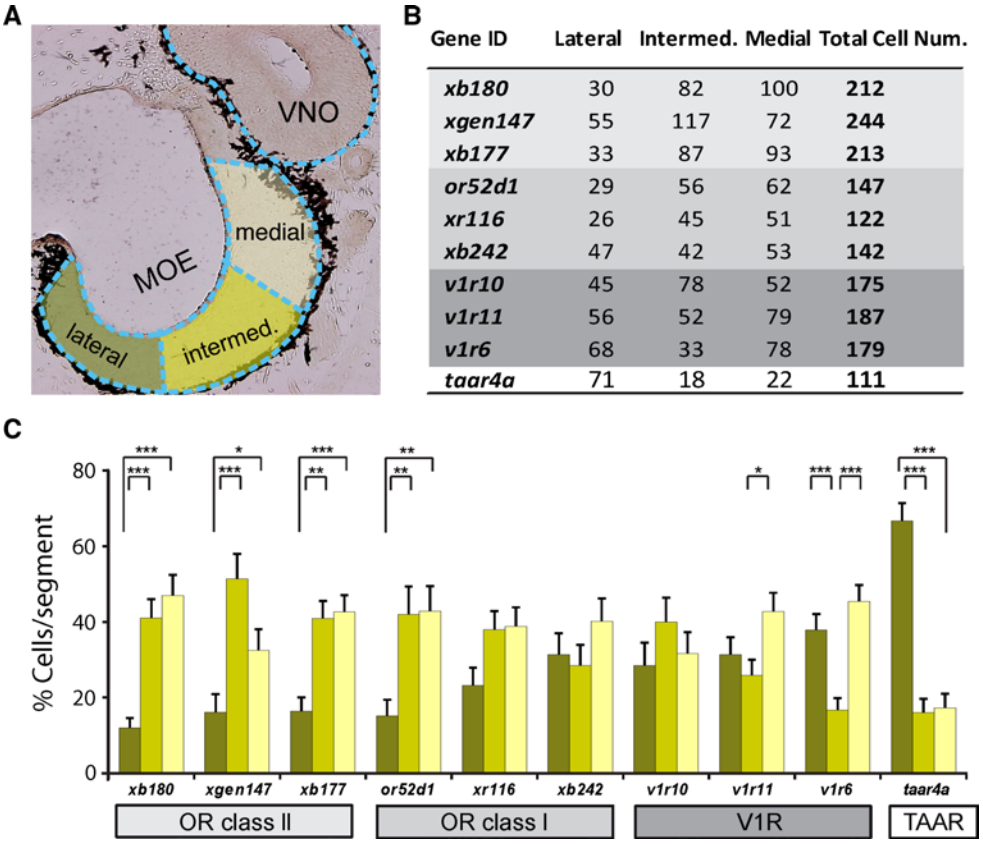

Fig. 7 Quantification of lateral-to-medial distribution of ten olfactory receptor genes. **a** Schematic illustration showing the three subdivisions of the MOE, lateral, intermediate, and medial, respectively. **b** Cumulative number of cells counted for each gene in lateral, intermediate, and medial subdivision and total number. *or* class II genes *light grey background*; *or* class I genes, *dark grey background*; *v1r* genes, *middle grey background*; *taar* gene, *white background*. **c** Quantitative evaluation of the spatial distribution for ten genes, same color code as in **a**, lateral (*dark green*), intermediate (*light green*) and medial (*yellow*) parts of the MOE. Percentage of cells in each segment was determined for each section, averaged over sections and shown as mean ± SEM. Significance was determined by *t* test and is denoted by *asterisks*: $*p < 0.05$, $**p < 0.01$, $***p < 0.002$, *error bars* show SEM

the MOE, and vice versa we find $G\alpha_i$ and $G\alpha_o$, markers of the lateral stream, to be depleted in the medial region of the MOE. The response to amino acids is strongly enriched in the lateral region, similar to the distribution of $G\alpha_i$ and $G\alpha_o$ immunoreactivity, as expected from the co-localization of these parameters in the lateral olfactory bulb. While alcohol, aldehyde, and ketone-responding cells were too sparse to allow an accurate determination of spatial distribution, we find the expected medial enrichment of forskolin responses, which serve as indicator of cAMP-responsive neurons, i.e., ciliated neurons. Interestingly, the forskolin distribution is considerably broader than the $G\alpha_{olf/s}$ distribution. While we cannot exclude methodological explanations (different thresholds could explain different steepness of the distribution), it is also conceivable that some ciliated neurons may not signal through $G\alpha_{olf/s}$, as has been observed for lamprey [62].

Medial and lateral enrichment factors range between 1.5 and 3-fold, and are thus clearly less pronounced than the near complete separation we observe for the corresponding parameters in the olfactory bulb. In other words, an incomplete segregation of different functionalities in the olfactory sensory surface is completed en route to the olfactory bulb by further sorting out of the axons of the corresponding receptor neuron subpopulations.

The medial olfactory stream may be signaling via class II odorant receptors

The distributions so far discussed presumably result from a summation over a multitude of different olfactory receptors, and expression patterns of individual receptor genes might deviate to some extent from the averaged distributions. However, a receptor distribution mimicking those of G proteins or odor responses would allow the hypothesis that such a receptor is expressed in the respective olfactory stream.

We found all three class II and one class I odorant receptor examined to be strongly depleted in the lateral region of the MOE, with ratios very similar to that of $G\alpha_{olf/s}$. We conclude that some class II (the so-called mammalian-like) *or* genes appear to be expressed in ciliated neurons of the medial olfactory stream. Further analysis will be required to see to what extent this is generalizable to all class II *or* genes. Class I (so-called fish-like) *or* genes may be more heterogeneous as we find already two different spatial patterns (medial enriched and ubiquitous) in the three genes analyzed. No candidates for laterally enriched *or* genes have been found, but we cannot exclude that other class I or class II genes among the large family of *or* genes might show such a distribution.

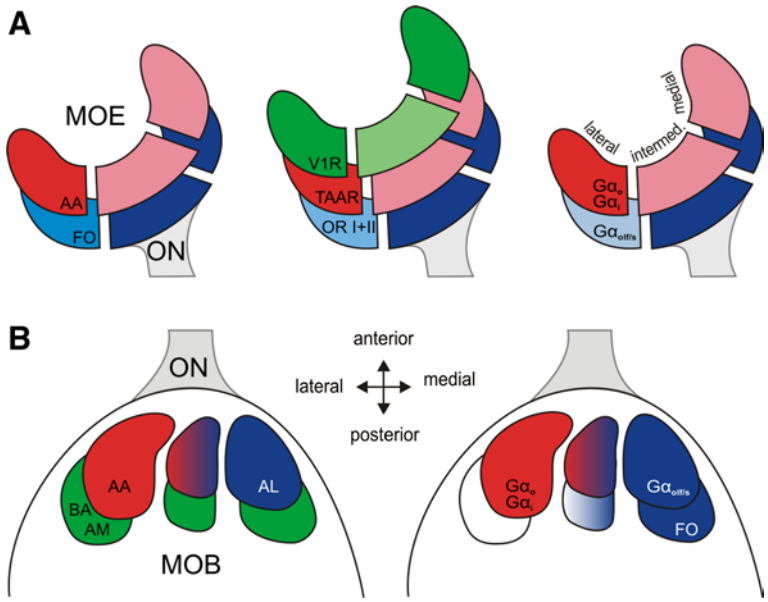

Fig. 8 Schematic representation of the lateral and medial olfactory stream in larval *Xenopus laevis*. **a** Spatial distributions observed in the MOE. The lateral stream (*red hues*) is characterized by amino acid responses (*left panel*), *taar* receptors (*middle panel*) and $G\alpha_i/G\alpha_o$ (*right panel*). The medial stream (*blue hues*) is represented by forskolin responses, all *or* class II and some *or* class I receptors, and expression of $G\alpha_{olf/s}$. Some receptors (*green hues*) are homogenously distributed or show a depletion in the intermediate region (*v1r* genes). **b** Spatial distributions observed in the MOB. The lateral stream (*red hues*) is characterized by amino acid responses (*left panel*), and expression of $G\alpha_i/G\alpha_o$ (*right panel*). The medial stream (*blue hues*) is represented by responses to alcohols, ketones, aldehydes and forskolin, and expression of $G\alpha_{olf/s}$. Responses to other odors (bile acids, amines, *green hues*) are rather homogenously distributed. *ON* olfactory nerve, *V1R* vomeronasal receptor genes of type 1, *V2R* vomeronasal receptor genes of type 2, *OR I* odorant receptor genes class I, *OR II* odorant receptor genes class II, *TAAR* trace amine-associated receptors, *AA* mixture of amino acids, *AL* mixture of alcohols, ketones and aldehydes, *AM* mixture of amines, *BA* mixture of bile acids, *FO* forskolin

A *taar* gene as candidate for the lateral odor-processing stream

Our data do suggest *taar4a* as a receptor gene candidate for the lateral olfactory stream. This came unexpectedly, since ligands for mammalian *taar* genes are believed to be mainly amines [45], which exhibit major biochemical differences to amino acids. In this context, it will be interesting to search for ligands of the *Xenopus taar* genes. Furthermore, responses to amino acids are much more frequent than that to the other three odor groups examined, and also very diverse [28], arguing for a sizable group of receptors dedicated to their detection, and not just two genes (of the three *taar* genes present in *Xenopus*, *taar1* is not expressed in the olfactory system).

The *v2r* gene family would appear to contain plausible candidates, since it contains over 300 genes in *Xenopus* [57], and one *v2r* receptor has been shown to be an amino acid receptor in two fish species [51, 52]. However, our probe, crossreacting with at least 75 different V2Rs and representing the largest subclade of the *Xenopus* V2R family [57], shows nearly exclusive expression in the VNO, consistent with findings by Hagino-Yamagishi and coworkers [15]. The occasional labeled cells in the MOE observed by us as well as others [15] are too rare to explain a major reactivity of this tissue. Furthermore, expression patterns for several genes from other V2R subclades also do not parallel the amino acid response pattern (A.S., S.I.K., unpublished observation). However, a truly comprehensive analysis of olfactory receptor families each comprising several hundred genes (*Xenopus or*, *v2r* genes, see [57, 69, 70]) is not feasible, and so the molecular nature of at least the majority of amino acid receptors remains an open question for now.

The fourth olfactory receptor gene family, *v1r* genes appear to be unlikely candidates for generating the complete lateral stream, as this rather small population of about two dozen receptors [57, 58] does not appear large enough. Moreover, the three representatives examined here show no lateral enrichment, but in two cases a near homogeneous distribution, and in one case a new pattern, a depletion restricted to the intermediate segment.

Xenopus laevis shows absence of correlation between aquatic life style and spatial segregation tendency

The present study revealed the existence of two distinct olfactory subsystems within the main olfactory system of larval *X. laevis*. A lateral and a medial odor-processing stream show clearly diverging odorant sensitivities, distinct

transduction mechanisms with differing G proteins, receptor neurons with different morphology (microvillous vs. ciliated), as well as differences in the expression frequencies of olfactory receptor genes, notwithstanding the absence of lateralization for some odor responses and receptors. These lateral and medial processing streams should not be confused with the segregation of the adult olfactory epithelium into a lateral and a medial diverticulum, which express class I and class II olfactory receptors, respectively [29]. During metamorphosis, complex reorganizations take place, and while the medial enrichment of larval *or* class II receptors is reminiscent of their expression in the medial diverticulum (also named principal cavity, or air nose) in the adult, the ubiquitous or medially enriched distribution of larval *or* class I receptors is clearly different from their restricted expression in the adult lateral diverticulum (other names are middle cavity, water nose). The presence of a vomeronasal epithelium in the adult medial diverticulum (posterolateral area of the principal cavity; see [71]) also has no parallel in the larval olfactory system [15].

Since the transition from aqueous to airborne olfaction has not yet occurred for the fully aquatic tadpoles of *X. laevis*, the distinct, if limited, tendency to spatial segregation appears unrelated to this transition and indeed may be an inherent characteristic of evolution in the lobe-finned fish lineage, cf. [5, 6]. In the ray-finned lineage there exist very few data concerning spatial segregation in the epithelium, but expression of *or* genes shows radially symmetric domains [53] unlike the left/right asymmetry observed here. Backtracing from small regions of the zebrafish olfactory bulb results in widespread labeled cells in the olfactory epithelium [72], unlike the more restricted distributions of backtraced neurons observed here. In conclusion, the olfactory system of *X. laevis* shows distinct, but incomplete segregation in the main olfactory system and thus appears well suited to investigate the molecular driving forces behind such olfactory regionalization.

Acknowledgments The authors thank Gudrun Federkeil, Christina Patzelt, and Mehmet Saltürk for expert technical help. We are grateful to Ashiq Hussain for introducing A.S. to the wet lab. Christian Muchowski and Mehmet Saltürk both kindly have provided two clones for in situ hybridization. The authors would also like to thank the reviewers for their valuable comments and suggestions. This work was supported by DFG Schwerpunktprogramm 1392 (I.M. and S.K.) and DFG Cluster of Excellence "Nanoscale Microscopy and Molecular Physiology of the Brain" (I.M.).

Conflict of interest The authors declare that they have no conflicts of interest.

References

1. Mombaerts P (2004) Genes and ligands for odorant, vomeronasal and taste receptors. Nat Rev Neurosci 5:263–278
2. Munger SD, Leinders-Zufall T, Zufall F (2009) Subsystem organization of the mammalian sense of smell. Annu Rev Physiol 71:115–140
3. Mori K, Sakano H (2011) How is the olfactory map formed and interpreted in the mammalian brain? Annu Rev Neurosci 34:467–499
4. Grüneberg H (1973) A ganglion probably belonging to the N. terminalis system in the nasal mucosa of the mouse. Z Anat Entwicklungsgesch 140:39–52
5. Gonzalez A, Morona R, Lopez JM, Moreno N, Northcutt RG (2010) Lungfishes, like tetrapods, possess a vomeronasal system. Front Neuroanat 4. Art no 130
6. Nakamuta S, Nakamuta N, Taniguchi K, Taniguchi K (2012) Histological and ultrastructural characteristics of the primordial vomeronasal organ in lungfish. Anat Rec (Hoboken) 295: 481–491
7. Taniguchi K, Saito S, Taniguchi K (2011) Phylogenic outline of the olfactory system in vertebrates. J Vet Med Sci 73:139–147
8. Hamdani el H, Doving KB (2007) The functional organization of the fish olfactory system. Prog Neurobiol 82:80–86
9. Korsching S (2009) The molecular evolution of teleost olfactory receptor gene families. Results Probl Cell Differ 47:37–55
10. Oka Y, Korsching SI (2011) Shared and unique G alpha proteins in the zebrafish versus mammalian senses of taste and smell. Chem Senses 36:357–365
11. Hansen A, Rolen SH, Anderson K, Morita Y, Caprio J et al (2003) Correlation between olfactory receptor cell type and function in the channel catfish. J Neurosci 23:9328–9339
12. Sato Y, Miyasaka N, Yoshihara Y (2005) Mutually exclusive glomerular innervation by two distinct types of olfactory sensory neurons revealed in transgenic zebrafish. J Neurosci 25: 4889–4897
13. Hayden S, Bekaert M, Crider TA, Mariani S, Murphy WJ et al (2010) Ecological adaptation determines functional mammalian olfactory subgenomes. Genome Res 20:1–9
14. Manzini I, Schild D (2010) Olfactory Coding in Larvae of the African Clawed Frog *Xenopus laevis*. In: Menini A (ed) The Neurobiology of Olfaction. Chap 4, CRC Press, Boca Raton
15. Hagino-Yamagishi K, Moriya K, Kubo H, Wakabayashi Y, Isobe N et al (2004) Expression of vomeronasal receptor genes in *Xenopus laevis*. J Comp Neurol 472:246–256
16. Mezler M, Konzelmann S, Freitag J, Rössler P, Breer H (1999) Expression of olfactory receptors during development in *Xenopus laevis*. J Exp Biol 202:365–376
17. Ji Y, Zhang Z, Hu Y (2009) The repertoire of G-protein-coupled receptors in *Xenopus tropicalis*. BMC Genomics 10:263
18. Manzini I, Heermann S, Czesnik D, Brase C, Schild D et al (2007) Presynaptic protein distribution and odour mapping in glomeruli of the olfactory bulb of *Xenopus laevis* tadpoles. Eur J Neurosci 26:925–934
19. Nieuwkoop PD, Faber J (1994) Normal table of *Xenopus laevis* (Daudin). Garland Publishing, Inc., New York
20. Czesnik D, Rössler W, Kirchner F, Gennerich A, Schild D (2003) Neuronal representation of odourants in the olfactory bulb of *Xenopus laevis* tadpoles. Eur J Neurosci 17:113–118
21. Manzini I, Schild D (2003) cAMP-independent olfactory transduction of amino acids in *Xenopus laevis* tadpoles. J Physiol 551:115–123
22. Manzini I, Schild D (2003) Multidrug resistance transporters in the olfactory receptor neurons of *Xenopus laevis* tadpoles. J Physiol 546:375–385

23. Manzini I, Schweer TS, Schild D (2008) Improved fluorescent (calcium indicator) dye uptake in brain slices by blocking multidrug resistance transporters. J Neurosci Methods 167:140–147
24. Junek S, Chen TW, Alevra M, Schild D (2009) Activity correlation imaging: visualizing function and structure of neuronal populations. Biophys J 96:3801–3809
25. Hassenklöver T, Kurtanska S, Bartoszek I, Junek S, Schild D et al (2008) Nucleotide-induced Ca2+ signaling in sustentacular supporting cells of the olfactory epithelium. Glia 56:1614–1624
26. Mezler M, Fleischer J, Conzelmann S, Korchi A, Widmayer P et al (2001) Identification of a nonmammalian Golf subtype: functional role in olfactory signaling of airborne odorants in *Xenopus laevis*. J Comp Neurol 439:400–410
27. Date-Ito A, Ohara H, Ichikawa M, Mori Y, Hagino-Yamagishi K (2008) *Xenopus* V1R vomeronasal receptor family is expressed in the main olfactory system. Chem Senses 33:339–346
28. Manzini I, Schild D (2004) Classes and narrowing selectivity of olfactory receptor neurons of *Xenopus laevis* tadpoles. J Gen Physiol 123:99–107
29. Freitag J, Krieger J, Strotmann J, Breer H (1995) Two classes of olfactory receptors in *Xenopus laevis*. Neuron 15:1383–1392
30. Gliem S, Schild D, Manzini I (2009) Highly specific responses to amine odorants of individual olfactory receptor neurons in situ. Eur J Neurosci 29:2315–2326
31. Carr WES, Derby CD (1986) Chemically stimulated feeding-behavior in marine animals—importance of chemical-mixtures and involvement of mixture interactions. J Chem Ecol 12:989–1011
32. Rolen SH, Sorensen PW, Mattson D, Caprio J (2003) Polyamines as olfactory stimuli in the goldfish *Carassius auratus*. J Exp Biol 206:1683–1696
33. Michel WC, Sanderson MJ, Olson JK, Lipschitz DL (2003) Evidence of a novel transduction pathway mediating detection of polyamines by the zebrafish olfactory system. J Exp Biol 206:1697–1706
34. Sorensen PW, Caprio J (1998) Chemoreception. In: Evans DH (ed) The physiology of fishes. CRC Press, Boca Raton, pp 251–261
35. Altner H (1962) Untersuchungen über Leistungen und Bau der Nase des südafrikanischen Krallenfrosches *Xenopus laevis* (Daudin, 1803). Z Vlg Physiol 45:272–306
36. Manzini I, Brase C, Chen TW, Schild D (2007) Response profiles to amino acid odorants of olfactory glomeruli in larval *Xenopus laevis*. J Physiol 581:567–579
37. Touhara K (2002) Odor discrimination by G protein-coupled olfactory receptors. Microsc Res Tech 58:135–141
38. Manzini I, Rössler W, Schild D (2002) cAMP-independent responses of olfactory neurons in *Xenopus laevis* tadpoles and their projection onto olfactory bulb neurons. J Physiol 545:475–484
39. Friedrich RW, Korsching SI (1998) Chemotopic, combinatorial, and noncombinatorial odorant representations in the olfactory bulb revealed using a voltage-sensitive axon tracer. J Neurosci 18:9977–9988
40. Korsching SI (2001) Odor maps in the brain: spatial aspects of odor representation in sensory surface and olfactory bulb. Cell Mol Life Sci 58:520–530
41. Friedrich RW, Korsching SI (1997) Combinatorial and chemotopic odorant coding in the zebrafish olfactory bulb visualized by optical imaging. Neuron 18:737–752
42. Hansen A, Reiss JO, Gentry CL, Burd GD (1998) Ultrastructure of the olfactory organ in the clawed frog, *Xenopus laevis*, during larval development and metamorphosis. J Comp Neurol 398:273–288
43. Wieland T (1987) 50 years of phalloidine: its discovery, characterization and current and future applications in cell research. Naturwissenschaften 74:367–373
44. Corbit KC, Aanstad P, Singla V, Norman AR, Stainier DY et al (2005) Vertebrate smoothened functions at the primary cilium. Nature 437:1018–1021
45. Liberles SD, Buck LB (2006) A second class of chemosensory receptors in the olfactory epithelium. Nature 442:645–650
46. Hussain A, Saraiva LR, Korsching SI (2009) Positive Darwinian selection and the birth of an olfactory receptor clade in teleosts. Proc Natl Acad Sci USA 106:4313–4318
47. Strotmann J, Wanner I, Helfrich T, Beck A, Meinken C et al (1994) Olfactory neurones expressing distinct odorant receptor subtypes are spatially segregated in the nasal neuroepithelium. Cell Tissue Res 276:429–438
48. Karunadasa DK, Chapman C, Bicknell RJ (2006) Expression of pheromone receptor gene families during olfactory development in the mouse: expression of a V1 receptor in the main olfactory epithelium. Eur J Neurosci 23:2563–2572
49. Wakabayashi Y, Mori Y, Ichikawa M, Yazaki K, Hagino-Yamagishi K (2002) A putative pheromone receptor gene is expressed in two distinct olfactory organs in goats. Chem Senses 27:207–213
50. Rodriguez I, Greer CA, Mok MY, Mombaerts P (2000) A putative pheromone receptor gene expressed in human olfactory mucosa. Nat Genet 26:18–19
51. Speca DJ, Lin DM, Sorensen PW, Isacoff EY, Ngai J et al (1999) Functional identification of a goldfish odorant receptor. Neuron 23:487–498
52. Luu P, Acher F, Bertrand HO, Fan J, Ngai J (2004) Molecular determinants of ligand selectivity in a vertebrate odorant receptor. J Neurosci 24:10128–10137
53. Weth F, Nadler W, Korsching S (1996) Nested expression domains for odorant receptors in zebrafish olfactory epithelium. Proc Natl Acad Sci USA 93:13321–13326
54. Meredith T, Hansen A (2010) Hemi-bulb organization in the elasmobrach brain. Chem Senses 35:A85
55. Oikawa T, Suzuki K, Saito TR, Takahashi KW, Taniguchi K (1998) Fine structure of three types of olfactory organs in *Xenopus laevis*. Anat Rec 252:301–310
56. Taniguchi K, Saito S, Oikawa T, Taniguchi K (2008) Phylogenic aspects of the amphibian dual olfactory system. J Vet Med Sci 70:1–9
57. Shi P, Zhang J (2007) Comparative genomic analysis identifies an evolutionary shift of vomeronasal receptor gene repertoires in the vertebrate transition from water to land. Genome Res 17: 166–174
58. Saraiva LR, Korsching SI (2007) A novel olfactory receptor gene family in teleost fish. Genome Res 17:1448–1457
59. Gaudin A, Gascuel J (2005) 3D atlas describing the ontogenic evolution of the primary olfactory projections in the olfactory bulb of *Xenopus laevis*. J Comp Neurol 489:403–424
60. Riddle DR, Wong LD, Oakley B (1993) Lectin identification of olfactory receptor neuron subclasses with segregated central projections. J Neurosci 13:3018–3033
61. Baier H, Korsching S (1994) Olfactory glomeruli in the zebrafish form an invariant pattern and are identifiable across animals. J Neurosci 14:219–230
62. Frontini A, Zaidi AU, Hua H, Wolak TP, Greer CA et al (2003) Glomerular territories in the olfactory bulb from the larval stage of the sea lamprey *Petromyzon marinus*. J Comp Neurol 465: 27–37
63. Hansen A, Anderson KT, Finger TE (2004) Differential distribution of olfactory receptor neurons in goldfish: structural and molecular correlates. J Comp Neurol 477:347–359
64. Lo YH, Bradley TM, Rhoads DE (1993) Stimulation of Ca(2+)-regulated olfactory phospholipase C by amino acids. Biochemistry 32:12358–12362
65. Ma L, Michel WC (1998) Drugs affecting phospholipase C-mediated signal transduction block the olfactory cyclic nucleotide-gated current of adult zebrafish. J Neurophysiol 79:1183–1192
66. Johnson BA, Leon M (2007) Chemotopic odorant coding in a mammalian olfactory system. J Comp Neurol 503:1–34

67. Lo YH, Bellis SL, Cheng LJ, Pang J, Bradley TM et al (1994) Signal transduction for taurocholic acid in the olfactory system of Atlantic salmon. Chem Senses 19:371–380
68. Tirindelli R, Dibattista M, Pifferi S, Menini A (2009) From pheromones to behavior. Physiol Rev 89:921–956
69. Niimura Y, Nei M (2005) Evolutionary dynamics of olfactory receptor genes in fishes and tetrapods. Proc Natl Acad Sci USA 102:6039–6044
70. Shi P, Zhang J (2009) Extraordinary diversity of chemosensory receptor gene repertoires among vertebrates. Results Probl Cell Differ 47:1–23
71. Föske H (1934) Das Geruchsorgan von *Xenopus laevis*. Z Anat Entwicklungsgesch 103:519–550
72. Baier H, Rotter S, Korsching S (1994) Connectional topography in the zebrafish olfactory system: random positions but regular spacing of sensory neurons projecting to an individual glomerulus. Proc Natl Acad Sci USA 91:11646–11650

2.2 *LATIMERIA chalumnae* (COELACANTH)

2.2.1 CHARACTERIZATION of TWO CHEMOSENSORY RECEPTOR FAMILIES

This section deals with the original research article published in the journal BioMed Central Genomics (Vol. 15, No. 650, published online on August, 2014). Supplementary data associated with this article can be found in the CD attached.

BMC Genomics

RESEARCH ARTICLE Open Access

Positive Darwinian selection in the singularly large taste receptor gene family of an 'ancient' fish, *Latimeria chalumnae*

Adnan S Syed and Sigrun I Korsching*

Abstract

Background: Chemical senses are one of the foremost means by which organisms make sense of their environment, among them the olfactory and gustatory sense of vertebrates and arthropods. Both senses use large repertoires of receptors to achieve perception of complex chemosensory stimuli. High evolutionary dynamics of some olfactory and gustatory receptor gene families result in considerable variance of chemosensory perception between species. Interestingly, both *ora/v1r* genes and the closely related *t2r* genes constitute small and rather conserved families in teleost fish, but show rapid evolution and large species differences in tetrapods. To understand this transition, chemosensory gene repertoires of earlier diverging members of the tetrapod lineage, i.e. lobe-finned fish such as *Latimeria* would be of high interest.

Results: We report here the complete T2R repertoire of L*atimeria chalumnae*, using thorough data mining and extensive phylogenetic analysis. Eighty *t2r* genes were identified, by far the largest family reported for any species so far. The genomic neighborhood of *t2r* genes is enriched in repeat elements, which may have facilitated the extensive gene duplication events resulting in such a large family. Examination of non-synonymous *vs.* synonymous substitution rates (dN/dS) suggests pronounced positive Darwinian selection in *Latimeria* T2Rs, conceivably ensuring efficient neo-functionalization of newly born *t2r* genes. Notably, both traits, positive selection and enrichment of repeat elements in the genomic neighborhood, are absent in the twenty *v1r* genes of *Latimeria*. Sequence divergence in *Latimeria* T2Rs and V1Rs is high, reminescent of the corresponding teleost families. Some conserved sequence motifs of Latimeria T2Rs and V1Rs are shared with the respective teleost but not tetrapod genes, consistent with a potential role of such motifs in detection of aquatic chemosensory stimuli.

Conclusions: The singularly large T2R repertoire of Latimeria may have been generated by facilitating local gene duplication *via* increased density of repeat elements, and efficient neofunctionalization *via* positive Darwinian selection. The high evolutionary dynamics of tetrapod *t2r* gene families precedes the emergence of tetrapods, i.e. the water-to-land transition, and thus constitutes a basal feature of the lobe-finned lineage of vertebrates.

Keywords: Coelacanth, Bitter taste, Pheromone, Phylogeny, Sarcopterygian, Evolution

Background

Chemosensation is an ancient sense, its origins going all the way back to unicellular organisms. In vertebrates and arthropods, two specialized senses have evolved. The olfactory sense serves a host of essential functions, among them search for food or prey, predator evasion, mate choice and reproduction, kin recognition and signalling of social status, whereas the gustatory sense is tasked with vital decisions about safety and desirability of food sources. Neuronal representation and the logic of coding sensory input are very different for vertebrate taste and smell [1-4]. Olfactory sensory neurons form one (teleost fish), two (lungfish, amphibians) or several (mammals) extended sensory epithelia, and directly project to the (rostral) brain, whereas small clusters of taste cells (taste buds) are found distributed across several nonsensory epithelia (oral cavity, gills, skin for teleost fish), and their innervating neurons connect to (caudal) brain stem neurons. Moreover, different receptor families

* Correspondence: sigrun.korsching@uni-koeln.de
Institute of Genetics, University of Cologne, 50674 Cologne, Germany

serve olfaction and taste [1-3]. Olfactory receptor genes are typically expressed in monogenic fashion, whereas co-expression of receptors shapes the response characteristics of taste cells [1-3]. All these differences notwithstanding, closely related families do segregate between these two senses, gustatory T2Rs *vs.* olfactory V1Rs, and T1Rs *vs.* V2Rs, respectively.

Basic features of olfactory and gustatory representation appear to be conserved across vertebrates [3-7]. However, the high evolutionary dynamics of olfactory and gustatory receptor gene families allows for considerable variance in neuronal representation of chemosensory signals between species [8]. In particular, the relative importance of different chemosensory receptor gene families appears to have changed drastically between tetrapods and teleosts [9-12]. Teleost fish species possess only very small *t2r* gene families, whereas a much larger variability has been observed in tetrapods, with up to 50 genes in an amphibian species [11]. Even more strikingly, the V1R-related *ora* gene repertoires of teleosts consist of the same six genes, with an occasional gene loss [10], whereas mammalian *v1r* gene repertoires are highly species-specific [13].

It has been proposed that chemosensory receptor family sizes adapt to the particular ecological environment of each species. Mammalian T2Rs and at least one fish T2R signal bitter taste [2,14], and bitter substances often occur as chemical defense mechanism of plants. Accordingly it has been suggested that the size of the T2R repertoire is larger in herbivorous than in carnivorous species [15]. Mammalian V1Rs are assumed to detect volatile pheromones [16], which could be related to the larger size and higher species specificity of mammalian V1R families. In contrast, the homologous ORA family of fishes is expected to detect hydrophilic substances, which may serve a different biological function. To examine such hypotheses it would be useful to establish the corresponding receptor repertoires of aquatic species from the tetrapod lineage.

Teleosts belong to the ray-finned lineage of vertebrates, whereas mammals and other tetrapods belong to the lobe-finned lineage, which also includes fish like coelacanths of the genus *Latimeria* and lungfish as very early diverging representatives [17]. One might expect the *v1r* and *t2r* gene repertoires of lobe-finned fishes to resemble those of ray-finned fishes more that those of land-living tetrapods. Alternatively, the higher evolutionary dynamics observed for tetrapods could be a common feature of the lobe-finned lineage of vertebrates. Recently, the genome of the coelacanth *Latimeria chalumnae* has been published [18], but initial gene searches have resulted in highly contradictory results, showing either a teleost-like small T2R repertoire of only 5 genes [15] or a large amphibian-like repertoire of 58 genes [19]. The V1R family size has alternatively been given as 15 or 20 genes [19,20]. To clarify these discrepancies, we performed a thorough bioinformatic analysis of the *Latimeria chalumnae* genome to delineate and characterize the *t2r* and *v1r* gene repertoires in this species.

We report here that *Latimeria* possess an unequaled large *t2r* gene repertoire of eighty genes that exhibit strong evidence for positive Darwinian selection, and whose genomic neighborhood shows increased density of repeat elements. Both these features are absent in the closely related *Latimeria* V1Rs, which nevertheless show much less negative selective pressure than their teleost counterparts. Together, these findings indicate that high evolutionary dynamics of *t2r* and *v1r* gene families are not linked to the loss of aquatic life style in tetrapods, but appear to be an ancient evolutionary characteristic of the lobe-finned lineage.

Results

To delineate the Latimeria *t2r* and *v1r* gene repertoires we performed a recursive search of the preliminary draft of the *Latimeria chalumnae* genome [18] provided by the Broad Institute [21], using representative T2R and V1R/ORA protein sequences from mouse, frog (*Xenopus tropicalis*) and zebrafish as initial queries. No additional candidates were found searching an independently sequenced Latimeria genome [20]. Candidate genes were evaluated by phylogenetic analysis, using a maximum-likelihood method, PhyMl-aLRT [22]. Published T2R and V1R/ORA sequences from lamprey (*Petromyzon marinus*), five teleost fish species, frog, and mouse were used as reference. Since *t2r* genes constitute the closest neighbors of *v1r/ora* genes, each group served as stringent outgroup for the other one. In initial analyses additional outgroups were used to delineate the combined V1R + T2R group of genes from other rhodopsin-like GPCRs, with very similar results.

We observe a clear-cut segregation with very high branch support between a monophyletic T2R and a monophyletic V1R/ORA group (Figure 1). This allows to unambiguously assign candidate genes to the respective family.

An unprecedentedly large T2R repertoire results from extensive gene duplications of a single ancestral t2r gene

Eighty *t2r* genes were identified in the *Latimeria* genome (Figures 1 and 2, Additional file 1 and Additional file 2), by far the largest repertoire found in any species so far, nearly double the size of the largest previously reported repertoire, *Xenopus tropicalis* (49 genes, [11]). Seventyfive of these *Latimeria t2r* genes have been missed in a recent multi-species study [15], possibly because validation criteria used there have eliminated many *bona fide t2r* genes. Twentytwo of *Latimeria t2r* genes have been missed in a recent multi-family study [19] that seems to have investigated only previously predicted genes,

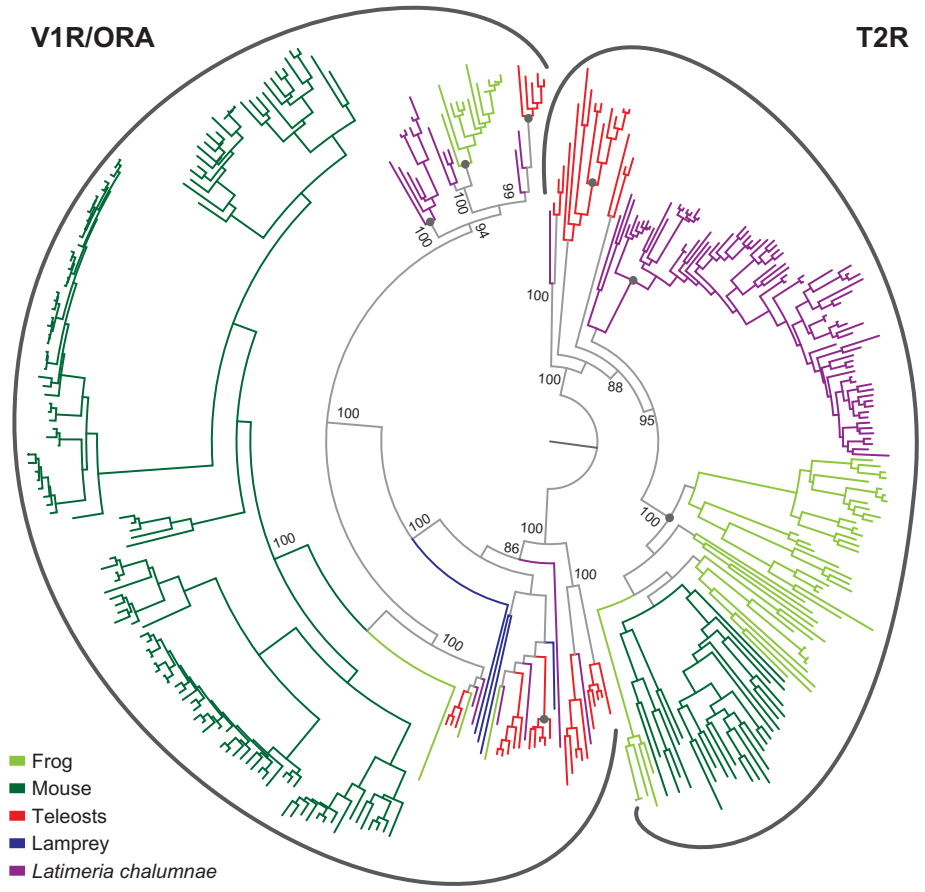

Figure 1 Monophyletic origin of the T2R and the V1R/ORA receptor family. The phylogenetic tree was generated using a maximum likelihood method (PhyML-aLRT) with SPR setting for tree optimization and chi square-based aLRT for branch support (given as percentage). Branches are color-coded for the respective species (*Latimeria chalumnae*, purple; mouse, dark green; *Xenopus tropicalis*, light green; lamprey, blue; 5 teleost fish species [zebrafish, stickleback, medaka, fugu, tetraodon], red). *t2r* of all species form a single subclade, as do all *v1r* genes. Grey filled circles indicate clades analysed for evidence of positive selection, see Figure 5. Gene sequences for *Xenopus tropicalis* and teleosts were taken from [11] for T2Rs and [10] for V1R/ORAs.

which in our experience [10,12,23,24] does not result in complete coverage of a chemosensory family. Our approach is comprehensive and does not rely on any prior annotation whatsoever, as our inclusion criterion is based solely on phylogenetic position of candidate genes, see Methods. Six of the 80 genes we report contain up to 2 stop codons and may either represent pseudogenes or databank inaccuracies. 74 genes have been validated as full length, and all 80 genes contain the expected motifs (see also Methods, and below).

The vast majority of *Latimeria t2r* genes (Lc_T2R05 to Lc_T2R80) appear to result from a single ancestral gene *via* extensive gene duplications (Figure 2). Another ancestral gene only went through 2 duplication events, resulting in Lc_T2R02 to Lc_T2R04, and no gene duplication was observed for Lc_T2R01, the third ancestral *Latimeria t2r* gene. We would like to point out that Lc_T2R01 is also the only *Latimeria t2r* gene with any ortholog in other species. Three teleost *t2r* genes, stickleback T2R3, puffer T2R1, and fugu T2R1 are direct orthologs of Lc_T2R01 (100% branch support, Figure 2). As such, Lc_T2R01 represents the first available evidence for a common origin of individual teleost and tetrapod *t2r* genes. In total, *Latimeria chalumnae* appears to possess three ancestral genes (Figure 2), two of which were subject to species-specific gene expansions. The extent of one of these gene duplications is unparalleled in any species investigated so far, but nevertheless places the Latimeria T2R family in the vicinity of tetrapod T2R repertoires, and far away from teleost T2R repertoires, which only comprise 3–6 genes [11].

The Latimeria V1R family possesses close orthologs/paralogs of all six teleost ora genes, but also exhibits several gene expansions characteristic of tetrapod V1R repertoires

Twenty *ora*-related *v1r* genes were identified in the *Latimeria* genome (Figures 1 and 3, Additional files 1 and 2),

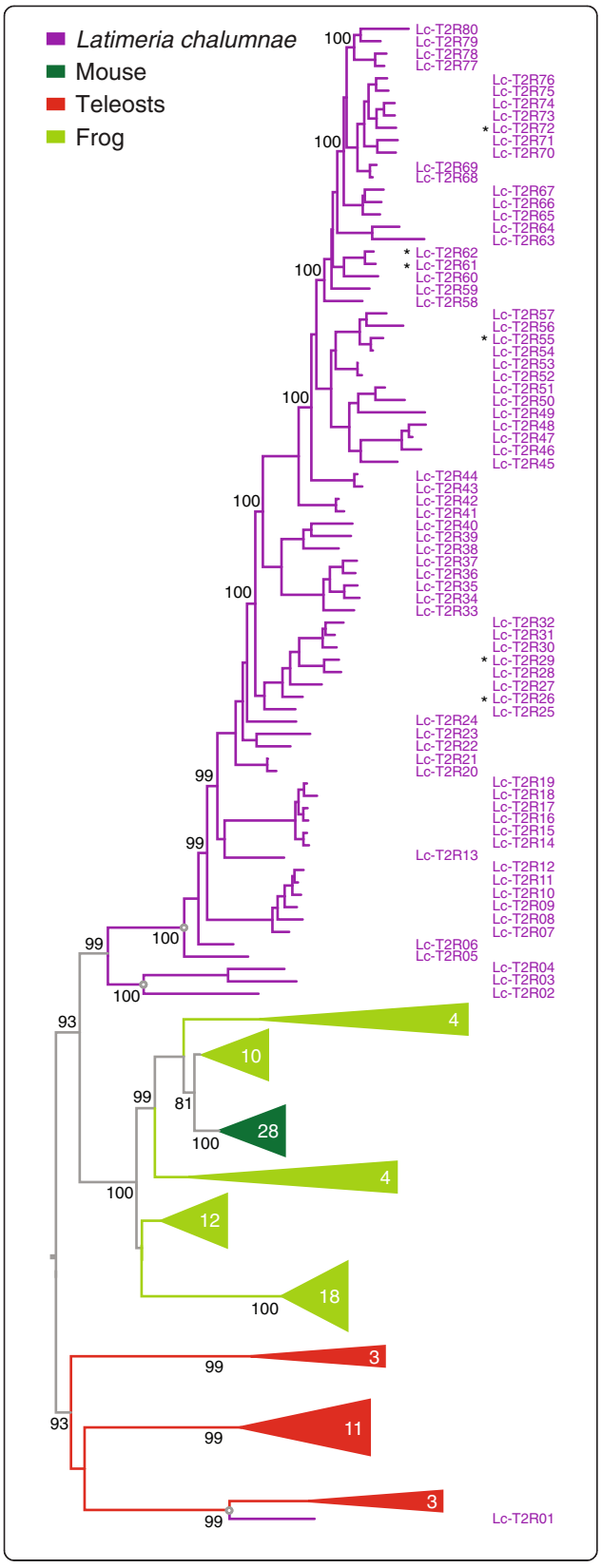

Figure 2 Three ancestral genes and a single large expansion in the Latimeria T2R family. Eighty T2R receptors of *Latimeria* were compared with T2R receptors of mouse, *Xenopus tropicalis*, and 5 teleost fishes (species and color code as given for Figure 1). The phylogenetic tree was generated as described for Figure 1; branch support is given as percentage. Asterisks, potential pseudogenes, see Methods for details. For accession numbers and genomic location of *Latimeria* genes see Additional file 1. Three ancestral genes are indicated by open circles at the respective nodes.

consistent with results of a recent phylogenetic study using data from an independent genome sequencing approach [20]. We expect this number to be very close to final, even though the genome assembly is still in draft stage [18], since the genome has been sequenced with high coverage (61 fold, [18]), and our gene identification approach is not sensitive to assembly quality. Phylogenetic analysis shows nine ancestral genes (Figure 3), six of which are shared with teleost fish (Lc_V1R01-06), and indeed three of these genes (Lc_V1R02, 03, 06) constitute direct one-to-one orthologs of the corresponding teleost *ora* genes, e.g. Lc_V1R02 is ortholog to ORA2 and so forth. The remaining 3 ancestral nodes are all located within the ORA1/ORA2 subclade, and exhibit varying degrees of gene expansion, similar to observations for later-derived species in the lobe-finned lineage such as frogs and mammals, *cf.* [25]. A small group of three *Latimeria v1r* genes (Lc_V1R08 to Lc_V1R10) emerges as sister clade to the main gene expansion in frog, whereas a larger group of 9 *Latimeria v1r* genes (Lc_V1R11 to Lc_V1R19) is more closely related to the (single) mammalian subclade of *v1r* genes (Figure 3, cf. [10]). These two gene expansions appear to have occurred independently within the *Latimeria* lineage, i.e. after divergence from the most recent common ancestor (MRCA) shared with tetrapods. Taken together, the *Latimeria* V1R repertoire shows the divergence characteristic of teleost ORA families and the gene expansion characteristic for tetrapod V1R families.

Motif analysis validates the phylogenetic assignment of Latimeria v1r and t2r genes and shows considerable species-specific conservation

T2R sequence identities can exceed 90% in pairwise comparisons, and the same holds true for pairwise comparisons of V1R sequences (*cf.* Additional file 1), consistent with an origin of such genes by recent gene duplications. However, overall both gene families are highly heterogenous, with frequent identity values between 40 to 50% and minimal identities down to 23% for T2R, and 19% for V1R sequences (Additional file 1). It therefore appeared instructive to analyse the evolution of conserved sequence motifs of T2R and V1R families in the tetrapod lineage, and to compare it to the teleost lineage. To the best of our knowledge such motif analysis

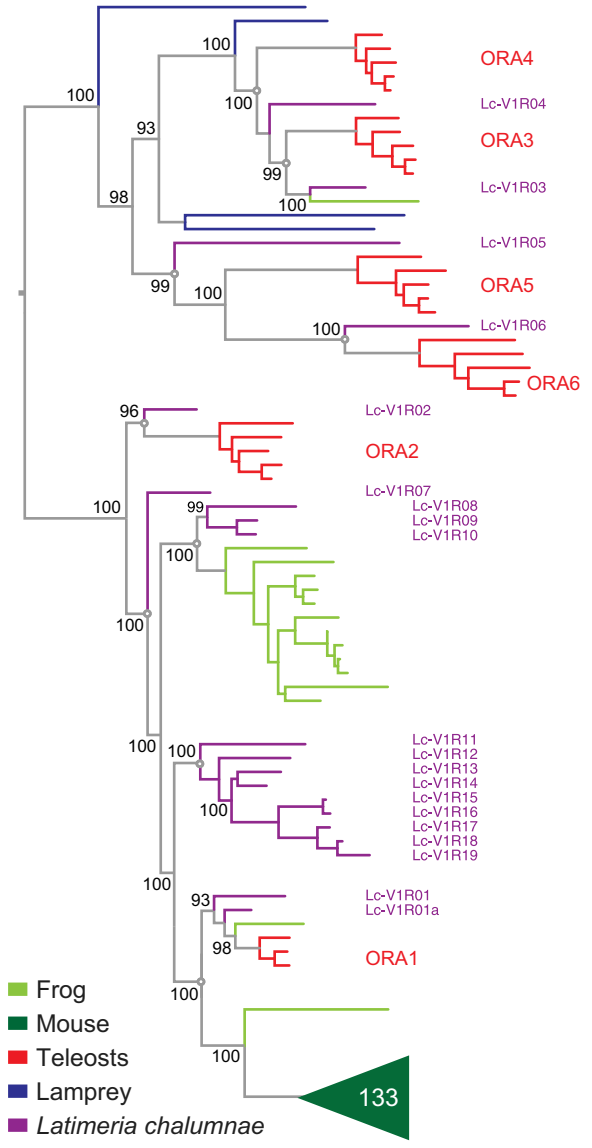

Figure 3 Teleost/tetrapod hybrid characteristics of the Latimeria V1R family. Twenty V1R receptors of *Latimeria* were compared with V1R and V1R-related ORA receptors of mouse, *Xenopus tropicalis*, lamprey and 5 teleost fishes (species and color code as given for Figure 1). The phylogenetic tree was generated as described for Figure 1. Branch support is given as percentage. For accession numbers and genomic location of *Latimeria* and lamprey genes see Additional file 1. Ancestral genes are indicated by open circles at the respective nodes.

comparing V1R and T2R families has not been performed in any species so far.

Thus we constructed separate multiple sequence alignments for tetrapod T2Rs (mouse and frog), tetrapod V1Rs (mouse and frog), teleost T2Rs and teleost V1R-related ORAs, visualized them as sequence logos [26], and compared them with those of *Latimeria* V1Rs and T2Rs (Figure 4, Additional file 1). Over 70 highly and moderately conserved amino acids were identified, organized in motifs of 1 to 3 amino acids, among them some motifs conserved in several GPCR families, and many motifs shared between *Latimeria* V1Rs and T2Rs, as expected from the close phylogenetic relationship of these two families (Figure 4). We identified 14 amino acid positions that are conserved in tetrapod and/or teleost *t2r*, but not in *v1r* genes. All but one show the same specificity in *Latimeria*. Furthermore, many amino acids are solely conserved in *Latimeria* T2Rs (22 amino acids) and two amino acids are only conserved in *Latimeria* V1R. In one case, the loss of the generally conserved cysteine in EC1 of *Latimeria* T2Rs is compensated by a cysteine in n-8 position, conserved only in *Latimeria* T2Rs. Either cysteine may form a disulfide bridge with a broadly conserved cysteine in EC2. Finally, ten positions are conserved differentially in T2Rs *vs*. V1Rs (Figure 4, Additional file 1). All these observations support the phylogeny-based assignment of *Latimeria t2r* and *v1r* genes (Figure 4, Additional file 1).

Amino acids that are differentially conserved between T2R and V1R receptors, e.g. Y_{T2R}/C_{V1R} in EC1, and $C..Y_{T2R}/S..Q_{V1R}$ in TM3, may be expected to be relevant for the functional differences between T2R and V1R receptors, and would be plausible candidates for a functional analysis by site-directed mutagenesis in future studies. In several cases residues conserved in *Latimeria* T2Rs and/or V1Rs are only conserved in either the teleost or the tetrapod lineages, e.g. a *Latimeria* T2R-specific KI motif in the IC2 region that is conserved in tetrapod T2Rs, but not in teleost T2Rs (Figure 4). Examples for motifs conserved in teleost T2Rs, but not in tetrapod T2Rs include a central Y in TM6 and in TM7 (Figure 4). Such pattern of conservation is consistent with *Latimeria* genes keeping features of the posited ancestral genes, that were differentially retained in later-deriving members of the lobe-finned lineage (tetrapods) and the ray-finned lineage (teleosts). It remains to be seen, whether residues shared with teleost, but not with tetrapod V1Rs and T2Rs, might be specifically relevant for aquatic chemosensation.

Overall, however, a high degree of divergence is visible within *Latimeria* T2Rs and within *Latimeria* V1Rs. Such high divergence might be generated by positive Darwinian selection, which has been shown to occur in several chemosensory receptor gene families [12,27-29]. We have therefore examined nucleotide substitution ratios to obtain an estimate for positive selection in *Latimeria t2r* and *v1r* gene families.

Pronounced positive selection in the T2R family suggested by dN/dS analysis

We compared the rate of **n**onsynonymous (dN) to **s**ynonymous (silent) nucleotide substitutions (*dN/dS*) separately for all codons, to obtain an estimate for the

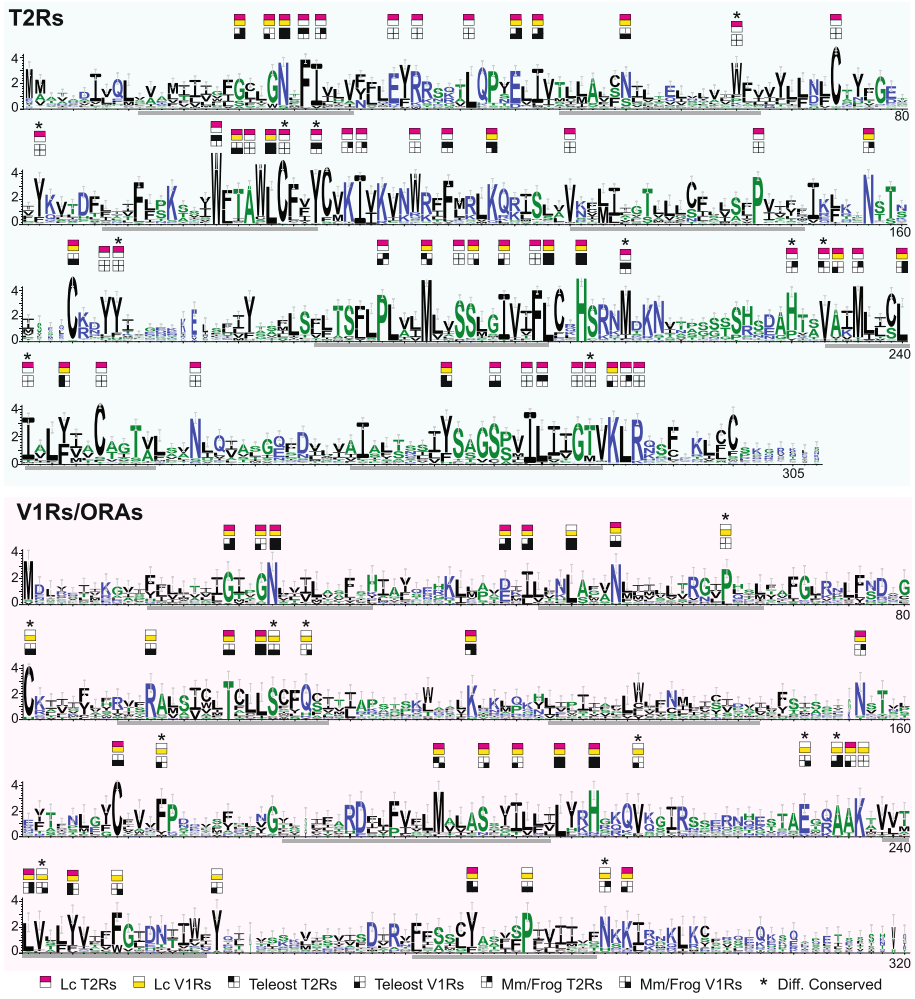

Figure 4 Motif analysis for Latimeria T2R and V1R/ORA receptors confirms results of the phylogenetic analysis. Sequence logos for 80 *Latimeria* T2Rs and 20 *Latimeria* V1Rs are shown. Letter height indicates the relative frequency with which a particular amino acid appears at that position. Amino acid conservation above 45% is indicated as follows: *Latimeria* T2Rs, magenta rectangle; *Latimeria* V1Rs, yellow rectangle; other T2Rs, upper black squares (teleost, left; mouse and frog, right); other V1Rs, lower black squares (teleost, left; mouse and frog, right). White squares and rectangles, no conservation found; asterisk, the same position is differently conserved between *Latimeria* T2Rs and V1Rs; grey bars, transmembrane domains.

evolutionary constraints acting on the *v1r* and *t2r* gene families of *Latimeria*. A value below 1 for dN/dS indicates negative selective pressure, i.e. purifying selection, whereas values larger than 1 suggest positive selection, i.e. selection for diversity [30]. dN/dS = 1 equals neutral selection. To avoid distortion of the dN/dS ratio by beginning saturation of synonymous substitutions [31] the dS values should not exceed a certain value, differently given as 2 or 3 [32]. We therefore verified that this condition was met for all *Latimeria* genes (dS < 0.5) and all genes from species we examined for comparative purposes (frog T2R and V1R frog, dS < 0.6; teleost fish T2R, dS < 0.5; teleost ORA2 and ORA4, 2.5 and 1.5, respectively). In order to obtain a stringent measure of positive selection we employ two different algorithms, single likelihood ancestor counting (SLAC) and fixed effects likelihood (FEL) to estimate dN/dS, and only report sites, for which both methods give the same prediction with a probability better than threshold, $p < 0.1$ (*cf.* [33].

We observe an impressive number of 28 positively selected sites in the *Latimeria t2r genes*, and a much smaller number of negatively selected sites (Figure 5A, Additional file 1). This is twice the number of positively selected sites in frog *t2r* genes (Figure 5A), and suggests a high evolutionary dynamic in Latimeria *t2r* genes, which is unexpected, since *Latimeria* genes generally are evolving slowly [34]. Many of the positively selected sites even show p values below 0.01 (Additional file 1). Positively selected sites are situated in extra- and intracellular compartments as well as most transmembrane regions

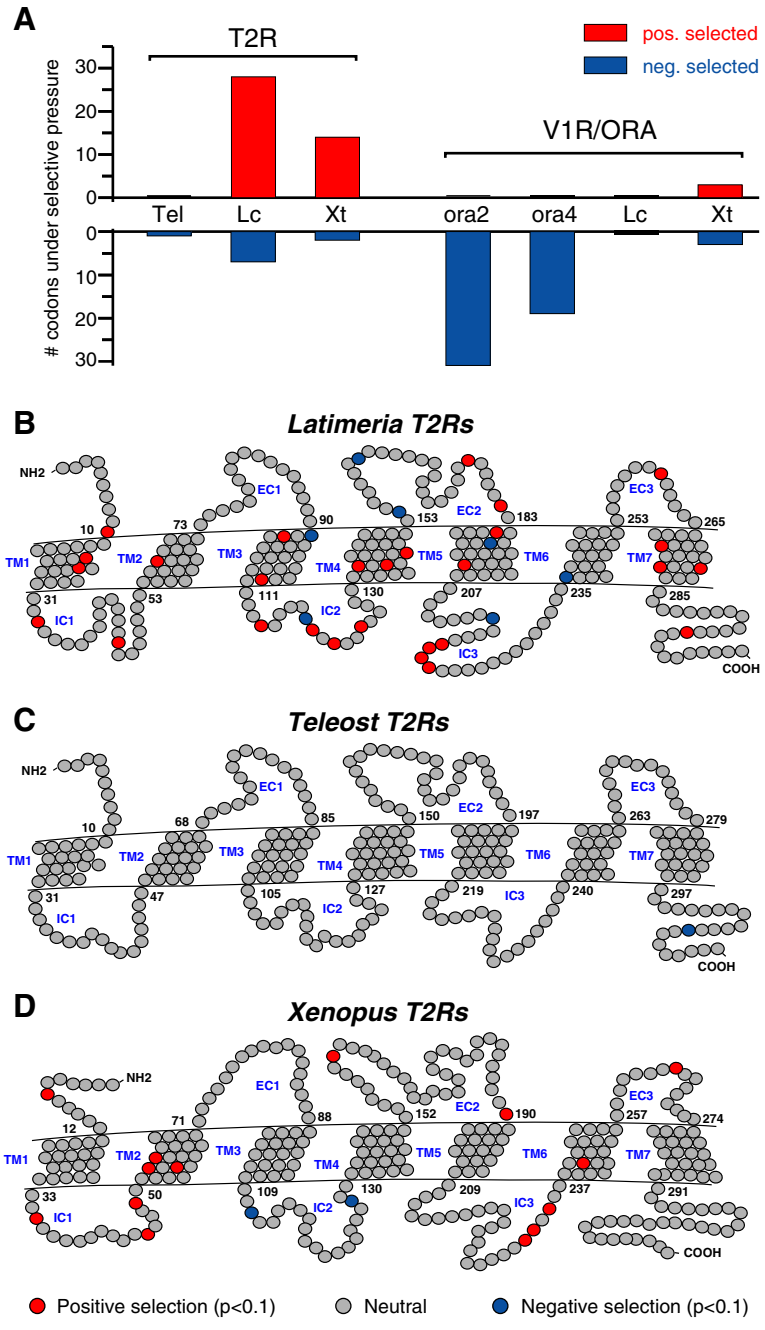

Figure 5 Evidence for extended positive selection in Latimeria t2r genes. Selective pressure for individual codons is shown as consensus of single likelihood ancestor counting (SLAC) and fixed effects likelihood (FEL) algorithm as implemented on the datamonkey server [62]. **A)** Number of positively and negatively selected sites ($p < 0.1$) for six clades depicted in Figure 1; tel, 7 teleost T2Rs; Lc, 76 Lc_T2Rs; Xt, 49 Xt_T2Rs; 5 ORA2; 5 ORA4, 9 Lc_V1Rs; 12 Xt_V1Rs. **B-D)** Results for T2R clades are presented as snake plot (negative selection in blue, $p < 0.1$, neutral selection in gray, positive selection in red, $p < 0.1$). **B)** Latimeria T2R sequences. Twentyeight codons show evidence for positive selection both with SLAC and FEL algorithms. **C)** Teleost T2R sequences. No evidence for positive selection. **D)** Frog T2R sequences. Fourteen codons show evidence for positive selection with both algorithms.

(Figure 5B). A small cluster of 4 contiguous positively selected sites occurs in the third intracellular loop, and another accumulation of four sites is observed in the preceding intracellular loop. A high variability in these loops could either diversify the interaction with signalling molecules or indirectly influence the positions of the transmembrane regions, which are believed to constitute the binding pocket for tastants [35]. Nearly half

of the positively selected sites (13 of 28) are within the transmembrane domains (Figure 5B), not significantly different from frog T2Rs (4 of 14 sites, $p > 0.2$, chi square test), and at least some of these sites could exert a direct influence on ligand binding.

In contrast, teleost *t2r* genes do not exhibit a single positively selected site (Figure 5A), suggesting that selection for diversity may be a characteristic feature of taste receptor evolution in the lobe-finned, but not the ray-finned lineage.

The V1R family exhibits neither pronounced positive nor negative selection

Teleost *ora* genes show very pronounced negative selection consistent with previous reports [10], whereas *Latimeria* and frog *v1r* genes exhibit no or nearly no negatively selected sites (Figure 5, Additional file 1). However, overall *v1r/ora* genes appear to be under higher evolutionary constraints than *t2r* genes, since we observe only rare positively selected sites in frog and none in Latimeria *v1r* genes (Figure 5). For *Latimeria v1r* genes neither negatively nor positively selected sites were found using both prediction methods, although one of the methods suggests the presence of some negatively selected sites. Thus it remains unresolved, whether *Latimeria v1r* genes are truly under neutral selection, or merely under weak purifying selection, undetected by the stringent search criteria applied.

Latimeria t2r and v1r genes are intronless

Mammalian T2Rs and V1Rs are monoexonic, while some teleost V1R-related ORAs are known to harbor 1 to 3 conserved introns [10]. We therefore evaluated all Latimeria T2R and V1R genomic sequences individually to obtain reliable exon/intron predictions. We find no evidence for introns in either gene family, including V1R03 and V1R04, orthologous respectively paralogous to intron-containing teleost *ora3* and *ora4* genes. Since the lamprey gene basal to both *v1r03*/*ora3* and *v1r04*/*ora4* is also intronless [36], we conclude that the intronless state is the ancestral feature, and that the intron gains resulting in polyexonic *ora3* and *ora4* genes have happened late in the vertebrate evolution, within the ray-finned lineage (Figure 6A).

Intergenic distances between Latimeria t2r genes are larger than between Latimeria v1r genes

Despite the generally small size of T2R-containing contigs, three quarters of *t2r* genes are found with neighboring *t2r* genes. Also, over two thirds of *v1r* genes are found with neighboring *v1r* genes, allowing calculation of intergenic distances (Figure 6B,C). It is noteworthy that *t2r* genes, with their larger evolutionary dynamics (see above), exhibit also larger intergenic distances, 31 kb median value compared to 16 kb for *v1r* genes (*cf.* Additional file 1). For two teleost *ora* gene pairs (*ora1/2* and *ora3/4*) we compared the genomic arrangement of their four *Latimeria* orthologs/paralogs (Figure 6B). The teleost *ora*3/4 gene pair is locked in tail-to-tail orientation at few kb distance, *cf.* [10]. While the corresponding *Latimeria* genes *v1r03* and *v1r04* are also neighbors, they are severalfold further apart and have head-to-tail orientation. The Latimeria *v1r01* and *v1r02* genes, on the other hand, share the head-to-head orientation of their teleost counterparts *ora1* and *ora2*, but lie much farther apart, with about 100 kb distance between *v1r01* and *v1r02*. Five *v1r01*-related genes are located in the intervening sequence, all sharing the orientation of *v1r01*, suggesting that several gene duplications of the ancestral *v1r01* gene resulted in breaking the ancestral close association of *v1r01* and *v1r02* (Figure 6B).

High density of repeat elements involved in gene duplication is observed close to t2r genes

Repeat elements may facilitate gene duplication by increasing the probability of illegitimate cross-over during meiosis. In particular LINE, SINE, and LTR elements (class I transposable elements, retrotransposons) have been shown to correlate with gene duplications and inversions [20,37-39]. An increased density of such elements close to *t2r* genes conceivably could provide a mechanism for the genesis of the record-sized T2R family. We have therefore analysed the distribution of repeat elements in the neighborhood of T2R clusters. Since drastically different average values for the contribution of repeat elements to the genome have been reported for Latimeria [18,20], we have generated a reference value ourselves, using ten randomly selected scaffolds. We find that on average T2R cluster regions (≥3 *t2r* genes) contain 4.6% more SINE sequence and 3.5% more LINE sequence than the reference regions (Figure 7A). LTR elements constitute a comparatively small proportion of all repeat elements, consistent with other reports [40], and show little difference between T2R cluster regions and reference regions (Figure 7A).

The strongest association of class I transposable elements with gene duplication is found within 5–10 kb distance from the respective genes [41]. In fact, there is evidence for duplication of such 5–10 kb regions for another class of chemosensory receptor genes [42]. We have therefore determined the density of LINE, SINE, and LTR elements in 20 kb sequence segments centered on each *t2r* gene that belongs to an identifiable cluster (47 genes) (Figure 7B). We report that the *t2r* surround regions exhibit a significantly higher density of LINE/SINE/LTR elements than the reference regions (13.9+/-0.8 *vs.* 7.2+/-0.6 elements/20 kb, respectively; mean+/-SEM, $p < 0.001$, two-sided t-test).

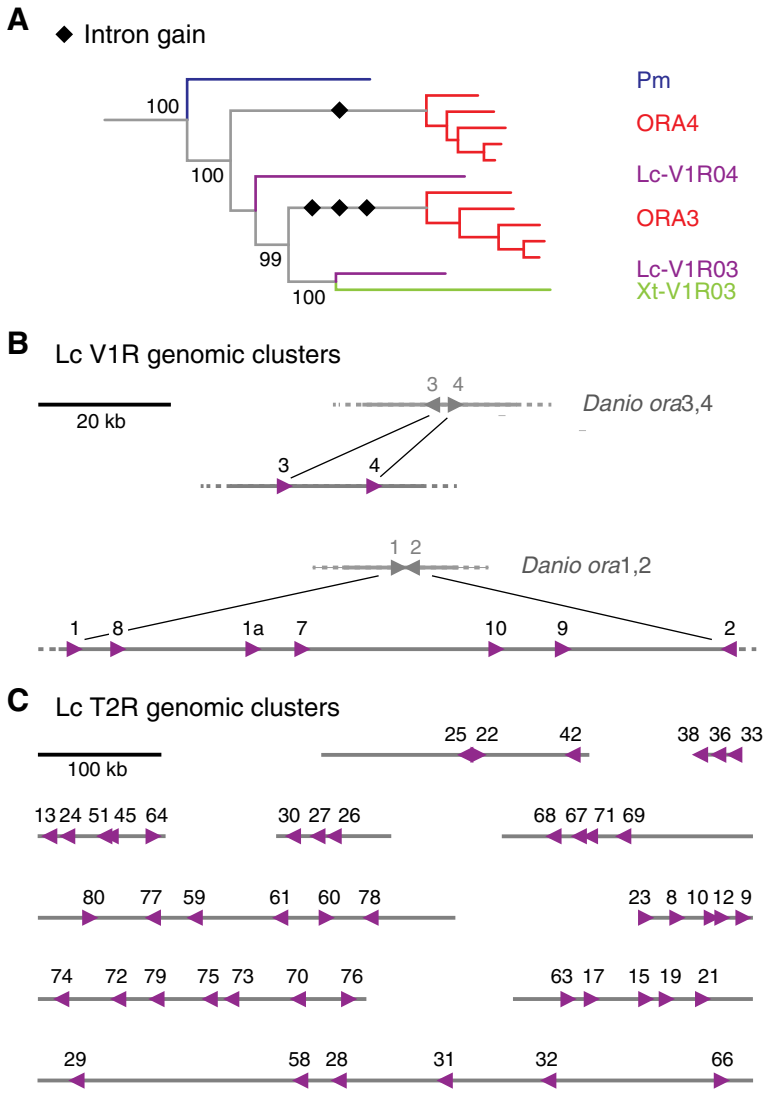

Figure 6 Genomic structure and location of Latimeria v1r and t2r genes. Panel **A**, phylogenetic origin of introns in the V1R/ora family. The subtree is taken from Figure 3; numbers indicate % branch support; black diamonds, intron gains. Panel **B**, comparison of the *Latimeria* V1R1/2 and V1R3/4 clades with the ORA1/2 and ORA3/4 gene pairs of teleosts. Numbers correspond to gene names; magenta triangles, *Latimeria* v1r genes; grey triangles, zebrafish genes; triangle pointing left, + strand; triangle pointing right, - strand; all gene distances drawn to scale. Panel **C**, *Latimeria t2r* gene clusters, full length of contigs is shown; numbers correspond to gene names; magenta triangles, *Latimeria* t2r genes; triangle pointing left, + strand; triangle pointing right, - strand; all gene distances drawn to scale. In comparison with an independent assembly [20], two contigs containing three and six genes (T2R25, 22, 42 and T2R29, 58, 28, 31, 32, 66, respectively), merge into a larger cluster of nine genes.

Finally we have determined for all *t2r* gene clusters the frequency of repeat elements in the entire contigs using small scale (1 kb) binning (Figure 7C). It is noticable that often pronounced peak frequencies occur in very close association to *t2r* genes, and on the other hand very few *t2r* genes are located in stretches of sequence devoid of repeat elements (Figure 7C). Taken together, analysis on three different length scales (gene cluster region, effective neighborhood range and 1 kb high resolution mapping) shows an enrichment in repeat elements in the genomic vicinity of *t2r* genes. These findings suggest that the high evolutionary dynamic of Latimeria *t2r* genes might be at least in part facilitated by an enrichment of class l transposons in the corresponding genomic regions.

v1r gene clusters show no increase in surround density of repeat elements

The *Latimeria* V1R family exhibits only moderate gene expansion, compared to the T2R family. Therefore it appeared instructive to compare the density of repeat elements in the vicinity of *v1r* genes to that found in reference regions as well as T2R clusters. We find on average that regions with V1R clusters (≥2 *v1r* genes) show slightly reduced LINE and SINE levels (1.0% and

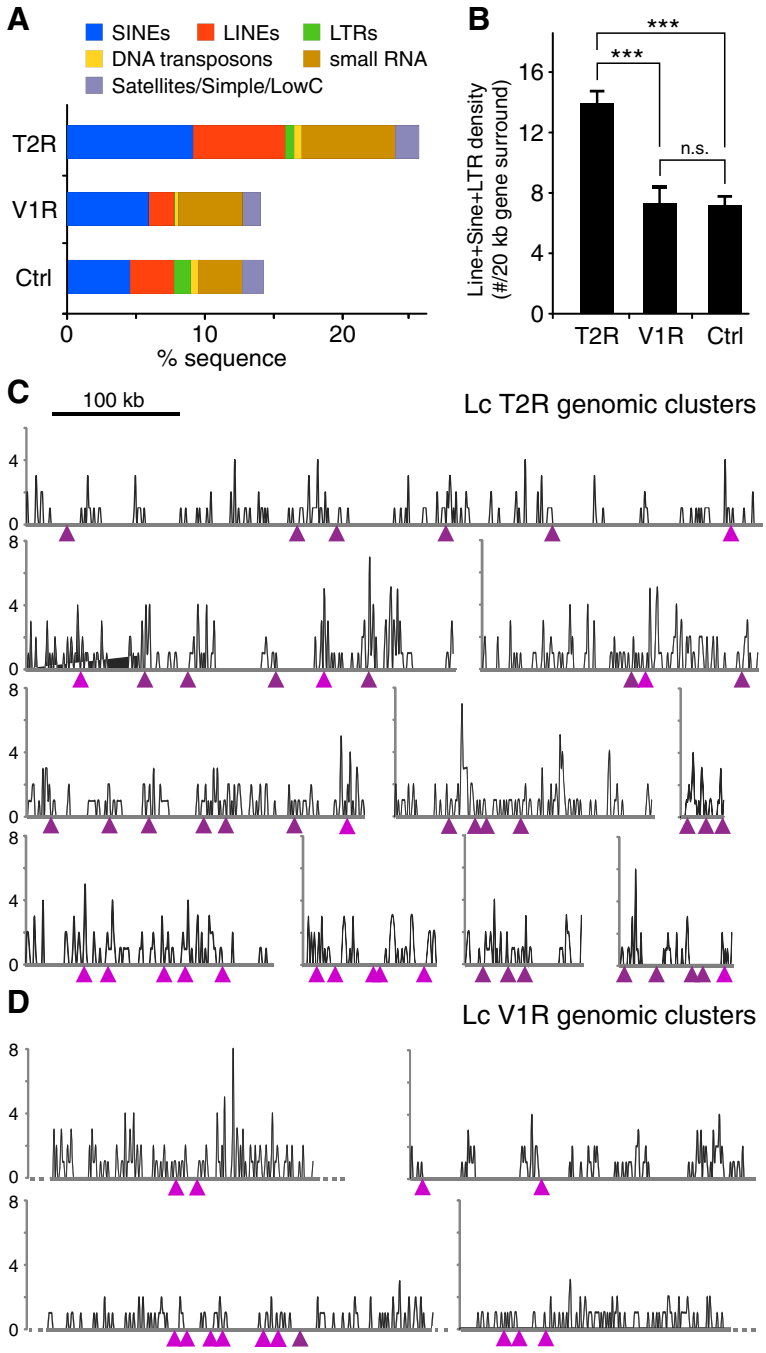

Figure 7 Repeat elements are enriched in T2R, but not in V1R genomic neighborhood. Transposable elements (repeat elements) were identified using RepeatMasker in ten *t2r* and four *v1r* gene clusters with up to 100 kb flanking regions and ten reference genomic regions (12.2 Mb total). **A)** Genomic sequence containing class I transposons (SINEs, LINEs, LTRs) and class II transposons (DNA transposons), small RNA, and Satellites/simple/low complexity repeats is determined as percent of total sequence in T2R and V1R clusters (each including 10 kb flanking regions) and the reference regions. Color code as indicated. **B)** Average density of class I transposons in 20 kb genomic segments centering on 47 *t2r* (T2R) and 14 *v1r* genes (V1R) and in 11.3 Mb reference region (Ctrl). Significance was evaluated by students t test (two-sided; ***, $p < 0.001$; n.s., not significant). **C, D)** The frequency of class I transposable elements is given as number of elements per kb sequence. The position of the genes is indicated by triangles; dark magenta, ++ (5'- > 3'); light magenta,+- (3'- > 5'). **C)** Ten contigs with *t2r* gene clusters are shown, from left to right and top to bottom, JH128085, JH128916, JH129648, JH129303, JH129750, JH132239, JH129824, JH130976, JH130917, JH130784. **D)** Four contigs with *v1r* gene clusters are shown, from left to right and top to bottom, JH126562, JH129249, JH126576, JH1276167.

1.8% of sequence below reference levels, respectively, Figure 7A). LTR elements are nearly completely absent (Figure 7A).

In the detailed analysis of 20 kb surround regions of *v1r* cluster genes the average frequency of retrotransposons is not significantly different from that observed in reference regions (Figure 7B). In contrast, the difference to *t2r* surround regions is highly significant ($p < 0.001$, t-test). In the small scale analysis only 1 of the 14 *v1r* genes present in clusters is associated with a noticable peak frequency of repeat elements, although several such peaks do exist in the larger vicinity (Figure 7D).

In summary, on all levels of analysis the genomic neighborhood of *v1r* genes is similar to control regions, whereas neighborhood regions of *t2r* genes show significant increases above control levels. Indeed, the frequency of repeat elements in *t2r* gene surrounds is double as large as that observed in *v1r* gene surrounds. Thus, the increased repeat density surrounding *t2r* genes is not a general feature of chemosensory genes in *Latimeria*, but is correlated with the unusually large increase in the T2R family size during coelacanth evolution.

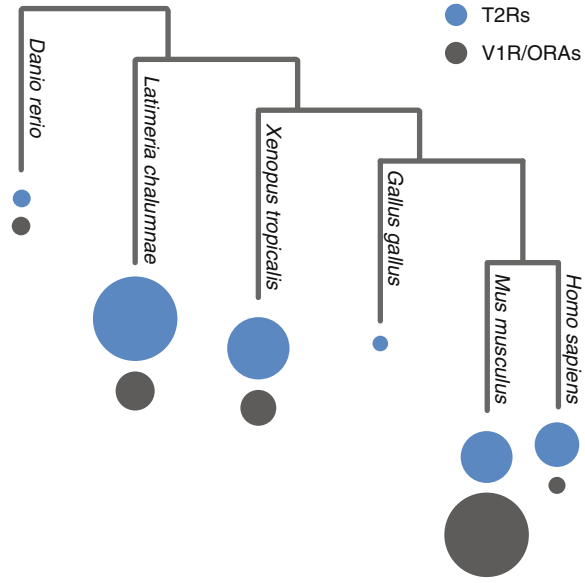

Figure 8 Evolutionary dynamic of vertebrate t2r and v1r gene repertoires. Species tree with the respective T2R (blue circle) and V1R/ORA (black circle) repertoires. Circle area is proportional to the size of the gene family. Values for *Latimeria* T2R and V1R families, this study; *t2r* gene family size for other species was taken from [11], teleost ORA and frog V1R family size from [10] and mouse V1R family size from [25].

Discussion

Coelacanths (*Latimeria*) are so-called living fossils, as they are one of the few extant fish in the lobe-finned lineage of vertebrates, from which all tetrapods emerged [17]. The fossil record shows remarkable morphological consistency since the early Devonian [43], consistent with a generally slow rate of molecular evolution in coelacanth genes [34]. Chemosensory receptor families are among the fastest evolving gene families [8], and thus we were interested in the evolutionary dynamics of such families in a coelacanth genome. In particular, two of these gene families, the closely related V1R/ORA and T2R families, are known to rapidly evolve in tetrapods [13], whereas the corresponding gene repertoires in teleost fish are small and highly conserved [10,11]. It is worth pointing out that this tetrapod/teleost difference is gene family-specific and cannot be generalized, since in another chemosensory gene family opposing trends are observed [12]. The sparse information available for cartilaginous and jawless fish [44] suggests that the teleost V1R/ORA repertoires may correspond to the ancestral situation.

We report here that *Latimeria chalumnae* possesses 80 *t2r genes*, of which at least 74 are intact genes, which is by far the largest repertoire size reported for any species (Figure 8), and nearly double as much as that of the frog *Xenopus tropicalis*, the largest known repertoire so far [11]. The biological purpose for *Latimeria* of such a large T2R receptoire is unknown. T2R receptors are bitter taste receptors in mammals [2], possibly also in teleost fish [45] and are assumed to mediate avoidance of potentially toxic food sources. It has been suggested that herbivores would require larger T2R repertoires to guard them against plant chemical defense mechanisms [15]. This correlation is weakened by our results, since plants are absent in the habitat of *Latimeria*, the deep sea (*Latimeria* feeds on various fish and cephalopods [46]). However, it cannot be excluded that *Latimeria* T2Rs might have extra-gustatory functions, as has been shown for mammalian T2Rs [47].

The unparalleled size of the Latimeria T2R repertoire is unexpected, given the overall low mutation rate in *Latimeria* genes, *cf.* [34]. It is noteworthy that all but four of the *Latimeria t2r* genes are derived from a single ancestral gene, thus the diversification of the T2R repertoire seen here constitutes a recent development within this lineage. The increase in *Latimeria* T2R family size appears to have arisen by repeated local gene duplications, since the large majority of *t2r* genes are found in small clusters in several short contigs, which presumably will coalesce into larger cluster(s) as the genome assembly becomes more refined. In fact, a comparison with an independent sequencing effort [20] showed two of the clusters found here merging into a larger cluster. The significantly higher density of transposable elements in the immediate vicinity of *t2r* genes may provide a means to facilitate/enhance gene duplication in this gene family and could thus be part of the mechanism responsible for generating the large T2R family. Additionally, closely

related neighboring *t2r* genes themselves might serve as recombination foci.

Genesis of a large gene repertoire requires not only gene duplications, but also an efficient path to neo-functionalization for these newly duplicated genes, which may involve positive selection. Indeed we found dN/dS values indicative of positive selection for a large number of sites localized in all three major compartments of the protein sequence (extracellular loops, transmembrane regions, intracellular loops), with small clusters in two intracellular loops. These sites might contribute either directly (sites in TMIII, TMV and TMVII, cf. [35]) or indirectly via overall conformational changes (sites in loops, other TMs) to diversification of *Latimeria* taste responses.

We wished to compare the extent of positive selection in *Latimeria t2r* genes to that observed in tetrapod and teleost chemosensory receptor families [12,27,48-50]. However, numerical comparison between results obtained by different algorithms is difficult, and so we also have examined dN/dS ratios for teleost and frog T2R repertoires here. We observe that Latimeria T2Rs by far show the most pronounced positive selection of all T2R families analysed, an unexpected result considering the generally low mutation rate in *Latimeria* genes, *cf.* [34]. We have also analysed V1R/ORA repertoires from *Latimeria*, teleost and frog, and did not find any evidence for positive selection in *Latimeria* V1Rs. Neither did *Latimeria* V1Rs exhibit the pronounced negative selection observed for the V1R-related *ora* genes of teleosts [10]. In other words, *Latimeria v1r* genes are drastically different from their teleost counterparts, and resemble more those of later diverging tetrapods (this manuscript, *cf.* [27,48-50]. In all within-species comparisons, V1Rs exhibited either more negative or less positive selection than T2Rs. Taken together, *Latimeria*, an early-diverged and aquatic-living vertebrate species with generally slow evolution, shows evidence for (near) neutral evolution of its V1R and fast evolution of its T2R repertoire.

It has previously been hypothesized that the difference between (small) teleost and (large) tetrapod T2R and V1R repertoires might reflect an adaptation to the terrestrial lifestyle [11]. Furthermore these differences have been contrasted with the absence of such drastic changes in V2R (and T1R) repertoires, resulting in large changes of the ratio of *v1r* to *v2r* genes upon the acquisition of the terrestrial life style [25]. However, the results we report here for the *Latimeria* V1R family and in particular the *Latimeria* T2R family do not strengthen this hypothesis. *Latimeria* is a purely aquatic organism with a medium-sized V1R and very large T2R repertoire, whereas its V2R repertoire is comparable to that of teleost fishes (Korsching, unpublished observation). Consequently, the difference in size between teleost and tetrapod T2R repertoires is not related to the water-to-land transition. Instead, frequent gene birth events in particular in the T2R family appear to be a general feature of the lobe-finned lineage of vertebrates, and need to be understood in that context. Of course, this does not exclude an additional role, aquired much later, in facilitating the water-to-land transition.

On the other hand, for another parameter, sequence divergence, both the V1R and T2R receptor families of *Latimeria* examined here are more similar to those of teleosts than to those of later diverging members of their own lobe-finned lineage. While *Latimeria* possess sister clades to all mouse and frog *t2r* genes, they have additionally retained a 'fish-like' taste receptor, unlike mouse and frog. Furthermore, *Latimeria* exhibits direct orthologs or paralogs of all six teleost *ora* genes, in contrast to the amphibian *Xenopus*, who lost the majority, and mammals, who lost all direct orthologs, and kept paralogs of only two *ora* genes. Thus, the *Latimeria* T2R and V1R repertoires are more divergent than the corresponding repertoires of the later-derived tetrapods from the same (lobe-finned) lineage. The gradual loss of ancestral *v1r* genes in the lobe-finned lineage correlates with loss of aquatic life style (obligatory for *Latimeria*, facultative for *Xenopus*, and mostly absent in mammals) and conceivably these six highly conserved V1R/ORA receptors are specialized for detection of purely aquatic odor stimuli.

Conclusions

Taken together we have shown hybrid features for the T2R and V1R receptor repertoire of a coelacanth, *Latimeria chalumnae*. Despite its basal position in the lobe-finned lineage, *t2r* genes of this species shows many species-specific gene duplications - conceivably facilitated by a high density of transposable elements - as well as evidence of positive Darwinian selection characteristic for later-diverged members of this lineage such as amphibians and mammals. At the same time, *Latimeria* retains most of the divergence characteristic of teleost chemosensory receptor repertoires, which to an increasing degree is lost in more modern representatives of the lobe-finned lineage. *Latimeria* thus provides a counter-example to the inverse correlation of genetic divergence and frequency of gene birth events apparent for several previously studied chemosensory repertoires of teleosts and tetrapods [8]. Furthermore, the large size of the *Latimeria* T2R repertoire, comparable to some of the smaller olfactory receptor gene families, *cf.* [8], suggests that the sense of taste may require unexpectedly high molecular complexity.

Methods

Sequence data mining and phylogenetic analysis

Using representative T2R and V1R amino acid sequences from mouse, *Xenopus tropicalis* and zebrafish as queries, we searched with tblastn for *t2r* and *v1r* genes in the

preliminary draft of the *Latimeria chalumnae* genome produced by the Broad Institute [21]. Homology regions above 200 amino acid length were considered further. Several sequences were manually edited to establish or to complete the ORF prediction, including six *t2r* genes, for which ≤2 stop codons/frame shifts were removed, resulting in each case in a full length sequence containing the expected motifs (*cf.* Figure 4) over the entire sequence length. These six genes are indicated with asterisks in the phylogenetic tree (Figure 2). No *t2r* candidate genes with more than 2 stop codons/frame shifts were found. This suggests to us that the edited bases could well have been due to sequencing errors in this draft assembly. One prediction of a small additional N-terminal exon (in V1R10) resulted in lower homology in the multiple sequence alignment, compared to the corresponding full length monoexonic prediction, and so the latter was included in further analysis. Sequences that are >98% identical in amino acid sequence are considered allelic variants [51], but could theoretically result from very recent gene duplications. In this case either adjacent or unambiguously different genomic location would be expected. No such cases were observed. Resulting sequences ranged from 287 to 316 amino acids for T2Rs, and 299 to 321 amino acids for V1Rs. All *Latimeria chalumnae* sequence data used in this article is included in Additional file 2. Sequences were aligned with MAFFT 7 [52], an online version of the multiple alignment tool MAFFT [53], using the E-INS-I strategy with the default parameters. Clustal Omega [54] was also used for alignment.

Phylogenetic analysis was performed with a Maximum likelihood algorithm (PhyML-aLRT) with SPR setting for tree optimization and chi square-based aLRT for branch support [22] on the phylemon2 server [55]. Branch support above 80% was considered significant. Candidate sequences had to fulfil the following stringent conditions to be accepted as *bona fide* unique T2Rs or V1Rs, respectively: a) the gene had to be located inside the corresponding phylogenetic tree with branch support over 80%; b) the sequence had to contain the motifs characteristic for that gene family; c) the sequence had to map to a unique, non-overlapping genomic position; d) the minimally accepted sequence difference of 2% had to be distributed along the sequence.

Sequences were named according to named orthologs or closest paralogs from other species, if applicable, and otherwise according to phylogenetic relationship. The assignment of Lc_V1R04 was confirmed by comparison with V1R-related ORA3 and ORA4-specific motifs.

Identity and similarity matrices and sequence logos

Pairwise alignments of the 20 V1R and 80 T2R amino acid sequences were performed using the SIAS webserver [56]. Identity and similarity values from all possible comparisons within each family were retrieved and are shown as matrix.

Sequence logos were generated using Sequence logo 3 [26]. Sequence alignments were manually edited using Jalview [57] and positions with gaps in over 90% of sequences were deleted. To align conserved motifs identified within Latimeria T2Rs, V1Rs, tetrapod T2Rs, V1Rs, teleost T2Rs and V1Rs, a multiple alignment including all six gene families was analysed. Transmembrane regions were predicted for multiple aligned sequences using PRALINE [58].

Analysis of transposable elements

Latimeria scaffolds containing *t2r* and *v1r* gene clusters were examined for repeat elements using RepeatMasker [59], which provides a detailed annotation of class I (retrotransposons) and class II transposable elements. Detailed analysis and graphical representation of results was performed using Excel, Open Office, and Adobe Illustrator. Class I transposable elements (LINE, SINE and LTR) encode a reverse transcriptase (RT) protein enabling a sometimes autonomous "copy and paste" mechanism. Class I elements are most relevant in facilitating gene duplication, inversion and translocation [37-39], and were analysed separately. For reference sequence we randomly chose ten *Latimeria* scaffolds totaling 11.3 Mb genomic sequence.

dN/dS analysis

The dN/dS ratios for the latimeria *t2r* and *v1r* gene families were calculated using nucleotide sequences aligned by MAFFT [52] and manually edited using Jalview [57] to match the amino acid alignments obtained in phylogenetic analysis. Codon based alignment was also employed using PAL2NAL [60]. To test the selective pressure on individual codons, we used the single likelihood ancestor counting (SLAC) package described in [61] and a fixed effects likelihood (FEL) method that directly estimates nonsynonymous and synonymous substitution rates at each site [33]. As significance cutoff we chose $p < 0.1$, in accordance with published procedures [33]. To achieve a high stringency of analysis, we required independent prediction of positive or negative selection by both methods. Thus we expect very few false-positives, and indeed no positively selected sites were predicted for several of the gene groups analysed. All dN/dS analyses were performed using the datamonkey server [62]. To exclude saturation bias, we confirmed that dS values for all comparisons were below critical values, *cf.* [32], using DnaSp software package [63].

Availability of supporting data

The data sets supporting the results of this article are included within the article and its additional files.

Additional files

Additional file 1: A list of tables containing *t2r* and *v1r* gene names, genomic location, previously reported synonyms, homology matrix, detailed motif analysis, and detailed dN/dS analysis.

Additional file 2: *Latimeria chalumnae* T2R and V1R protein sequences in fasta format and three phylogenetic tree files in Newick format that were used in construction of phylogenetic trees shown in Figures 1, 2 and 3.

Competing interests
The authors declare no competing interests.

Authors' contributions
SIK and ASS designed research, ASS and SIK performed research, ASS analysed data, ASS and SIK prepared figures, SIK wrote the paper. Both authors read and approved the final manuscript.

Acknowledgements
We thank the Deutsche Forschungsgemeinschaft for financial support (grants Ko-1046/5-1 and Ko-1046/5-2 to SIK).

Received: 3 March 2014 Accepted: 29 July 2014
Published: 5 August 2014

References
1. Mombaerts P: **Genes and ligands for odorant, vomeronasal and taste receptors.** *Nat Rev Neurosci* 2004, **5:**263–278.
2. Mueller KL, Hoon MA, Erlenbach I, Chandrashekar J, Zuker CS, Ryba NJ: **The receptors and coding logic for bitter taste.** *Nature* 2005, **434:**225–229.
3. Mori K, Sakano H: **How is the olfactory map formed and interpreted in the mammalian brain?** *Annu Rev Neurosci* 2011, **34:**467–499.
4. Kapsimali M, Barlow LA: **Developing a sense of taste.** *Semin Cell Dev Biol* 2013, **24:**200–209.
5. Baier H, Korsching S: **Olfactory glomeruli in the zebrafish form an invariant pattern and are identifiable across animals.** *J Neurosci* 1994, **14:**219–230.
6. Friedrich RW, Korsching SI: **Chemotopic, combinatorial, and noncombinatorial odorant representations in the olfactory bulb revealed using a voltage-sensitive axon tracer.** *J Neurosci* 1998, **18:**9977–9988.
7. Friedrich RW, Korsching SI: **Combinatorial and chemotopic odorant coding in the zebrafish olfactory bulb visualized by optical imaging.** *Neuron* 1997, **18:**737–752.
8. Nei M, Niimura Y, Nozawa M: **The evolution of animal chemosensory receptor gene repertoires: roles of chance and necessity.** *Nat Rev Genet* 2008, **9:**951–963.
9. Grus WE, Shi P, Zhang J: **Largest vertebrate vomeronasal type 1 receptor gene repertoire in the semiaquatic platypus.** *Mol Biol Evol* 2007, **24:**2153–2157.
10. Saraiva LR, Korsching SI: **A novel olfactory receptor gene family in teleost fish.** *Genome Res* 2007, **17:**1448–1457.
11. Dong D, Jones G, Zhang S: **Dynamic evolution of bitter taste receptor genes in vertebrates.** *BMC Evol Biol* 2009, **9:**12.
12. Hussain A, Saraiva LR, Korsching SI: **Positive Darwinian selection and the birth of an olfactory receptor clade in teleosts.** *Proc Natl Acad Sci U S A* 2009, **106:**4313–4318.
13. Young JM, Massa HF, Hsu L, Trask BJ: **Extreme variability among mammalian V1R gene families.** *Genome Res* 2010, **20:**10–18.
14. Ishimaru Y, Okada S, Naito H, Nagai T, Yasuoka A, Matsumoto I, Abe K: **Two families of candidate taste receptors in fishes.** *Mech Dev* 2005, **122:**1310–1321.
15. Li D, Zhang J: **Diet shapes the evolution of the vertebrate bitter taste receptor gene repertoire.** *Mol Biol Evol* 2014, **31**(2):303–309.
16. Dulac C, Torello AT: **Molecular detection of pheromone signals in mammals: from genes to behaviour.** *Nat Rev Neurosci* 2003, **4:**551–562.
17. Zardoya R, Meyer A: **Evolutionary relationships of the coelacanth, lungfishes, and tetrapods based on the 28S ribosomal RNA gene.** *Proc Natl Acad Sci U S A* 1996, **93:**5449–5454.
18. Amemiya CT, Alfoldi J, Lee AP, Fan S, Philippe H, Maccallum I, Braasch I, Manousaki T, Schneider I, Rohner N, Organ C, Chalopin D, Smith JJ, Robinson M, Dorrington RA, Gerdol M, Aken B, Biscotti MA, Barucca M, Baurain D, Berlin AM, Blatch GL, Buonocore F, Burmester T, Campbell MS, Canapa A, Cannon JP, Christoffels A, De Moro G, Edkins AL, *et al*: **The African coelacanth genome provides insights into tetrapod evolution.** *Nature* 2013, **496:**311–316.
19. Picone B, Hesse U, Panji S, Van Heusden P, Jonas M, Christoffels A: **Taste and odorant receptors of the coelacanth-A gene repertoire in transition.** *J Exp Zool B Mol Dev Evol* 2013, Sep 18, doi:10.1002/jez.b.22531. [Epub ahead of print].
20. Nikaido M, Noguchi H, Nishihara H, Toyoda A, Suzuki Y, Kajitani R, Suzuki H, Okuno M, Aibara M, Ngatunga BP, Mzighani SI, Kalombo HW, Masengi KW, Tuda J, Nogami S, Maeda R, Iwata M, Abe Y, Fujimura K, Okabe M, Amano T, Maeno A, Shiroishi T, Itoh T, Sugano S, Kohara Y, Fujiyama A, Okada N: **Coelacanth genomes reveal signatures for evolutionary transition from water to land.** *Genome Res* 2013, **23:**1740–1748.
21. **Broad Institute.** 2012 [http://www.ensembl.org/Latimeria_chalumnae/Info/Index]
22. Guindon S, Dufayard JF, Lefort V, Anisimova M, Hordijk W, Gascuel O: **New algorithms and methods to estimate maximum-likelihood phylogenies: assessing the performance of PhyML 3.0.** *Syst Biol* 2010, **59:**307–321.
23. Syed AS, Sansone A, Nadler W, Manzini I, Korsching SI: **Ancestral amphibian v2rs are expressed in the main olfactory epithelium.** *Proc Natl Acad Sci U S A* 2013, **110:**7714–7719.
24. Oka Y, Saraiva LR, Kwan YY, Korsching SI: **The fifth class of Galpha proteins.** *Proc Natl Acad Sci U S A* 2009, **106:**1484–1489.
25. Shi P, Zhang J: **Comparative genomic analysis identifies an evolutionary shift of vomeronasal receptor gene repertoires in the vertebrate transition from water to land.** *Genome Res* 2007, **17:**166–174.
26. Crooks GE, Hon G, Chandonia JM, Brenner SE: **WebLogo: a sequence logo generator.** *Genome Res* 2004, **14:**1188–1190.
27. Zhou Y, Dong D, Zhang S, Zhao H: **Positive selection drives the evolution of bat bitter taste receptor genes.** *Biochem Genet* 2009, **47:**207–215.
28. Shi P, Zhang J, Yang H, Zhang YP: **Adaptive diversification of bitter taste receptor genes in Mammalian evolution.** *Mol Biol Evol* 2003, **20:**805–814.
29. Kosiol C, Vinar T, da Fonseca RR, Hubisz MJ, Bustamante CD, Nielsen R, Siepel A: **Patterns of positive selection in six Mammalian genomes.** *PLoS Genet* 2008, **4:**e1000144.
30. Nei M, Gojobori T: **Simple methods for estimating the numbers of synonymous and nonsynonymous nucleotide substitutions.** *Mol Biol Evol* 1986, **3:**418–426.
31. Gojobori T: **Codon substitution in evolution and the "saturation" of synonymous changes.** *Genetics* 1983, **105:**1011–1027.
32. Mank JE, Axelsson E, Ellegren H: **Fast-X on the Z: rapid evolution of sex-linked genes in birds.** *Genome Res* 2007, **17:**618–624.
33. Kosakovsky Pond SL, Frost SD: **Not so different after all: a comparison of methods for detecting amino acid sites under selection.** *Mol Biol Evol* 2005, **22:**1208–1222.
34. Lampert KP, Fricke H, Hissmann K, Schauer J, Blassmann K, Ngatunga BP, Schartl M: **Population divergence in East African coelacanths.** *Curr Biol* 2012, **22:**R439–R440.
35. Behrens M, Meyerhof W: **Bitter taste receptor research comes of age: from characterization to modulation of TAS2Rs.** *Semin Cell Dev Biol* 2013, **24:**215–221.
36. Libants S, Carr K, Wu H, Teeter JH, Chung-Davidson YW, Zhang Z, Wilkerson C, Li W: **The sea lamprey Petromyzon marinus genome reveals the early origin of several chemosensory receptor families in the vertebrate lineage.** *BMC Evol Biol* 2009, **9:**180.
37. Kazazian HH Jr: **Mobile elements: drivers of genome evolution.** *Science* 2004, **303:**1626–1632.
38. Bourque G: **Transposable elements in gene regulation and in the evolution of vertebrate genomes.** *Curr Opin Genet Dev* 2009, **19:**607–612.
39. Ohshima K: **RNA-mediated gene duplication and retroposons: retrogenes, LINEs, SINEs, and sequence specificity.** *Int J Evol Biol* 2013, **2013:**424726.
40. Forconi M, Chalopin D, Barucca M, Biscotti MA, De Moro G, Galiana D, Gerdol M, Pallavicini A, Canapa A, Olmo E, Volff JN: **Transcriptional activity of transposable elements in coelacanth.** *J Exp Zool B Mol Dev Evol* 2013, Sep 3, doi:10.1002/jez.b.22527. [Epub ahead of print].
41. Estecio MR, Gallegos J, Vallot C, Castoro RJ, Chung W, Maegawa S, Oki Y, Kondo Y, Jelinek J, Shen L, Hartung H, Aplan PD, Czerniak BA, Liang S, Issa JP: **Genome architecture marked by retrotransposons modulates predisposition to DNA methylation in cancer.** *Genome Res* 2010, **20:**1369–1382.

42. Lane RP, Cutforth T, Axel R, Hood L, Trask BJ: **Sequence analysis of mouse vomeronasal receptor gene clusters reveals common promoter motifs and a history of recent expansion.** *Proc Natl Acad Sci U S A* 2002, **99:**291–296.
43. Zhu M, Yu X, Lu J, Qiao T, Zhao W, Jia L: **Earliest known coelacanth skull extends the range of anatomically modern coelacanths to the Early Devonian.** *Nat Commun* 2012, **3:**772.
44. Grus WE, Zhang J: **Origin of the genetic components of the vomeronasal system in the common ancestor of all extant vertebrates.** *Mol Biol Evol* 2009, **26:**407–419.
45. Oike H, Nagai T, Furuyama A, Okada S, Aihara Y, Ishimaru Y, Marui T, Matsumoto I, Misaka T, Abe K: **Characterization of ligands for fish taste receptors.** *J Neurosci* 2007, **27:**5584–5592.
46. Fricke H, Hissmann K, Schauer J, Erdmann M, Moosa MK, Plante R: **Biogeography of the Indonesian coelacanths.** *Nature* 2000, **403:**38.
47. Behrens M, Meyerhof W: **Gustatory and extragustatory functions of mammalian taste receptors.** *Physiol Behav* 2011, **105:**4–13.
48. Gilad Y, Man O, Glusman G: **A comparison of the human and chimpanzee olfactory receptor gene repertoires.** *Genome Res* 2005, **15:**224–230.
49. Hohenbrink P, Radespiel U, Mundy NI: **Pervasive and ongoing positive selection in the vomeronasal-1 receptor (V1R) repertoire of mouse lemurs.** *Mol Biol Evol* 2012, **29:**3807–3816.
50. Sugawara T, Go Y, Udono T, Morimura N, Tomonaga M, Hirai H, Imai H: **Diversification of bitter taste receptor gene family in western chimpanzees.** *Mol Biol Evol* 2011, **28:**921–931.
51. Zhang X, Rodriguez I, Mombaerts P, Firestein S: **Odorant and vomeronasal receptor genes in two mouse genome assemblies.** *Genomics* 2004, **83:**802–811.
52. Katoh K, Standley DM: **MAFFT multiple sequence alignment software version 7: improvements in performance and usability.** *Mol Biol Evol* 2013, **30:**772–780.
53. Katoh K, Misawa K, Kuma K, Miyata T: **MAFFT: a novel method for rapid multiple sequence alignment based on fast Fourier transform.** *Nucleic Acids Res* 2002, **30:**3059–3066.
54. Sievers F, Wilm A, Dineen D, Gibson TJ, Karplus K, Li W, Lopez R, McWilliam H, Remmert M, Soding J, Thompson JD, Higgins DG: **Fast, scalable generation of high-quality protein multiple sequence alignments using Clustal Omega.** *Mol Syst Biol* 2011, **7:**539.
55. Sanchez R, Serra F, Tarraga J, Medina I, Carbonell J, Pulido L, de Maria A, Capella-Gutierrez S, Huerta-Cepas J, Gabaldon T, Dopazo J, Dopazo H: **Phylemon 2.0: a suite of web-tools for molecular evolution, phylogenetics, phylogenomics and hypotheses testing.** *Nucleic Acids Res* 2011, **39:**W470–W474.
56. Reche P: **SIAS.** 2013 [http://imed.med.ucm.es/Tools/sias.html]
57. Waterhouse AM, Procter JB, Martin DM, Clamp M, Barton GJ: **Jalview Version 2–a multiple sequence alignment editor and analysis workbench.** *Bioinformatics* 2009, **25:**1189–1191.
58. Pirovano W, Feenstra KA, Heringa J: **PRALINETM: a strategy for improved multiple alignment of transmembrane proteins.** *Bioinformatics* 2008, **24:**492–497.
59. Smit AFA, Hubley R, Green P: **RepeatMasker Open 4.0.3.** [http://www.repeatmasker.org/] 1996-2010.
60. Suyama M, Torrents D, Bork P: **PAL2NAL: robust conversion of protein sequence alignments into the corresponding codon alignments.** *Nucleic Acids Res* 2006, **34:**W609–W612.
61. Suzuki Y, Gojobori T: **A method for detecting positive selection at single amino acid sites.** *Mol Biol Evol* 1999, **16:**1315–1328.
62. Kosakovsky Pond SL, Frost SDW: **Datamonkey: rapid detection of selective pressure on individual sites of codon alignments.** *Bioinformatics* 2005, **21:**2531–2533.
63. Librado P, Rozas J: **DnaSP v5: a software for comprehensive analysis of DNA polymorphism data.** *Bioinformatics* 2009, **25:**1451–1452.

doi:10.1186/1471-2164-15-650
Cite this article as: Syed and Korsching: Positive Darwinian selection in the singularly large taste receptor gene family of an 'ancient' fish, *Latimeria chalumnae*. *BMC Genomics* 2014 **15**:650.

3 EXTENDED DISCUSSION

"The capacity of DNA to store information vastly exceeds that of any other known system"

Dr. Michael Denton

3.1 *XENOPUS laevis* (AFRICAN CLAWED FROG)

The olfactory system architecture of teleost fishes is very different from that of tetrapods. In tetrapods olfactory system is segregated in multiple subsystems with distinct segregation even within subsystems, whereas a single sensory surface with little internal segregation is observed in the teleost fishes, although they possess all but one of the different olfactory receptor gene families, which segregate into different subsystems in tetrapods. Amphibians occupy an important position in the evolution of olfactory systems as being the first vertebrates to possess a separate vomeronasal organ. Furthermore, amphibians have biphasic life cycle, aquatic larvae *vs*. terrestrial adults, which makes them a good model for understanding how chemical signaling functions in aquatic versus terrestrial environments. Finally, studying early diverging tetrapods is crucial in determining at which point during evolution vertebrate olfactory receptor families localized and became functional in the vomeronasal system. In my PhD thesis I have examined the olfactory system of the anuran amphibian *Xenopus laevis*, an early diverging tetrapod. Most of my work is on *Xenopus* tadpole which is fully aquatic and has olfactory system showing clear morphological separation into two subsystems, the MOE and the VNO (Manzini and Schild 2010).

3.1.1 EARLY DIVERGING V2R GENES are EXPRESSED in MOE

Previously it was thought that all *v2r* genes are expressed in the VNO, based on expression data for a few V2Rs (Hagino-Yamagishi et al. 2004). However, at that time no genome project for *Xenopus* existed and so these studies could not provide a systematic phylogenetic analysis of the V2R gene family. With the availability of the genome sequence of *Xenopus tropicalis*, a close relative of *Xenopus laevis*, a recent study found *Xenopus tropicalis* to have the largest V2R gene family repertoire reported so far, with well over 300 genes (Figure 2) (Ji et al. 2009). Using the V2R gene family information from Ji et al., 2009, we employed phylogenetic analysis to identify four

major subgroups and selected seven representative genes belonging to all four subgroups, and cloned their orthologs in *Xenopus laevis* (Syed et al. 2013). Two subgroups represent later diverging genes according to phylogenetic analysis, and all genes selected from those two subgroups (v2r-A2a, v2r-A2b, v2r-A2c and v2r-E-1) are expressed in the VNO.

However, very unexpectedly, all genes analyzed from the two earlier diverging subgroups (v2r-A1a, v2r-A1b and v2r-C) are expressed exclusively in the MOE (Syed et al. 2013). These results represent a major subpopulation of V2Rs, since all selected probes except v2r-C cross-react with many neighboring *v2r* genes of the subtree, (Syed et al. 2013). The *v2r-C* gene nevertheless labels a large population of neurons in the MOE, possibly because it may be a co-receptor for many other *v2r* genes, as has been shown both for its mammalian and teleost orthologs (Martini et al. 2001, DeMaria and Ngai 2010, Ishii and Mombaerts 2011).

This segregation of a single olfactory receptor family into two main olfactory organs is unprecedented. There have been reports about isolated TAAR and OR genes being expressed outside the MOE and in fact outside the olfactory system (Fleischer et al. 2007, Tian and Ma 2008), but never before major phylogenetic subdivisions of a single olfactory receptor family were found to be expressed in different olfactory organs. The function and the mechanism for such segregation are currently unknown, but it is tempting to speculate that the earlier diverging V2R genes still have functional roles comparable to those of their teleost counterparts, who are also expressed in the MOE, whereas the later diverging V2R genes may have acquired functions comparable to their mammalian counterparts, which are expressed in the VNO as well. In this sense, the bimodal expression of V2R genes observed in *Xenopus* would represent an evolutionary transition point, possibly between aquatic and terrestrial olfaction.

3.1.2 TRPC2 EXPRESSION in BOTH OLFACTORY SUBSYSTEMS of *XENOPUS* PARALLELS THE COMBINED V2R EXPRESSION

TRPC2 is a marker for microvillous neurons, which is shown to be expressed in the single olfactory surface of the teleost fish but is restricted to the VNO in the terrestrial amphibian and tetrapods (Sato et al. 2005, Liman and Dulac 2007). TRPC2 is

shown to be a crucial channel for the signal transduction activated by V1R and V2R expressing sensory neurons in the rodent VNO (Liberles 2014). Thus we expected TRPC2 to be expressed both with early diverging and late diverging V2R genes, i.e. in both MOE and VNO. TRPC2 expression in anuran species was not known, so we performed homology cloning and *in situ* hybridization to localize cells expressing TRPC2. We found that TRPC2 is expressed in the VNO as well as in the MOE (Sansone et al. 2014). This bimodal expression constitutes a unique finding unlike any other species investigated so far. For teleost fish TRPC2 is restricted to the MOE, and for all terrestrial living species, including a salamander, TRPC2 is restricted to the VNO (Kiemnec-Tyburczy et al. 2012, Liberles 2014), always paralleling the V2R expression in those species. The same parallelism was observed in *Xenopus laevis* and might allow searching for V2R gene expression patterns in novel species by analyzing the expression of the much more conserved TRPC2 gene.

3.1.3 SPATIAL EXPRESSION ARCHITECTURE of *XENOPUS* OLFACTORY RECEPTOR FAMILIES in MOE

Our work has shown that TRPC2 and a large subpopulation of the V2R gene family are expressed in the MOE, suggesting the main olfactory system of amphibians is similar to that of teleost fishes, including the cellular and genetic components that are already confined to the VNO in terrestrial vertebrates. Having expression of all four olfactory receptor families in the MOE draws our attention to look whether and how expression of these olfactory families may be segregated or intertwined. Our work combined from three studies gives a complete description of the spatial architecture of olfactory receptor gene family expression in the MOE (Gliem et al. 2013, Syed et al. 2013, Sansone et al. 2014). We found non-random distributions of cells expressing particular receptors in two dimensions, apical to basal and medial to lateral in the MOE (Figure 4).

Firstly, we looked at apical to basal distributions of four olfactory receptor gene families (TAAR, OR class I and class II, V1R and V2R), along with olfactory marker protein (OMP) and TRPC2 as marker for ciliated and microvillous neurons respectively. We report that TRPC2 expressing cells preferentially take a basal position while OMP

expressing cells are present closer to the apical surface of the MOE. These two distributions of TRPC2 and OMP do not have sharp borders, instead, after an initial rise there is a gradual decrease in the frequency of expression from basal to apical, with peak positions characteristically different between these two markers (Syed et al. 2013, Sansone et al. 2014). Furthermore, MOE-specific V2R genes are expressed basally, like the TRPC2 expressing cells (Sansone et al. 2014), and one OR and one TAAR gene are expressed apically like the OMP-expressing cells (Syed et al. 2013).

Secondly, we analyzed medial-to-lateral distribution of these receptors and reported OMP-positive cells being present in all three segments, with a slight depletion in the lateral segment, whereas TRPC2 and V2R-positive cells are uniformly present from medial-to-lateral in the MOE. We found all three members of OR class II and one member of OR class I to be strongly depleted in the lateral region of MOE, whereas two OR class I genes have heterogeneous expression patterns (medial enriched and ubiquitous). Furthermore, two out of three V1R genes showed near homogeneous distribution, whereas other showed depletion in the intermediate zone. The TAAR gene family has only two members involved in olfaction, which exhibit very dissimilar expression patterns: for one gene the large majority of cells is found in the lateral part of MOE (Figure 4) (Gliem et al. 2013), while the second gene is expressed homogeneously in all three regions (unpublished observation).

When evaluating the spatial expression patterns of all olfactory receptors examined, we find that the two axes studied - medial to lateral and apical to basal - appear to be specified independently. Apical expression zones can be uniform (OMP), medial-enriched (OR) or lateral-enriched (TAAR4a), basal expression zones can be uniform (V2Rs) or lateral-enriched. In other words, a particular preferred position on one axis does not predict a preferred position in the second axis.

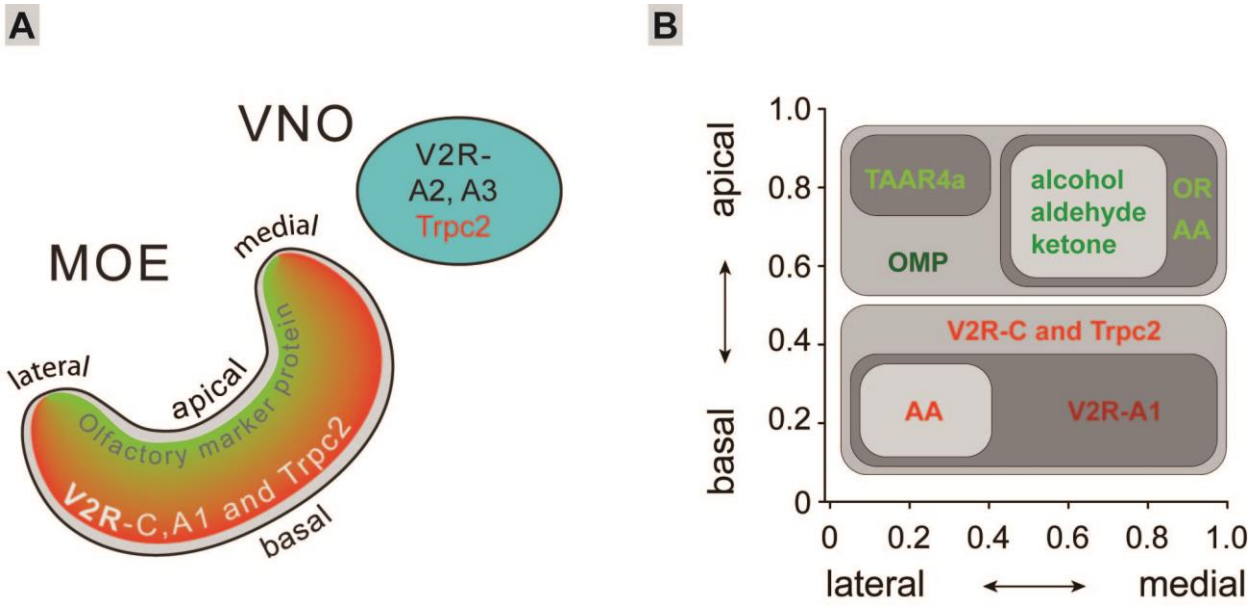

Figure 4: Bimodal and zonal topology of V2R, TRPC2, OMP gene expression and odor responses. (Left) Complementary expression in MOE (OMP, V2R, TRPC2) and VNO (v2r-A2 and v2r-A3, TRPC2 genes). Within the MOE, gradients of expression frequency are observed. A basal zone (red) contains the V2R and TRPC2, whereas an apical zone (green) contains OMP2 as well as an odorant receptor; alcohol, aldehyde, and ketone responses (not depicted). (Right) A 2D schematic representation of the center region of each odor response and gene expression analyzed. Amino acid responses are heterogeneous, basal in the lateral segment, but apical in the intermediate and medial regions. In all, multiple subdivisions are observed, resulting in a highly complex pattern. (Figure modified after Syed et al 2013)

3.1.4 MAPPING the ODOR RESPONSES to the OLFACTORY RECEPTORS SPATIAL DISTRIBUTION in MOE

We looked at the spatial distribution of cells responsive to four different odors (amino acids and alcohols, aldehydes and ketones) in medial-to-lateral and apical to basal zones of MOE. We found amino acid-responsive cells are enriched in the lateral region and are basal within the lateral region, but that smaller populations of amino acid-responsive cells in the medial and intermediate region are preferentially located apically, suggesting a heterogenous population of OSN to be responsible for amino acid detection. We hypothesize that amino acid responses are the sum of a lateral population of microvillous, V2R-expressing OSNs plus a medial and intermediate population of OMP-expressing OSNs. Our findings parallel a previous observation of

ciliated OSNs responding to amino acids in some fish species (Hansen et al. 2003). In contrast, responses to alcohol, aldehyde and ketones are distributed evenly in all three regions from medial to lateral, and show a preferentially apical location, suggesting their expression in ciliated OSNs that express class II or class I OR gene family (Gliem et al. 2013, Syed et al. 2013). To conclude, a correlation of olfactory receptor gene expression patterns with a spatial pattern of an odor responses suggests potential ligands for these receptors, which has of course to be examined directly in further experiments.

To summarize, we have shown a two dimensional architecture of *Xenopus* MOE, in which distributions can vary independently for each dimension. Our findings about the bimodal expression of V2R and TRPC2 in the VNO as well as in the MOE in the *Xenopus* tadpole shows closer similarities of the *Xenopus* MOE to the single sensory epithelium of fishes than to the multi-organ olfactory system of mammals. This intermediate segregation of the olfactory system makes *Xenopus* an ideal model system to investigate the cellular and molecular forces governing the evolution of the vertebrate olfactory system.

3.2 COELACANTH CHEMOSENSORY RECEPTOR REPERTOIRE MORE SIMILAR to TETRAPODS than RAY-FINNED FISHES

Coelacanth (*Latimeria chalumnae*), also known as a living fossil, is a critically endangered species belonging to the family of Latimeriidae. *Latimeria chalumnae* holds an important branch point in evolution as they are the oldest known living lineage of the lobe-finned fishes which was believed to be extinct since the time of dinosaurs (70 million years ago). A genome sequencing study of *Latimeria chalumnae* points at the slow rate of molecular evolution in *Latimeria* genes (Amemiya et al. 2013), this phenomena got us interested to look at the evolutionary dynamics of chemosensory receptor families, in particular V1R and T2R gene families, which are known to rapidly evolve in tetrapods but are small and moderately to highly conserved in teleost fishes (Korsching 2009, Young et al. 2010).

3.2.1 AN UNPRECEDENTEDLY LARGE T2R FAMILY of LIVING FOSSIL

We reported *Latimeria chalumnae* possesses the largest T2R gene family described for any species so far (Figure 5). T2Rs are bitter taste receptors in tetrapods which enable animals to detect and prevent from ingestion structurally distinct toxic compounds. It has been proposed that herbivores possess larger T2R repertoires to guard them against plant chemical defense mechanisms (Li and Zhang 2013). This hypothesis is greatly weakened by our findings, as *Latimeria* lives in deep sea water around 150- 200 meters deep and their diet consists mainly on squids, eels, small sharks and other animals that are found in the deep sea. The biological purpose of the large T2R gene family is unknown, but we can speculate this family might be involved in extra-gustatory functions similar to mammalian T2Rs (Behrens and Meyerhof 2011).

In depth T2R phylogenetic analysis shows three ancestral genes. Only one gene, T2R01, has any ortholog in other species, interestingly in teleost fish, not in tetrapods, and this gene is located most basally in the phylogenetic tree, suggesting T2R01 to be closest to the ancestral T2R gene (Syed and Korsching 2014). Nearly all T2Rs arose *via* multiple gene duplications from another single ancestral gene. We have looked for potential mechanisms generating and maintaining such a large family size. Transposable elements play a key role in gene duplication and indeed we found twice

the density of transposable elements in the immediate vicinity of T2R gene clusters compared to the control group, a highly significant enrichment. For a possible mechanism stabilizing newly duplicated genes we have investigated the selective pressure acting on T2R genes. We have performed dN/dS analysis as an indicator of positive or negative selection and could show pronounced positive selection in the major regions of the protein sequence (extracellular loops, transmembrane regions, intracellular loops), with small clusters in two intracellular loops. Positively selected sites in TMIII, TMV and TMVII might contribute either directly (Behrens and Meyerhof 2013) or indirectly via overall conformational changes to diversification of *Latimeria* taste responses.

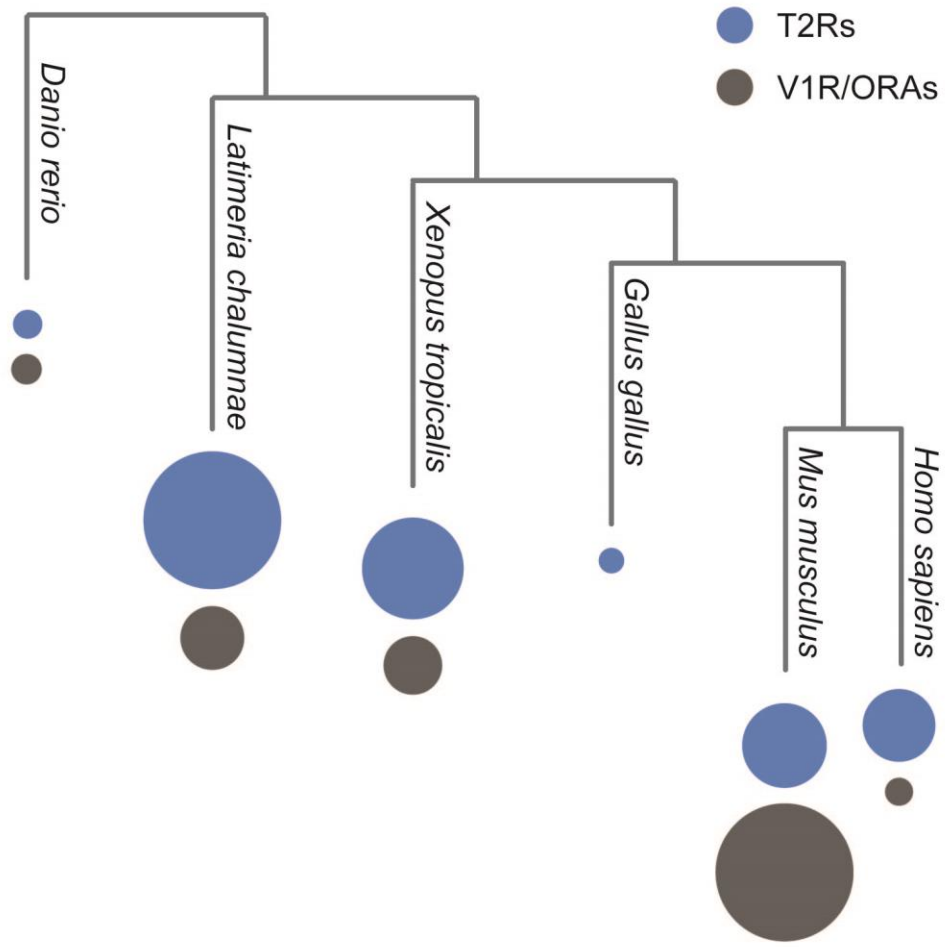

Figure 5: Evolutionary dynamic of vertebrate T2R and V1R gene repertoires. Species tree with the respective T2R (blue circle) and V1R/ORA (black circle) repertoires. Circle area is proportional to the size of the gene family. Values for Latimeria T2R and V1R families, this study; t2r gene family size for other species was taken from (Dong et al., 2009) , teleost ORA and frog V1R family size from (Saraiva and Korsching 2007) and mouse V1R family size from (Shi and Zhang 2007). Figure taken from (Syed and Korsching 2014).

3.2.2 V1R GENE REPERTOIRE SIMILAR to TETRAPOD V1R REPERTOIRES

Through data mining of the *Latimeria* genome we identified twenty V1R/ORA genes (Figure 5). V1R phylogenetic analysis reveals nine ancestral genes, six of which have orthologs in teleost fishes. Transposable elements are not enriched in the surrounding of V1R gene clusters, in contrast to the T2R gene environment. Similarly, dN/dS analysis show neither pronounced positive nor negative selection in *Latimeria* V1R gene family, reminiscent of the properties of *Xenopus* V1Rs. Thus, enrichment of repeat elements in the neighborhood of T2R genes is not a general feature of chemosensory receptors in *Latimeria*, but is correlated with the unusually large increase in the T2R family size during *Latimeria* evolution (Syed and Korsching 2014).

In teleosts the V1R-related ORA gene family is conserved and consists of just six gene members, whereas tetrapod V1R gene repertoires are highly species-specific, from 20 members in frog and reaching up to 210 family members in mouse (Grus et al. 2007). The *Latimeria* V1R gene family has the features of both teleost (having all six ancestral V1R genes), and tetrapod species (species-specific expansion). It had been argued that the species-specific expansions characteristic for tetrapod V1R repertoires were related to the water-to-land transition, i.e. the detection of airborne chemicals (Shi and Zhang 2007). This hypothesis is weakened by the presence of species-specific expansions in coelacanth, and suggests that the expansion of the V1R gene family is not related to terrestrial adaption.

Taken together, our work provides several insights into the chemosensory system of a lobe-finned fish, *Latimeria chalumnae.* The singularly large T2R family may have resulted from an interplay of local gene duplication facilitated *via* neighboring transposable elements, and an efficient neofunctionalization of duplicated genes *via* positive Darwinian selection. In contrast, the *Latimeria* V1R gene family does not show

positive selection or enrichment of repeat elements in the genomic neighborhood. Nevertheless, its family size shows intermediate signatures between ray-finned fish and tetrapods, since it possesses all orthologs of the six ORA genes of ray-finned fishes, and furthermore small species-specific gene expansions which are characteristic for tetrapod V1R families. Finally, *Latimeria* is a critically endangered species, which can't be used as a model organism for functional studies, however due to its significant branch point in evolution and availability of its genome sequence, *Latimeria* provides an excellent anchor point for understanding the evolution of chemosensory receptor families and using the evolutionary viewpoint to derive hypotheses about their function.

4 REFERENCES

Ahuja, G., S. B. Nia, V. Zapilko, V. Shiriagin, et al. (2014). "Kappe neurons, a novel population of olfactory sensory neurons." Sci Rep **4**: 4037.

Alioto, T. S. and J. Ngai (2005). "The odorant receptor repertoire of teleost fish." BMC Genomics **6**: 173.

Alioto, T. S. and J. Ngai (2006). "The repertoire of olfactory C family G protein-coupled receptors in zebrafish: candidate chemosensory receptors for amino acids." BMC Genomics **7**: 309.

Amemiya, C. T., J. Alfoldi, A. P. Lee, S. Fan, et al. (2013). "The African coelacanth genome provides insights into tetrapod evolution." Nature **496**(7445): 311-6.

Behrens, M., O. Frank, H. Rawel, G. Ahuja, et al. (2014). "ORA1, a zebrafish olfactory receptor ancestral to all mammalian V1R genes, recognizes 4-hydroxyphenylacetic acid, a putative reproductive pheromone." J Biol Chem **289**(28): 19778-88.

Behrens, M. and W. Meyerhof (2009). "Mammalian bitter taste perception." Results Probl Cell Differ **47**: 203-20.

Behrens, M. and W. Meyerhof (2011). "Gustatory and extragustatory functions of mammalian taste receptors." Physiol Behav **105**(1): 4-13.

Behrens, M. and W. Meyerhof (2013). "Bitter taste receptor research comes of age: from characterization to modulation of TAS2Rs." Semin Cell Dev Biol **24**(3): 215-21.

Borowsky, B., N. Adham, K. A. Jones, R. Raddatz, et al. (2001). "Trace amines: identification of a family of mammalian G protein-coupled receptors." Proc Natl Acad Sci U S A **98**(16): 8966-71.

Boschat, C., C. Pelofi, O. Randin, D. Roppolo, et al. (2002). "Pheromone detection mediated by a V1r vomeronasal receptor." Nat Neurosci **5**(12): 1261-2.

Breslin, P. A. and A. C. Spector (2008). "Mammalian taste perception." Curr Biol **18**(4): R148-55.

Buck, L. and R. Axel (1991). "A novel multigene family may encode odorant receptors: a molecular basis for odor recognition." Cell **65**(1): 175-87.

Buck, L. B. (2000). "The molecular architecture of odor and pheromone sensing in mammals." Cell **100**(6): 611-8.

Bunzow, J. R., M. S. Sonders, S. Arttamangkul, L. M. Harrison, et al. (2001). "Amphetamine, 3,4-methylenedioxymethamphetamine, lysergic acid diethylamide, and metabolites of the catecholamine neurotransmitters are agonists of a rat trace amine receptor." Mol Pharmacol **60**(6): 1181-8.

Chandrashekar, J., C. Kuhn, Y. Oka, D. A. Yarmolinsky, et al. (2010). "The cells and peripheral representation of sodium taste in mice." Nature **464**(7286): 297-301.

Chang, S., Y. W. Chung-Davidson, S. V. Libants, K. G. Nanlohy, et al. (2013). "The sea lamprey has a primordial accessory olfactory system." BMC Evol Biol **13**: 172.

Clapp, T. R., L. M. Stone, R. F. Margolskee and S. C. Kinnamon (2001). "Immunocytochemical evidence for co-expression of Type III IP3 receptor with signaling components of bitter taste transduction." BMC Neurosci **2**: 6.

Conigrave, A. D., S. J. Quinn and E. M. Brown (2000). "L-amino acid sensing by the extracellular Ca2+-sensing receptor." Proc Natl Acad Sci U S A **97**(9): 4814-9.

Date-Ito, A., H. Ohara, M. Ichikawa, Y. Mori, et al. (2008). "Xenopus V1R vomeronasal receptor family is expressed in the main olfactory system." Chem Senses **33**(4): 339-46.

DeMaria, S., A. P. Berke, E. Van Name, A. Heravian, et al. (2013). "Role of a ubiquitously expressed receptor in the vertebrate olfactory system." J Neurosci **33**(38): 15235-47.

DeMaria, S. and J. Ngai (2010). "The cell biology of smell." J Cell Biol **191**(3): 443-52.

Doty, R. L. (2008). "The olfactory vector hypothesis of neurodegenerative disease: is it viable?" Ann Neurol **63**(1): 7-15.

Doty, R. L. (2009). "The olfactory system and its disorders." Semin Neurol **29**(1): 74-81.

Dulac, C. (2000). "Sensory coding of pheromone signals in mammals." Curr Opin Neurobiol **10**(4): 511-8.

Firestein, S. (2001). "How the olfactory system makes sense of scents." Nature **413**(6852): 211-8.

Fleischer, J., K. Schwarzenbacher and H. Breer (2007). "Expression of trace amine-associated receptors in the Grueneberg ganglion." Chem Senses **32**(6): 623-31.

Freitag, J., J. Krieger, J. Strotmann and H. Breer (1995). "Two classes of olfactory receptors in Xenopus laevis." Neuron **15**(6): 1383-92.

Freitag, J., G. Ludwig, I. Andreini, P. Rossler, et al. (1998). "Olfactory receptors in aquatic and terrestrial vertebrates." J Comp Physiol A **183**(5): 635-50.

Fulle, H. J., R. Vassar, D. C. Foster, R. B. Yang, et al. (1995). "A receptor guanylyl cyclase expressed specifically in olfactory sensory neurons." Proc Natl Acad Sci U S A **92**(8): 3571-5.
Germana, A., G. Montalbano, R. Laura, E. Ciriaco, et al. (2004). "S100 protein-like immunoreactivity in the crypt olfactory neurons of the adult zebrafish." Neurosci Lett **371**(2-3): 196-8.
Gibbs, R. A., G. M. Weinstock, M. L. Metzker, D. M. Muzny, et al. (2004). "Genome sequence of the Brown Norway rat yields insights into mammalian evolution." Nature **428**(6982): 493-521.
Gliem, S., A. S. Syed, A. Sansone, E. Kludt, et al. (2013). "Bimodal processing of olfactory information in an amphibian nose: odor responses segregate into a medial and a lateral stream." Cell Mol Life Sci **70**(11): 1965-84.
Glusman, G., I. Yanai, I. Rubin and D. Lancet (2001). "The complete human olfactory subgenome." Genome Res **11**(5): 685-702.
Gonzalez, A., R. Morona, J. M. Lopez, N. Moreno, et al. (2010). "Lungfishes, like tetrapods, possess a vomeronasal system." Front Neuroanat **4**.
Grus, W. E., P. Shi and J. Zhang (2007). "Largest vertebrate vomeronasal type 1 receptor gene repertoire in the semiaquatic platypus." Mol Biol Evol **24**(10): 2153-7.
Hagino-Yamagishi, K., K. Moriya, H. Kubo, Y. Wakabayashi, et al. (2004). "Expression of vomeronasal receptor genes in Xenopus laevis." J Comp Neurol **472**(2): 246-56.
Halpern, M. (1987). "The organization and function of the vomeronasal system." Annu Rev Neurosci **10**: 325-62.
Hansen, A., J. O. Reiss, C. L. Gentry and G. D. Burd (1998). "Ultrastructure of the olfactory organ in the clawed frog, Xenopus laevis, during larval development and metamorphosis." J Comp Neurol **398**(2): 273-88.
Hansen, A., S. H. Rolen, K. Anderson, Y. Morita, et al. (2003). "Correlation between olfactory receptor cell type and function in the channel catfish." J.Neurosci. **23**(28): 9328-39.
Hansen, A. and B. S. Zielinski (2005). "Diversity in the olfactory epithelium of bony fishes: development, lamellar arrangement, sensory neuron cell types and transduction components." J Neurocytol **34**(3-5): 183-208.
Hasen, N. S. and S. C. Gammie (2009). "Trpc2 gene impacts on maternal aggression, accessory olfactory bulb anatomy and brain activity." Genes Brain Behav **8**(7): 639-49.
Hashiguchi, Y. and M. Nishida (2007). "Evolution of trace amine associated receptor (TAAR) gene family in vertebrates: lineage-specific expansions and degradations of a second class of vertebrate chemosensory receptors expressed in the olfactory epithelium." Mol Biol Evol **24**(9): 2099-107.
Herrada, G. and C. Dulac (1997). "A novel family of putative pheromone receptors in mammals with a topographically organized and sexually dimorphic distribution." Cell **90**(4): 763-73.
Hu, J., C. Zhong, C. Ding, Q. Chi, et al. (2007). "Detection of near-atmospheric concentrations of CO2 by an olfactory subsystem in the mouse." Science **317**(5840): 953-7.
Hussain, A., L. R. Saraiva, D. M. Ferrero, G. Ahuja, et al. (2013). "High-affinity olfactory receptor for the death-associated odor cadaverine." Proc Natl Acad Sci U S A **110**(48): 19579-84.
Hussain, A., L. R. Saraiva and S. I. Korsching (2009). "Positive Darwinian selection and the birth of an olfactory receptor clade in teleosts." Proc Natl Acad Sci U S A **106**(11): 4313-8.
Ishii, T. and P. Mombaerts (2011). "Coordinated coexpression of two vomeronasal receptor V2R genes per neuron in the mouse." Mol.Cell Neurosci. **46**(2): 397-408.
Ishii, T. and P. Mombaerts (2011). "Coordinated coexpression of two vomeronasal receptor V2R genes per neuron in the mouse." Mol Cell Neurosci **46**(2): 397-408.
J, N. P. a. F. (1994). "Normal Table of Xenopus laevis (Daudin)." (Garland, New York).
Ji, Y., Z. Zhang and Y. Hu (2009). "The repertoire of G-protein-coupled receptors in Xenopus tropicalis." BMC Genomics **10**: 263.
Juilfs, D. M., H. J. Fulle, A. Z. Zhao, M. D. Houslay, et al. (1997). "A subset of olfactory neurons that selectively express cGMP-stimulated phosphodiesterase (PDE2) and guanylyl cyclase-D define a unique olfactory signal transduction pathway." Proc Natl Acad Sci U S A **94**(7): 3388-95.
Kapur, A. and L. B. Haberly (1998). "Duration of NMDA-dependent synaptic potentiation in piriform cortex in vivo is increased after epileptiform bursting." J Neurophysiol **80**(4): 1623-9.
Kiemnec-Tyburczy, K. M., S. K. Woodley, R. A. Watts, S. J. Arnold, et al. (2012). "Expression of vomeronasal receptors and related signaling molecules in the nasal cavity of a caudate amphibian (Plethodon shermani)." Chem Senses **37**(4): 335-46.

Kimoto, H., S. Haga, K. Sato and K. Touhara (2005). "Sex-specific peptides from exocrine glands stimulate mouse vomeronasal sensory neurons." Nature **437**(7060): 898-901.
Korsching, S. (2009). "The molecular evolution of teleost olfactory receptor gene families." Results Probl Cell Differ **47**: 37-55.
Lazic, S. E., A. O. Goodman, H. E. Grote, C. Blakemore, et al. (2007). "Olfactory abnormalities in Huntington's disease: decreased plasticity in the primary olfactory cortex of R6/1 transgenic mice and reduced olfactory discrimination in patients." Brain Res **1151**: 219-26.
Leinders-Zufall, T., P. Brennan, P. Widmayer, P. C. S, et al. (2004). "MHC class I peptides as chemosensory signals in the vomeronasal organ." Science **306**(5698): 1033-7.
Leinders-Zufall, T., R. E. Cockerham, S. Michalakis, M. Biel, et al. (2007). "Contribution of the receptor guanylyl cyclase GC-D to chemosensory function in the olfactory epithelium." Proc Natl Acad Sci U S A **104**(36): 14507-12.
Li, D. and J. Zhang (2013). "Diet Shapes the Evolution of the Vertebrate Bitter Taste Receptor Gene Repertoire." Mol Biol Evol.
Li, D. and J. Zhang (2014). "Diet shapes the evolution of the vertebrate bitter taste receptor gene repertoire." Mol Biol Evol **31**(2): 303-9.
Liberles, S. D. (2014). "Mammalian pheromones." Annu Rev Physiol **76**: 151-75.
Liberles, S. D. and L. B. Buck (2006). "A second class of chemosensory receptors in the olfactory epithelium." Nature **442**(7103): 645-50.
Liberles, S. D., L. F. Horowitz, D. Kuang, J. J. Contos, et al. (2009). "Formyl peptide receptors are candidate chemosensory receptors in the vomeronasal organ." Proc Natl Acad Sci U S A **106**(24): 9842
Liman, E. R. and C. Dulac (2007). Frontiers in NeuroscienceTRPC2 and the Molecular Biology of Pheromone Detection in Mammals. TRP Ion Channel Function in Sensory Transduction and Cellular Signaling Cascades. W. B. Liedtke and S. Heller. Boca Raton (FL), CRC Press
Taylor & Francis Group, LLC.Liman, E. R. and H. Innan (2003). "Relaxed selective pressure on an essential component of pheromone transduction in primate evolution." Proc Natl Acad Sci U S A **100**(6): 3328-32.
Lindemann, L., M. Ebeling, N. A. Kratochwil, J. R. Bunzow, et al. (2005). "Trace amine-associated receptors form structurally and functionally distinct subfamilies of novel G protein-coupled receptors." Genomics **85**(3): 372-85.
Manzini, I. and D. Schild (2010). Frontiers in NeuroscienceOlfactory Coding in Larvae of the African Clawed Frog Xenopus laevis. The Neurobiology of Olfaction. A. Menini. Boca Raton (FL), CRC PressLlc.
Martini, S., L. Silvotti, A. Shirazi, N. J. Ryba, et al. (2001). "Co-expression of putative pheromone receptors in the sensory neurons of the vomeronasal organ." J.Neurosci. **21**(3): 843-8.
Matsunami, H. and L. B. Buck (1997). "A multigene family encoding a diverse array of putative pheromone receptors in mammals." Cell **90**(4): 775-84.
Meredith, T. L., S. M. Kajiura and A. Hansen (2013). "The somatotopic organization of the olfactory bulb in elasmobranchs." J Morphol **274**(4): 447-55.
Meyer, M. R., A. Angele, E. Kremmer, U. B. Kaupp, et al. (2000). "A cGMP-signaling pathway in a subset of olfactory sensory neurons." Proc Natl Acad Sci U S A **97**(19): 10595-600.
Mezler, M., S. Konzelmann, J. Freitag, P. Rossler, et al. (1999). "Expression of olfactory receptors during development in Xenopus laevis." J Exp Biol **202**(Pt 4): 365-76.
Mombaerts, P. (2004). "Love at first smell--the 2004 Nobel Prize in Physiology or Medicine." N Engl J Med **351**(25): 2579-80.
Mueller, K. L., M. A. Hoon, I. Erlenbach, J. Chandrashekar, et al. (2005). "The receptors and coding logic for bitter taste." Nature **434**(7030): 225-9.
Nakamuta, S., N. Nakamuta, K. Taniguchi and K. Taniguchi (2012). "Histological and ultrastructural characteristics of the primordial vomeronasal organ in lungfish." Anat Rec (Hoboken) **295**(3): 481-91.
Nei, M., Y. Niimura and M. Nozawa (2008). "The evolution of animal chemosensory receptor gene repertoires: roles of chance and necessity." Nat Rev Genet **9**(12): 951-63.
Nelson, G., J. Chandrashekar, M. A. Hoon, L. Feng, et al. (2002). "An amino-acid taste receptor." Nature **416**(6877): 199-202.
Nelson, G., M. A. Hoon, J. Chandrashekar, Y. Zhang, et al. (2001). "Mammalian sweet taste receptors." Cell **106**(3): 381-90.
Niimura, Y. and M. Nei (2003). "Evolution of olfactory receptor genes in the human genome." Proc Natl Acad Sci U S A **100**(21): 12235-40.

Niimura, Y. and M. Nei (2007). "Extensive gains and losses of olfactory receptor genes in mammalian evolution." PLoS One **2**(8): e708.
Oka, Y., L. R. Saraiva and S. I. Korsching (2012). "Crypt neurons express a single V1R-related ora gene." Chem Senses **37**(3): 219-27.
Picone, B., U. Hesse, S. Panji, P. Van Heusden, et al. (2014). "Taste and odorant receptors of the coelacanth--a gene repertoire in transition." J Exp Zool B Mol Dev Evol **322**(6): 403-14.
Riviere, S., L. Challet, D. Fluegge, M. Spehr, et al. (2009). "Formyl peptide receptor-like proteins are a novel family of vomeronasal chemosensors." Nature **459**(7246): 574-7.
Sansone, A., A. S. Syed, E. Tantalaki, S. I. Korsching, et al. (2014). "Trpc2 is expressed in two olfactory subsystems, the main and the vomeronasal system of larval Xenopus laevis." J Exp Biol **217**(Pt 13): 2235-8.
Saraiva, L. R. and S. I. Korsching (2007). "A novel olfactory receptor gene family in teleost fish." Genome Res **17**(10): 1448-57.
Sato, H., I. Naito, R. Momota, Y. Naomoto, et al. (2007). "The differential distribution of type IV collagen alpha chains in the subepithelial basement membrane of the human alimentary canal." Arch Histol Cytol **70**(5): 313-23.
Sato, Y., N. Miyasaka and Y. Yoshihara (2005). "Mutually exclusive glomerular innervation by two distinct types of olfactory sensory neurons revealed in transgenic zebrafish." J Neurosci **25**(20): 4889-97.
Shi, P. and J. Zhang (2006). "Contrasting modes of evolution between vertebrate sweet/umami receptor genes and bitter receptor genes." Mol Biol Evol **23**(2): 292-300.
Shi, P. and J. Zhang (2007). "Comparative genomic analysis identifies an evolutionary shift of vomeronasal receptor gene repertoires in the vertebrate transition from water to land." Genome Res **17**(2): 166-74.
Sun, L., H. Wang, J. Hu, J. Han, et al. (2009). "Guanylyl cyclase-D in the olfactory CO2 neurons is activated by bicarbonate." Proc Natl Acad Sci U S A **106**(6): 2041-6.
Syed, A. S. and S. I. Korsching (2014). "Positive Darwinian selection in the singularly large taste receptor gene family of an 'ancient' fish, Latimeria chalumnae." BMC Genomics **15**: 650.
Syed, A. S., A. Sansone, W. Nadler, I. Manzini, et al. (2013). "Ancestral amphibian v2rs are expressed in the main olfactory epithelium." Proc Natl Acad Sci U S A **110**(19): 7714-9.
Tian, H. and M. Ma (2008). "Differential development of odorant receptor expression patterns in the olfactory epithelium: a quantitative analysis in the mouse septal organ." Dev Neurobiol **68**(4): 476-86.
Walz, A., P. Feinstein, M. Khan and P. Mombaerts (2007). "Axonal wiring of guanylate cyclase-D-expressing olfactory neurons is dependent on neuropilin 2 and semaphorin 3F." Development **134**(22): 4063-72.
Yang, D., Q. Chen, B. Gertz, R. He, et al. (2002). "Human dendritic cells express functional formyl peptide receptor-like-2 (FPRL2) throughout maturation." J Leukoc Biol **72**(3): 598-607.
Yarmolinsky, D. A., C. S. Zuker and N. J. Ryba (2009). "Common sense about taste: from mammals to insects." Cell **139**(2): 234-44.
Yasuoka, A. and K. Abe (2009). "Gustation in fish: search for prototype of taste perception." Results Probl Cell Differ **47**: 239-55.
Yoshii, K., C. Yoshii, Y. Kobatake and K. Kurihara (1982). "High sensitivity of Xenopus gustatory receptors to amino acids and bitter substances." Am J Physiol **243**(1): R42-8.
Young, J. M., H. F. Massa, L. Hsu and B. J. Trask (2010). "Extreme variability among mammalian V1R gene families." Genome Res **20**(1): 10-8.
Young, J. M., B. M. Shykind, R. P. Lane, L. Tonnes-Priddy, et al. (2003). "Odorant receptor expressed sequence tags demonstrate olfactory expression of over 400 genes, extensive alternate splicing and unequal expression levels." Genome Biol **4**(11): R71.
Young, J. M. and B. J. Trask (2007). "V2R gene families degenerated in primates, dog and cow, but expanded in opossum." Trends Genet **23**(5): 212-5.
Zhang, J. and D. M. Webb (2003). "Evolutionary deterioration of the vomeronasal pheromone transduction pathway in catarrhine primates." Proc Natl Acad Sci U S A **100**(14): 8337-41.
Zhang, X. and S. Firestein (2002). "The olfactory receptor gene superfamily of the mouse." Nat Neurosci **5**(2): 124-33.
Zhao, G. Q., Y. Zhang, M. A. Hoon, J. Chandrashekar, et al. (2003). "The receptors for mammalian sweet and umami taste." Cell **115**(3): 255-66.

5 SUMMARY

Chemosensation (smell and taste) is essential for the detection of chemical signals, which enables animals to perform essential biological functions such as to find, recognize and assess food cues, to localize prey and avoid predators, to recognize kin, to identify suitable mates, and analyse food quality. In humans, smell, almost more than any other sense, has the ability to recall up memories, and to change moods. The smell molecules or odors are detected by a specialized set of G protein-coupled receptors called olfactory receptors; these olfactory receptors are expressed in olfactory sensory neurons located in the olfactory epithelium of vertebrates. Unlike tetrapods, which have 2 or more specialized olfactory subsystems, teleost fishes possess a single sensory surface.

The aim of my doctoral thesis is to investigate the evolution of chemosensory receptor gene repertoires from the perspective of comparative genomics. I have mainly focused on two evolutionary relevant animal models, *Latimeria chalumnae* and *Xenopus laevis*. *Latimeria chalumnae* are also called “living fossil” and are considered the oldest living lineage of Sarcopterygii (lobe-finned fish and tetrapods). *Xenopus laevis* (African clawed frog*)* is of great evolutionary importance as it is embodies the evolutionary transition between aquatic and terrestrial environment.

In my thesis I have combined rigorous bioinformatics analysis with a molecular biological approach to characterize chemosensory receptor repertoires. For two of these repertoires that are characteristically different between teleost fish and tetrapods I could show that *Latimeria chalumnae* exhibits the tetrapod, not the teleost features. Furthermore, I demonstrated *Latimeria* to possess the largest taste receptor type 2 gene family reported for any species, showed pronounced positive Darwinian selection in this gene family, and identified a possible evolutionary mechanism for generating this large family. In an amphibian species (*Xenopus laevis*), I could show that expression zones for several olfactory receptors are specified independently along two perpendicular axes, the first such demonstration for any species. In this species I revealed a novel bimodal expression pattern for type 2 vomeronasal receptors, with phylogenetically ‘ancient’ receptors being expressed in the main olfactory epithelium like their teleost fish counterparts, whereas ‘modern’ receptors are expressed in the vomeronasal epithelium like their mammalian counterparts. These findings establish *Xenopus laevis*, an established olfactory model system for functional analysis as highly suitable to study the transition from aquatic to terrestrial olfaction at the molecular level.

6 ZUSAMMENFASSUNG

Chemosensorische Systeme (Geruchs- und Geschmackssinn) sind essentiell für die Wahrnehmung chemischer Stimuli. Er befähigt Tiere zur Ausführung essentieller biologischer Funktionen und Verhaltensweisen, darunter das Finden, Erkennen, Erreichen und Bewerten von Nahrungsquellen, die Lokalisation von Beute und Fressfeinden, die Erkennung von verwandten Artgenossen und die Identifikation geeigneter Geschlechtspartner. Beim Menschen hat der Geruch, vielleicht mehr als jeder andere Sinn, die Fähigkeit, Erinnerungen zu wecken und Gemütsstimmungen zu verändern. Die Duftmoleküle werden von spezialisierten G-Protein gekoppelten Rezeptoren erkannt, welche bei Vertebraten in sensorischen Neuronen des olfaktorischen Epithels lokalisiert sind. Im Gegensatz zu Tetrapoden, die zwei oder mehr spezialisierte olfaktorische Subsysteme aufweisen, haben Teleosten nur ein olfaktorisches Organ.

Das Ziel meiner Dissertation ist die Entschlüsselung der evolutionären Zusammenhänge verschiedener chemosensorischer Rezeptorgen-Repertoires vom Standpunkt der vergleichenden Genetik. Dabei habe ich mich auf zwei evolutionär relevante Modellspezies konzentriert: *Latimeria chalumnae* und *Xenopus laevis. Latimeria chalumna*, auch als lebendes Fossil bezeichnet, wird als der älteste rezente Vertreter der Sarcopterygii (Fleischflosser und Tetrapoden) angesehen. *Xenopus laevis* (afrikanischer Klauenfrosch) ist ebenfalls von enormer evolutionärer Bedeutung, da die Amphibien den Übergang von der aquatischen zur terrestrischen Lebensweise verkörpern.

In meiner Arbeit habe ich bioinformatische Analysen mit einem molekularbiologischen Ansatz kombiniert, um chemosensorische Rezeptorgen-Repertoires zu charakterisieren. Für zwei dieser Genfamilien, die sich bei Teleosten und Tetrapoden in charakteristischer Weise unterscheiden, konnte ich zeigen, dass *Latimeria chalumnae* Eigenschaften des Tetrapoden-Repertoires aufweist, nicht aber des der Teleosten. Weiterhin konnte ich zeigen, dass *Latimeria* die größte bekannte Typ 2 Geschmacksrezeptor Genfamilie aller untersuchten Spezies aufweist und diese einer positiven Selektion im Sinne Darwins unterliegt. In der Arbeit habe ich mögliche evolutionäre Mechanismen der Entstehung solch einer großen Genfamilie aufgezeigt. Für eine amphibische Spezies (*Xenopus laevis*) konnte ich, erstmalig in diesem Forschungsgebiet, demonstrieren, dass die Expression verschiedener olfaktorischer Rezeptoren in der sensorischen Oberfläche in zwei Dimensionen unabhängig voneinander festgelegt wird. In dieser Spezies beobachtete ich außerdem ein neuartiges bimodales Expressionsmuster für Typ 2 vomeronasale Rezeptoren: Phylogenetisch „ursprünglichere“ Rezeptoren werden, genau wie die entsprechenden Rezeptoren bei Teleosten, im olfaktorischen Epithel exprimiert. Hingegen werden

„moderne“ Rezeptoren, ebenso wie deren Pendants bei Säugetieren, im vomeronasalen Epithel exprimiert. Diese Erkenntnisse machen *Xenopus laevis,* der bereits ein bewährtes Modell für funktionelle Analysen in der Geruchsforschung ist, nun auch zu einem geeigneten und äußerst interessanten Modell zu Untersuchung des Geruchssinnes im Übergang von der aquatischen zur terrestrischen Lebensweise.

7 APPENDIX

OE:	Olfactory epithelium
OSN:	Olfactory sensory neuron
GPCR:	G protein-coupled receptor
MOB:	Main olfactory bulb
MOE:	Main olfactory epithelium
OB:	Olfactory bulb
TRPC2:	Transient receptor potential cation channel, subfamily C, member 2
OSN:	Olfactory sensory neuron
OMP:	Olfactory marker protein
GC:	Guanylyl cyclase
OR:	Olfactory receptor
TAAR:	Trace Amine-Associated Receptor
FPR:	Formyl peptide receptor
V1R:	Vomeronasal receptors type 1
V2R:	Vomeronasal receptors type 2
VNO:	Vomeronasal organ
VR:	vomeronasal receptor
X.l:	*Xenopus laevis*
X.t:	*Xenopus tropicalis*
Lc:	*Latimeria chalumnae*
Actinopterygii:	Ray-finned fish
Sarcopterygii:	Lobe-finned fish
T2R:	Taste receptor, type 2
T1R:	Taste receptor, type 1
TRC:	Taste receptor cell

8 ACKNOWLEDGEMENT

This study was performed in the lab of Prof. Dr. Sigrun I. Korsching in the Institute of Genetics, University of Cologne, Cologne, Germany and was supported by a grant from the DFG Schwerpunktprogramm/ SPP 1392: Integrative Analysis of Olfaction.

First and foremost, I want to thank my supervisor Prof. Sigrun Korsching for all her contributions of time, ideas and funding to make my PhD experience productive and stimulating. She provided me with an excellent environment where I had incredible freedom to delve into different scientific techniques and methods, which helped broaden my scientific horizon. The many discussions and suggestions in the lab, on the sandy beaches, and even at the airport terminals are unforgettable and priceless.

I would also like to acknowledge Dr. Ivan Manzini for the guidance and introducing me to *Xenopus* model system. Many thanks to Prof. Dr. Kay Hofmann and to Prof. Dr. Wolfgang Walkowiak for accepting to be in my thesis committee, and for the interest in my work.

The members of the Olfis (AG Korsching) have contributed immensely to my personal and professional life, and I take this opportunity to thank everyone (past and current) lab members, Dr. Ashiq Hussain, Dr.Yuichiro Oka, Ivan, Gaurav, Venkatesh, Daniel, Milan, Vladimir, Shahrzad, Dr. Veronika Zapilko, Kanika, Mehreen, and Mehmet, for a great atmosphere and useful discussions.

Special thanks to Prof. Korsching, Kanika and Dr. Ashiq Hussain for critical discussion of my thesis draft, suggestions, and proof reading. Also special thanks to Milan for translating abstract into German language.

My past four years in Cologne was made enjoyable in large part due to many friends that became a part of my life. Many thanks to Reka, Lisa, Anna, Umit, Mehreen, Kanika for their valuable friendship, support, inspiration, company, for always being there for me and making my stay in Germany memorable and priceless.

This acknowledgment would be incomplete without giving thanks to my parents and siblings. Both have instilled many admirable qualities in me and given me a good foundation with which to meet life.

9 AUTHOR CONTRIBUTIONS

I am first author or shared first author in all the studies underlying this dissertation. My contributions are listed below for each study.

Syed, A. S., A. Sansone, W. Nadler, I. Manzini, et al. (2013). "**Ancestral amphibian v2rs are expressed in the main olfactory epithelium**." Proc Natl Acad Sci U S A **110**(19): 7714-9.

Designed Research	Performed Research	Analyzed Data	Designed Figures	Wrote Paper
Yes	Yes	Yes	Yes	Yes

Sa Sansone, A., **A. S. Syed**, E. Tantalaki, S. I. Korsching, et al. (2014). "**Trpc2 is expressed in two olfactory subsystems, the main and the vomeronasal system of larval Xenopus laevis**." J Exp Biol **217**(Pt 13): 2235-8.

Designed Research	Performed Research	Analyzed Data	Designed Figures	Wrote Paper
No	Yes	Yes	Yes	No

Gliem, S., **A. S. Syed**, A. Sansone, E. Kludt, et al. (2013). "**Bimodal processing of olfactory information in an amphibian nose: odor responses segregate into a medial and a lateral stream**." Cell Mol Life Sci **70**(11): 1965-84.

Designed Research	Performed Research	Analyzed Data	Designed Figures	Wrote Paper
No	Yes	Yes	Yes	No

Syed, A. S. and S. I. Korsching (2014). "**Positive Darwinian selection in the singularly large taste receptor gene family of an 'ancient' fish, Latimeria chalumnae**." BMC Genomics **15**: 650.

Designed Research	Performed Research	Analyzed Data	Designed Figures	Wrote Paper
Yes	Yes	Yes	Yes	No

10 ERKLÄRUNG (DECLARATION)

Ich versichere, dass ich die von mir vorgelegte Dissertation selbstständig angefertigt, die benutzten Quellen und Hilfsmittel vollständig angegeben und die Stellen in der Arbeit - einschließlich Tabellen, Karten und Abbildungen -, die anderen Werken im Wortlaut oder dem Sinn nach entnommen sind, in jedem Einzelfall als Entlehnung kenntlich gemacht habe; dass diese Dissertation noch keiner anderen Fakultät oder Universität zur Prüfung vorgelegen hat; dass sie - abgesehen von den unten angegebenen Teilpublikationen – noch nicht veröffentlicht worden ist, sowie dass ich eine solche Veröffentlichung vor Abschluss des Promotionsverfahrens nicht vornehmen werde. Die Bestimmungen dieser Promotionsordnung sind mir bekannt. Die von mir vorgelegte Dissertation ist von Prof. Dr. Sigrun. I. Korsching betreut worden.

Köln, den 017. Nov, 2014

Teilpublikationen:

1: **Syed AS**, Korsching SI. Positive Darwinian selection in the singularly large taste receptor gene family of an 'ancient' fish, Latimeria chalumnae. BMC Genomics. 2014 Aug 5;15:650.

2: Sansone A*, **Syed AS***, Tantalaki E, Korsching SI, Manzini I. Trpc2 is expressed in two olfactory subsystems, the main and the vomeronasal system of larval Xenopus laevis. J Exp Biol. 2014 Jul 1;217(Pt 13):2235-8. (shared first author)

3: **Syed AS**, Sansone A, Nadler W, Manzini I, Korsching SI. Ancestral amphibian v2rs are expressed in the main olfactory epithelium. Proc Natl Acad Sci U S A. 2013 May 7;110(19):7714-9.

4: Gliem S*, **Syed AS***, Sansone A, Kludt E, Tantalaki E, Hassenklöver T, Korsching SI, Manzini I. Bimodal processing of olfactory information in an amphibian nose: odor responses segregate into a medial and a lateral stream. Cell Mol Life Sci.2013 Jun;70(11):1965-84

(* shared first authors)

Adnan S. Syed

Date of Birth: 21/11/1983 **Citizenship:** Pakistani

Mobile Number: +49-176-3416476

Email Address: adnan.shahzad@gmail.com

Languages: English [fluent], Urdu/Hindi [native speaker] , Italian [beginner], German [beginner]

Current Address: Zuelpicherstr. 58e, 50674, Cologne, Germany.

Motivation

An enthusiastic, adaptive and fast-learning person with a broad and acute interest in the field of neuroscience. I particularly enjoy using multidisciplinary approach to answer scientific phenomenas.

Education

PhD in Neuroscience 2010 – 2014

Institute for Genetics, University of Cologne, Germany.

Dissertation Title: Integrative analysis of branch points in the evolution of chemosensory receptor repertoires: unexpected properties of amphibian olfactory and coelacanth taste receptors

BS(Hons)/Msc in Bioinformatics 2002 – 2006

Muhammad Ali Jinnah University Islamabad, Pakistan.

Thesis: In-silico study of pathogenicity and human gastric colonization of *helicobacter pylori*

Work Experience

Research Fellow Feb-2009 – Mar-2010

European Institute of Oncology, Milan, Italy

I worked as a research fellow in Bioinformatics & Comparative Genomics" Lab, where we focused on understanding the similar

system level properties of genes that have been found mutated in different types of cancer.

Lecturer May-2007 – Dec-2008

Kohat University of Science and Technology, Kohat, Pakistan

I worked as a lecturer in the department of biotechnology and genetic engineering. My responsibilities included teaching bioinformatics as a subject, and establishment of bioinformatics research lab.

Research Fellow Feb-2006 – May-2007

National Centre of Excellence in Molecular Biology, Lahore, Pakistan

I worked as a research fellow in bioinformatics research group at CEMB. My responsibilities included conducting bioinformatics practical labs, providing in-house bioinformatics expertise and support.

Publications

1: **Syed AS**, Korsching SI. Positive Darwinian selection in the singularly large taste receptor gene family of an 'ancient' fish, Latimeria chalumnae. BMC Genomics. 2014 Aug 5;15:650.

2: Sansone A**, **Syed AS****, Tantalaki E, Korsching SI, Manzini I. Trpc2 is expressed in two olfactory subsystems, the main and the vomeronasal system of larval Xenopus laevis. J Exp Biol. 2014 Jul 1;217(Pt 13):2235-8.

3: Sansone A, Hassenklöver T, **Syed AS**, Korsching SI, Manzini I. Phospholipase C and diacylglycerol mediate olfactory responses to amino acids in the main olfactory epithelium of an amphibian. PLoS One. 2014 Jan 28;9(1):e87721.

4: **Syed AS**, Sansone A, Nadler W, Manzini I, Korsching SI. Ancestral amphibian v2rs are expressed in the main olfactory epithelium. Proc Natl Acad Sci U S A. 2013 May 7;110(19):7714-9.

5: Gliem S**, **Syed AS****, Sansone A, Kludt E, Tantalaki E, Hassenklöver T, Korsching SI, Manzini I. Bimodal processing of olfactory information in an amphibian nose: odor responses segregate into a medial and a lateral stream. Cell Mol Life Sci.2013 Jun;70(11):1965-84

6: **Syed AS**, D'Antonio M, Ciccarelli FD. Network of Cancer Genes: a web resource to analyze duplicability, orthology and network properties of cancer genes. Nucleic Acids Res. 2010 Jan;38

** Shared first author

Manuscripts Submitted / In Preparation

1: Luis R. Saraiva, Gaurav Ahuja, **Syed AS**, Ivan Ivandic, John C. Marioni, Sigrun I. Korsching, and Darren W. Logan. Molecular and neuronal homology between the olfactory systems of zebrafish and mouse. **(Submitted)**.

2: **Syed AS** et al., The third nose of an amphibian expresses ancestral V2Rs. (In preparation)

3: **Syed AS** et al., Distinct basal and apical response domains for amines in an amphibian olfactory epithelium correlate with spatial heterogeneity of TAAR olfactory receptors. (In preparation)

4: **Syed AS** et al., Ancient grandeur of the TAAR olfactory receptor repertoire in the living fossil coelacanth. (In preparation)

5: Gaurav Ahuja, Vera Reichel, **Syed AS**, Yuichiro Oka and Sigrun Korsching. Fuzzy topology for zebrafish olfactory receptors of the V2R-related OlfC family. (In preparation)

Technical Skills

Programming	Java, Bio Java, C#, C++, Perl, PHP.
Database	Ms SQL Server, Visual Basic, Ms Access, J builder
Graphics	Dream Viewer, MS Front Page, HTML
Wet lab skills	DNA/RNA Extraction, PCR, Primer Designing, Restriction Mapping, In situ hybridization, Immunohistochemistry
Bioinformatics	Phylogenetics, Biological databases, Molecular modelling and docking softwares, Molecular visualization softwares

Presentations & Conferences

1: **Invited talk** presented at Turkish-German workshop on molecular neuroscience in September 2014, held in Istanbul, Turkey.

2: **Poster** presented at European chemoreception workshop in August 2013, held in Leuven, Belgium.

3: **Poster** presented at 8th FENS forum of neuroscience meeting in July 2012, held in Barcelona, Spain.

Interests and Activities

I achieved black belt in martial arts (Shotokan) with discipline, motivation and dedication through regular exercise and practice. I have won over 12 medals including 6 gold, at district and national level championships. Additionally, I love socialising with friends and family, watching TED talks, solving puzzles and computing games in my spare time.

References

References will be furnished upon request